BeFo

STIFTELSEN BERGTEKNISK FORSKNING
ROCK ENGINEERING RESEARCH FOUNDATION

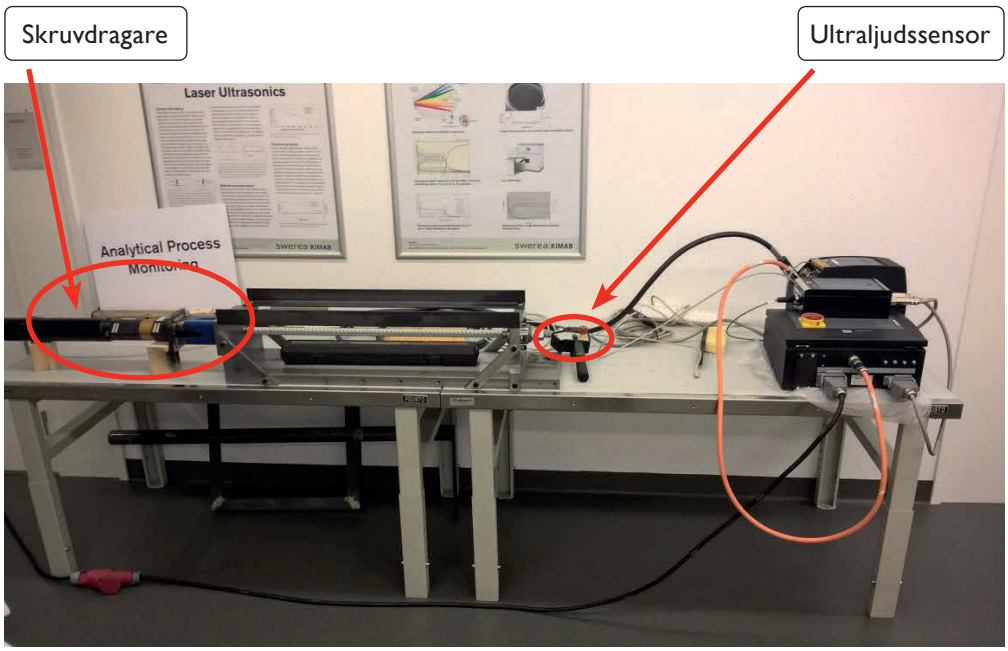

UTVÄRDERING AV STRUKTURKOMPONENTER

Peter Lundin

BeFo Rapport 164

STIFTELSEN BERGTEKNISK FORSKNING
ROCK ENGINEERING RESEARCH FOUNDATION

UTVÄRDERING AV STRUKTURKOMPONENTER

Evaluation of loaded structural components

Peter Lundin

BeFo Rapport 164
Stockholm 2024
ISSN 1104 – 1773
ISRN BEFO-R-164-SE

Förord

I alla tider har det varit önskvärt att kunna mäta hur mycket ett material är belastat. Detta kan enkelt göras i provutrustningar men ute i fält eller i monterat skick är det oftast väldigt svårt, för att inte säga omöjligt, att konstatera hur mycket ett material är belastat. I stort sett alla industrigrenar har belastade strukturelement i form av stänger. Stängerna är ofta kritiska för produktens användning och människor riskerar ofta att komma till skada om deras lastbärande förmåga är reducerad. Formen på dessa kritiska stänger skiljer mellan olika industrigrenar. Inom t.ex. bilindustrin är det belastade stänger i form av åtdragna skruvar i kritiska skruvförband främst i motorer och hjulupphängningar medan det i tunnel- och gruvindustrin är stänger i form av bergbultar som håller berget på plats som är kritiska. Alla områden har med sina varierande miljöer egna krav på hanterbarhet och olika informationsbehov av den belastade stången men dock gemensamt för alla är behovet av att kunna mäta belastningsgraden i dessa stänger för att säkerställa kvalitet samt säkerhet. Bergbult gjuts ofta in i berget spänningsfritt men vid eventuella framtida påkänningar av bulten skulle den tänkta mätmetoden kunna konstatera om berget är i rörelse eller inte. För väg- och järnvägstunnlar är detta av stort intresse eftersom dessa anläggningar dimensioneras för 120 års drift.

I det här forskningsprojektet har en ultraljudsbaserad mätmetod utvecklats som ska kunna övervaka åldrandet hos redan installerade stänger vilket kommer möjliggöra ett bättre och mer välanpassat underhåll samt optimera användandet av t.ex. bergrum. Metoden utnyttjar det faktum att hastigheten hos olika typer av ultraljudsvågor förändrar sig olika beroende på lasten i materialet vågorna fortplantar sig i. Mätmetoden samt hårdvara utvecklades och förfinades genom kontrollerade mätningar i labbet där bergbultar av olika material spändes fast i en mätrigg och undersöktes med ultraljud vid olika laster. Resultaten från labbmätningarna visade att mätmetoden har stor potential för att övervaka och undersöka belastade strukturelement. Projektet avslutades med ett fältförsök där ett tjugotal berg-monterade bultar undersöktes. Mätningarna visade att både metod och hårdvara har tillräcklig stabilitet för att tillförlitliga mätningar ska kunna utföras.

Medverkande i projektet har varit Peter Lundin/Swerea KIMAB och Johan Carlson/LTU som utförare. Erik Persson/Atlas Copco, Kjell Windelhed/ÅF Infrastructure AB, Tommy Elison/BESAB, Erik Swedberg/LKAB, Anders Asp/Pretec samt Per Tengborg/BeFo medverkande i arbets- och referensgruppen och bidrog med värdefulla insatser.

Detta projekt är stödprojekt till ett Formasprojekt (samma titel) som beviljades 2012 under utlysningen Geoinfra. Medlemskonsortiet i detta och i Formasprojektet är Swerea KIMAB (forskningsutövare), Luleå tekniska universitet, LTU (forskningsutövare), Atlas Copco, ÅF, Pretec, BESAB, Lunds universitet och LKAB. Formas och BeFo finansierar projekten.

Stockholm

Per Tengborg

Sammanfattning

I alla tider har det varit önskvärt att kunna mäta hur mycket ett material är belastat. Detta kan enkelt göras i provutrustningar men ute på fältet eller i monterat skick är det oftast väldigt svårt, för att inte säga omöjligt, att konstatera hur mycket ett material är belastat. I stort sett alla industrigrenar har belastade strukturelement i form av stänger. Stängerna är ofta kritiska för produktens användning och människor riskerar ofta att komma till skada om deras lastbärande förmåga är reducerad. Formen på dessa kritiska stänger skiljer mellan olika industrigrenar. Alla områden har med sina varierande miljöer egna krav på hanterbarhet och olika informationsbehov av den belastade stången men gemensamt för alla är dock behovet av att kunna mäta belastningsgraden i dessa stänger för att säkerställa kvalitet samt säkerhet. Bergbult gjuts ofta in i berget spänningsfritt men vid eventuella framtida påkänningar av bulten skulle den studerade mätmetoden kunna konstatera om berget är i rörelse eller inte. För väg- och järnvägstunnlar är detta av stort intresse eftersom dessa anläggningar dimensioneras för 120 års drift. En utvecklad mätmetod skulle även kunna användas för att övervaka åldrandet hos redan installerade stänger. Detta skulle t.ex. möjliggöra ett bättre och mer välanpassat underhåll. Syftet med projektet har varit att utveckla och utvärdera en metod för att mäta spänningen i belastade stänger, främst för att övervaka dragspänningen i väldigt kritiska stänger som en del av det periodiska underhållet.

Den ultraljudsmetod som använts i detta projekt har sitt ursprung i två fenomen: Hookes lag och den akustoelastiska effekten. Hookes lag säger att bultens förlängning är direkt proportionell mot kraften i bulten. Detta är sant så länge töjningen sker i det elastiska området. Den akustoelastiska effekten säger att våghastigheten (longitudinell (VL) och transversell (VT)) är kopplade till materialets elastiska egenskaper och töjning genom de akustoelastiska koefficienterna AL och AT. Om Hookes lag kombineras med den akustoelastiska effekten får man, med några antaganden, en lösning för time-of-flight (TOF) under töjning av materialet. Om man använder hastigheten för en av ultraljudsvågorna har man en differentiell metod som kräver att TOF mäts i varje bult före och efter att bulten dras åt alternativt att man vet den exakta längden av bulten efter åtdragandet. Detta gör att en-vågsmetoden inte är applicerbar för undersökning av redan monterade bultar, till exempel bergbultar. I detta projekt har möjligheterna att använda två-vågsmetoden undersökts vilket undanröjer kravet på vetskap om bultens längd. Två-vågsmetoden använder kvoten mellan TOF på de två olika vågtyperna. Detta möjliggör en skattning av åtdragningskraften i redan monterade bultar. Dock krävs en viss kalibrering då bultar från olika batcher beter sig olika samt att man behöver ha koll på temperaturen i bulten. Det finns en del utmaningar med att bestämma TOF i en ultraljudsvåg som har färdats en lång väg (t.ex. i en bergbult). Utseendet på ultraljudsresponsen ändrar sig något med utbredningsväg (ex. lång bult ger lång gångväg). Utseendet på eko nr.1 kommer således att se lite annorlunda ut än på eko nr. 2. Detta beror på dispersion där olika frekvenser rör sig med olika hastighet genom materialet. Mätningarna som gjordes i detta projekt visade dock att dispersionen var väldigt svag och en jämförelse mellan analysmetoderna ren korskorrelation och korskorrelation av en demodulerad version av ekot i ultraljudet kunde göras. Den senare metoden visade sig korrelera bäst med uppmätta krafter i bulten men den enklare rena korskorrelationen fungerar helt ok i enklare fall.

Resultaten från mätningarna i labbet visade att det är möjligt att, genom att mäta ultraljudshastighet för två vågtyper, beräkna klämkraften i en (berg)bult utan att ha kännedom om bultens längd. Den uppmätta klämkraften visar på en linjär koppling om den plottas som

funktion av TOF-kvoten vilket var väntat. Mätningarna som utfördes i Citybanan på bultar med okänd längd och klämkraft visar väldigt konsistenta resultat. Längden på var enskild bult kunde beräknas och stämde bra överens med specifikationerna på respektive bult. Klämkraften kunde inte beräknas absolut då man skulle behöva kalibrera mot varje bults respektive batch men det man kunde se var att varje bult satt med samma klämkraft i berget. Detta resultat var också förväntat då bultarna sitter väldigt nära varandra och det inte ska vara några skillnader inbördes mellan bultarna med avseende på klämkraft.

Detta projekt har visat att kvoten på TOF för olika vågmoder (longitudinell- och transversell) varierar linjärt med avseende på klämkraft i en bult på bultar upp till 6.6m. Två olika metoder för att skatta kvoten på TOF har utvärderats och används en korskorrelation baserad på demodulerade ultraljudsekon ger anpassningen av en rät linje ett R^2-värde på 0.979.

Nyckelord: bergbultar, tunnel, infrastruktur, oförstörande provning, ofp, ultraljud, ultraljudsmätning, piezo

Summary

Rods and bolts are commonly used as structural elements in a variety of applications. In the automotive and aviation industry they are used in engines and suspensions and in the energy industries they are used in reactor tanks, generator turbines etc. In infrastructural constructions, load bearing rods and bolts are used e.g. in railings and bridges. Concerning underground constructions, rock bolts are used to secure the stability of tunnels. To use a sufficient number of bolts with appropriate specifications and to mount them correctly is therefore of great importance not only for safety but also for economic reasons. Accurate methods for characterizing and monitoring the condition of rock bolts and other structural elements would, in addition to increasing the safety, also enable an optimized use of the bolts as well as the whole structure.

This report presents results from laboratory and a field measurement using a combined longitudinal (L) and transversal (T) wave ultrasonic technique for measuring the tightening force applied to a rock bolt. The time-of-flights (TOF) of either wave mode can be used to estimate the tightening of the bolt, given that the TOF or exact length of the bolt, prior to tightening, is known. In this project we show that by using two wave modes, some of this calibration can be avoided, and that the result depends essentially only on the ratio of TOFs for the two wave modes. Since wave propagation over long distances in rock bolts can be assumed to be dispersive, the main challenge is therefore to accurately estimate the TOF of the two wave modes, by either taking the dispersion into account or by a method which is not too sensitive to limited dispersive effects.

There are different challenges that occur when TOF is to be determined with an ultrasonic wave that has travelled through a long (rock) bolt. The shape of the pulses changes slightly with propagation distance (long bolt -> longer distance). This poses challenges when trying to too estimate TOF between the first end second echo since the dispersion implies the TOF is frequency dependent. The effect is, however, not very prominent and therefore a comparison between a standard cross-correlation technique for TOF estimation to the performance of using the signal envelopes can be made. The results show that the signal envelope method correlates better with the result but the standard cross-correlation method (which is easier) can be sufficient enough in some easier cases.

The laboratory measurements were performed on different kinds of rock bolts; carbon steel (with- and without epoxy) and stainless steel. The bolts mounted inside Citybanan in Stockholm (field test) are carbon steel bolts without epoxy. The bolts in the laboratory were mounted in a rig, were 1.1m bolts could be used, designed to withstand large strain. In the initial measurements a nut (M12) was screwed onto a thread of the bolt with a torque wrench (150-800Nm). In later measurements the rig was modified in order to fit an automatic torque wrench with more control of real applied torque (degrees, force, etc.). This is commercial equipment from Atlas Copco which was one of the partners in the project.

The results from the measurements in laboratory shows that it is possible to, by measuring ultrasonic velocity of two different wave modes, calculate the clamping force in a (rock) bolt). The torque, which is correlated to the clamping force, shows a linear dependence if plotted as a function of TOF-ratio which is as suspected. The measurements made in Citybanan on bolts with unknown length and clamping force showed very consistent results. The length could be

calculated, it differed between 2 meter to 3 meter, and the clamping force was equal in all mounted bolts. The bolts are mounted very close to each other so no large deviation between the bolts was expected and the results from the ultrasonic measurements verified that.

The project has shown that the ratio of the TOFs between transversal- and longitudinal waves varies linearly with the torque (clamping force) applied in a (rock) bolt over a measurement distance equivalent to a bolt length up to 6.6 meters. Two different methods for estimating the TOF ratio were evaluated and the envelope based cross-correlation technique showed that, despite presence of some dispersion, the straight line model could be adopted with an R^2 value of 0.979.

Keywords: rock bolts, tunnels, infrastructure, non-destructive testing, ndt, ultrasound, ultrasonic testing, piezo

Innehållsförteckning

1 Inledning

Hösten 2012 startades forskningsprojektet *Utvärdering av belastade strukturelement* med inriktning att ta fram en ny metod för att oförstörande kunna undersöka klämkraften i en monterad bergbult. Genom detta så skulle man kunna säkerställa bultens status och kunna upptäcka eventuella riskområden i till exempelvis tunnlar.

Projektets mål var att utveckla en metod för att mäta spänningen i belastade stänger, främst för att övervaka dragspänningen i väldigt kritiska stänger som en del av det periodiska underhållet. Metoden kommer också kunna användas för att verifiera produktionsmetoder och optimera montering av bergbultar. Under projektets gång visade det sig att även bultens längd kunde mätas med stor noggrannhet samt att indikationer från defekter kan observeras i signalen. Syftet med en sådan här teknik skulle med andra ord vara två saker: att kunna säkerställa att berget inte genomgått förändringar sedan montering av bultar och att rasrisk skulle vara förestående samt att kunna effektivisera/optimera monteringen av bultar och således inte behöva montera fler än nödvändigt.

I dagsläget finns det ingen kommersiell utrustning som oförstörande kan mäta klämkraft i bergbultar. För att oförstörande undersöka ingjutningskvaliteten hos en ingjuten bult finns en tillgänglig utrustning, Boltometern. Även Boltometern använder sig av ultraljud, men av typen Guided Waves. Guided Waves är förhållandevis lågfrekventa och rör sig mestadels på ytan av objektet man undersöker. Den metod som använts i detta projekt bygger på en annan ultraljudsbaserad metod där man i stället för Guided Waves använder mer högfrekventa ultraljudsvågor som rör sig genom bulken på (inuti) objektet. För att kunna mäta klämkraft, utan kunskap om objektets egenskaper som t.ex. längd, med ultraljud behöver man använda två vågmoder: longitudinell- och transversell. Då kombinationen av dessa vågor används benämns det ofta Två-vågsteknik och här har just denna teknik i kombination med högfrekvent ultraljud används.

2 Bakgrund

Skruvförband, stag och bultar är väldigt vanliga strukturelement i varierande applikationer. I till exempel fordons- och flygindustrin används dessa i motorer och i fjädringar samt i energiindustrin används de exempelvis i reaktortankar och turbiner. I infrastruktursektorn används bultar för att bära last och används till exempel i broar. Angående underjordiska konstruktioner, till exempel tunnlar, används bergbultar för att säkerställa stabiliteten i berget. Att använda ett tillräckligt antal bultar som har tillräckligt bra egenskaper och sedan montera dem korrekt är därför av stor vikt inte bara säkerhetsmässigt utan även av ekonomiska orsaker. Noggranna metoder för att karakterisera och övervaka tillståndet i en bergbult och andra strukturelement skulle, i tillägg till att öka säkerheten, också möjliggöra ett optimerat användande av bultar och hela strukturen där de sitter. Exempelvis skulle livstiden på en tunnel kunna bli anpassad efter strukturens faktiska fysiska tillstånd i stället för, som brukligt är, avgöras på antaganden.

Det finns ingen utrustning tillgänglig kommersiellt idag som använder ultraljud med två vågmoder (Bi-wave) för att bestämma klämkraften i bultar. Det finns däremot några andra ultraljudsmetoder som används för att försöka bestämma tillståndet i bultar. Ett instrument är GRANIT^{TM} som är utvecklat av universitetet i Aberdeen. GRANIT^{TM} använder en accelerometer för att mäta frekvensresponsen i en bult efter det att man har inducerat en puls i bulten med hjälp av en ”lufthammare”. Frekvensresponsen kommer vara olika mellan bultar med olika klämkraft. Uppsamlad data analyseras inte på plats (i fält) utan skickas och analyseras hos GRANIT^{TM} vilket gör metoden tidskrävande. Frekvensresponsen är också känslig för ingjutning vilket medför att denna metod inte lämpar sig så bra för t.ex. bergbultar. En annan utrustning för undersökning av bergbultar som använder sig av ultraljud är Boltometern. Metoden som används bygger på Guided Waves vilket är ultraljud med mycket lägre frekvenser än vad som brukligt används för att undersöka bulken på ett objekt. Guided Waves färdas mestadels på ytan och Boltometern är framtagen för att kontrollera ingjutningskvalitéten på bultarna. Detta skiljer sig signifikant från metoden som använts i detta projekt där ultraljudet har en mycket högre frekvens och färdas mestadels i bulten och ingjutningskvaliteten blir således troligtvis osynlig.

I traditionella ultraljudsundersökningar är ultraljudsproben antingen handhållen eller monterad på motoriserade steg. Proben genererar en ultraljudssignal som propagerar genom objektet och interagerar med materialet. Det finns olika tekniker för att generera ultraljud, några exempel är piezoelektrisk prob, EMAT-prob eller med hjälp utav en laserpuls. Den vanligaste samt i någon mån den enklaste är med hjälp av en piezoelektrisk prob som dock kräver någon form utav kopplingsmedium vilket kan omöjliggöra mätningar i vissa situationer. EMAT är en elektromagnetisk prob som inte kräver kopplingsmedium men den metoden har väldigt svårt att generera olika typer av vågor samt är betydligt svagare än piezo-metoden vilket försvårar mätningar på långa/tjocka objekt. Att inducera ultraljud med en laserpuls har många fördelar då tekniken är helt kontaktfri men dessa system är mycket mer kostsamma, komplicerade att använda och är

den ”svagaste” av de nämnda här och kan således inte användas på till exempel bergbultar. I detta projekt har piezo- samt EMAT-tekniken utvärderats och använts under mätningarna.

3 Teori

3.1 Grundläggande idé

Ultraljudsmetoden som använts för att beräkna resultaten i detta projekt härrör från en kombination av två fenomen: Hookes lag och den akustoelastiska effekten. Hookes lag säger att töjningen av en bult är direkt proportionell mot lasten applicerad på bulten. Detta är sant så länge bulten är under plastisk deformation. Den akustoelastiska effekten säger att ultraljudvågens hastighet (longitudinell hastighet V_L och transversell hastighet V_T) är kopplade till materialets elastiska karakteristik och spänning (σ) genom de akustoelastiska koefficienterna A_L och A_T [1] [2].

Hookes lag säger att:

$$L_\sigma = L_e\left(10\frac{\sigma}{E}\right) \qquad [1]$$

$$L_0 = L_e + L_h \qquad [2]$$

där L_0 och L_σ är den totala längden på bulten utan spänning och efter att spänning σ, respektive L_e är längden på den del som är påverkad av spänning, L_h är den opåverkade delen och E är Youngs modul.

Den akustoelastiska effekten säger att:

$$V_{L,T}^{\sigma} = V_{L,T}^{0}\left(10A_{L,T^{\sigma}}\right) \qquad [3]$$

$$V_{L,T}^{0} = \frac{2L_0}{T_{L,T}^{0}} \qquad [4]$$

där $V^0_{L,T}$ och $V^\sigma_{L,T}$ är hastigheten på ultraljudsvågen genom bulten vid spänning noll- respektive spänning σ och $A_{L,T}$ är de akustoelastiska koefficienterna. L,T betyder att uttrycket gäller för både longitudinella (L)- och transversella (T) vågor.

Om man kombinerar Hookes lag och den akustoelastiska effekten samt gör antagandet att $A_{L,T\sigma} << 1$ och att $(1+A_{L,T\sigma})-1 \approx (1+A_{L,T\sigma})$ får man en lösning för Time-of-Flight (TOF) under spänning enligt:

$$T_{L,T}^{\sigma} \approx T_{L,T}^{0}\left(\frac{L_e}{L_0}\left(E^{-1} - A_{L,T}\right)\sigma + 1\right) \qquad [5]$$

Om en en-vågsteknik (antingen L- eller T-våg) används måste några kalibreringar göras för att kunna beräkna spänningen i bulten [3]. Om man använder en longitudinell våg kan kraften F som appliceras på en bult bestämmas genom

$$F = \frac{1}{B}(T_L^{\sigma} - T_L^{0}) \qquad [6]$$

där B är en konstant som bestämmas genom kalibrering samt där T^0_L och T^σ_L är uppmätt TOF före respektive efter åtdragning av bulten.

En-vågsmetoden är en differentiell metod som kräver att TOF mäts med ultraljud i varje bult före- och efter åtdragning eller att den exakta längden på bulten är känd om bulten ska undersökas efter åtdragning. Detta gör att en-vågsmetoden är olämplig och i verkligheten omöjlig att använda för undersökning av monterade bergbultar där till exempel längden på bulten är okänd (med den noggrannhet som behövs).

Två-vågsmetoden använder kvoten mellan TOF för de olika vågmoderna (longitudinell och transversell). Kvoten av denna TOF, som ges av ekvation 5, blir

$$\frac{T_T^\sigma}{T_L^\sigma} \approx \frac{T_T^0 L_e (E^{-1} - A_T)\sigma + 1}{T_L^0 L_e (E^{-1} - A_L)\sigma + 1} \approx \frac{T_T^0 L_e}{T_L^0 L_e}(A_L - A_T)\sigma + \frac{T_T^\sigma}{T_L^\sigma} \qquad [7]$$

Ekvation 7 ger i sin tur

$$\frac{T_T^\sigma}{T_L^\sigma} \approx BF + C \xrightarrow{yields} F \approx \frac{\frac{T_T^\sigma}{T_L^\sigma} - C}{B} \qquad [8]$$

med

$$C = \frac{T_T^0}{T_L^0} = \frac{V_T^0}{V_L^0} \qquad [9]$$

Så, om man kan mäta TOF för båda vågmoderna (L och T) är behovet av att veta den exakta längden och behovet av att mäta före åtdragning eliminerad. Detta möjliggör med andra ord estimering av åtdragningskraften (klämkraft F) i bultar som redan är monterade. Man måste dock göra några kalibreringsmätningar innan. För att komma åt konstanterna B och C, se Ekvation 9, behöver man kalibrera TOF på varje batch av bultar.

3.2 Bestämning av TOF

Denna del beskriver lite av utmaningarna med att bestämma TOF för ultraljudspulser som har propagerat genom ett långt objekt (alternativt under lång tid). Resultatet från en av mätningarna i labbet ligger som grund för att enklare kunna beskriva vad som händer med signalen och vilka svårigheter som dyker upp då man mäter på en lång bult.

Figur 1 visar den uppmätta ultraljudssignalen från en mätning i labbet. Bulten är obelastad och är heller inte ingjuten, se kapitel Experiment för mer detaljerad beskrivning av själva labbuppställningen. I figurerna ser vi tre ekon för den longitudinella vågen och två pulser för den transversella vågen. Figur 2 och Figur 3 visar inzoomande ekon, första och andra longitudinella och transversella ekot, från Figur 1 där de heldragna linjerna är den anpassade formen på ekot. I de inzoomade ekona kan man se att formen på ekona ändras något då pulsen färdas längre i ett objekt, se exempelvis de transvesella vågorna i Figur 3. Detta komplicerar beräkningen då man ska uppskatta TOF mellan första och andra ekot eftersom dipersionen innebär att TOF är frekvensberoende. Här är dock effekten ganska liten och därför gjordes en jämförelse mellan två metoder för att bestämma TOF: standard korskorrelation och korskorrelation där man använder sig av formen på respektive eko.

Låt $p_1[n]$, $p_2[n]$, $s_1[n]$ och $s_2[n]$ vara den digitaliserade versionen av första respektive andra ekot för den longitudinella (p)- samt den transversella vågen (s) och låt η_T och η_L vara diskreta ekvivalenter till tidsförskjutningen T_T ock T_L. Uppgiften blir således att lösa η_T och η_L, det vill säga tidsdifferensen mellan $p_1[n]$ och $p_2[n]$ samt $s_1[n]$ och $s_2[n]$. Eftersom vi primärt är intresserade av att bestämma kvoten, TOFR, mellan uppskattningen av TOF

$$TOFR = \frac{T_T}{T_L} \approx \frac{\eta_T}{\eta_L} \qquad [10]$$

kan TOF uppskattas antingen i sampel eller i sekunder.

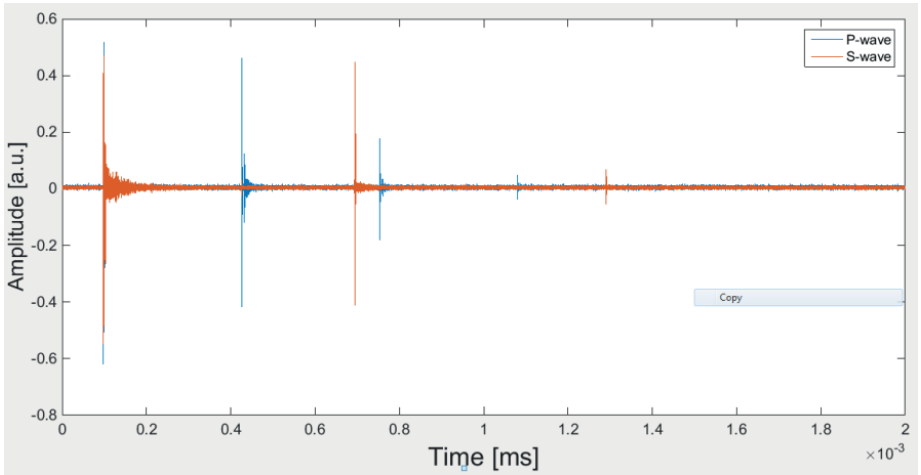

Figur 1 Uppmätt ultraljudssignal i en 1.1 meter lång, obelastad, bult. Röd kurva: longitudinell signal, Blå kurva: transversell signal.

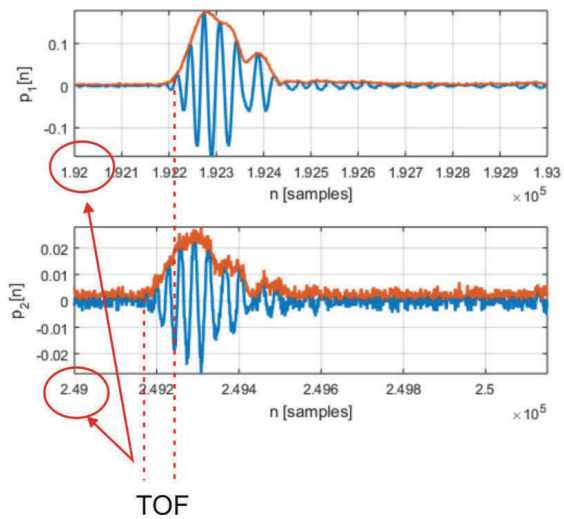

Figur 2 Inzoomad version av första- och andra longitudinella ekot (blå kurvor) i Figur 1 tillsammans med dess demodulerade motsvarigheter (röda kurvor).

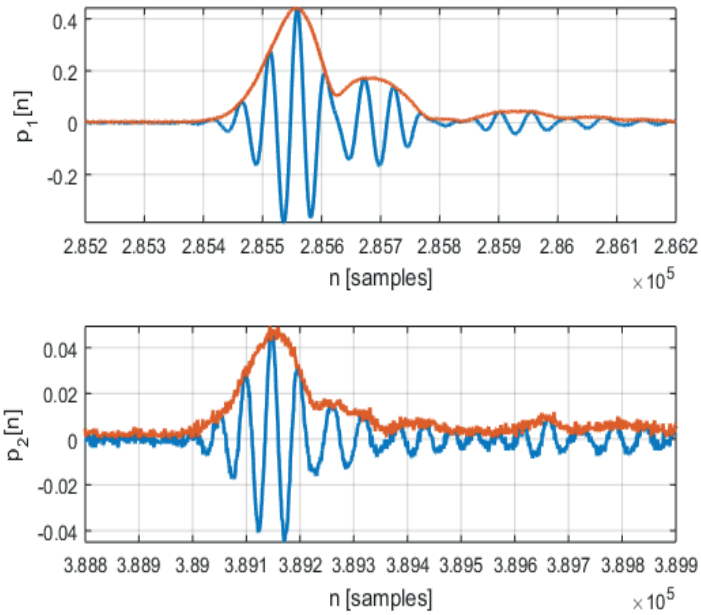

Figur 3 Inzoomad version av första- och andra transversella ekot (blå kurvor) i Figur 1 tillsammans med dess demodulerade motsvarigheter (röda kurvor).

3.2.1 Standardkorskorrelation

Antag att det andra ekot för den longitudinella- och den transversella vågen, $p_2[n]$ eller $s_2[n]$, enbart är skalad och tidsförskjutna versioner av de första ekona, $p_1[n]$, $s_1[n]$, så att

$$p_2[n] = ap_1[n - \eta_L] + w_1[n] \quad [11]$$
$$s_2[n] = bs_1[n - \eta_T] + w_2[n] \quad [12]$$

där $w_1[n]$ och $w_2[n]$ antas Gaussiskt brus och a och b reella skalärer så kommer ”maximum likelihood” uppskattningen av tidsförskjutningen vara [ekv.4]

$$\eta_L^* = arg_{\eta L} max \sum_{n=0}^{N-1} p_1[n]p2[n + \eta_L] \quad [13]$$
$$\eta_T^* = arg_{\eta T} max \sum_{n=0}^{N-1} s_1[n]s2[n + \eta_T] \quad [14]$$

Time-of-Flight kvoten baserad på standard-korskorrelation, TOFR enligt Ekvation 10, kan således bestämmas som kvoten av Ekvation 14 och Ekvation 13.

3.2.2 Korskorrelation av demodulerade pulser

Om dispersion gör sig synlig i signalen blir inte antagandena i Ekvation 11 och Ekvation 12 helt uppfyllda och därför blir TOF mellan pulserna inte längre en skalär utan ska definieras som en funktion som beror av frekvens. Detta skulle involvera en uppskattning av TOF i frekvensdomänen vilket ökar beräkningskomplexiteten märkbart för metoden. Här utvärderas i stället om en korskorrelation där man anpassar formen på pulsen är tillräcklig i fall där man har väldigt liten dispersion. Formen på en signal x[n] kan beräknas som

$$x^*[n] = abs(x[n] + j\mathrm{H}\{x[n]\}) \qquad [15]$$

där $\mathrm{H}\{\cdot\}$ är Hilbert transformen. Låt $\tilde{}$ vara operationen för att demodulera pulserna, vilket då ger att TOF-uppskattningen baserad på korskorrelation av demodulerade pulser blir

$$\eta_L^{*e} = arg_{\eta_L^e} max \sum_{n=0}^{N-1} p_1^*[n] p_2^*[n + \eta_L^e] \qquad [16]$$

$$\eta_T^{*e} = arg_{\eta_T^e} max \sum_{n=0}^{N-1} s_1^*[n] s_2^*[n + \eta_T^e] \qquad [17]$$

Kvoten mellan TOF kommer nu i stället från TOF-uppskattningarna $\eta^{*e}{}_T$ och $\eta^{*e}{}_T$ där *e* bara säger att den är ”baserad på dem demodulerade pulsen”.

För att summera har vi nu två formler för att uppskatta kvoten definierad i Ekvation 8. Den första, baserad på standardkorskorrelation

$$TOFR = \frac{T_T^\sigma}{T_L^\sigma} = \frac{\eta_T^*}{\eta_L^*} \qquad [18]$$

och den andra baserad på en korskorrelation av demodulerade pulser

$$TOFR^e = \frac{T_T^\sigma}{T_L^\sigma} = \frac{\eta_T^{*e}}{\eta_L^{*e}} \qquad [19]$$

4 Experiment

Alla experiment och mätningar utfördes hos Swerea KIMAB i Kista. Ultraljudsutrustningen bestod av ett SNAP-mätsystem från Ritec Inc. SNAP-systemet har två toneburst pulskällor vardera med en maximal uteffekt på 5 KW RMS @ 0.3% intermittens. Optimala frekvensområdet är 0.25-7 MHz. Om man, som i mätningarna i detta projekt, använder piezo-elektriska prober behövs en 50 Ω terminator (RT-50) efter utgången från SNAP-systemet. En variabel högeffektssdämpare (RA-30) är monterad före en diplexer (RDX-6), denna används om systemet körs i puls-eko mod. Den mottagna signalen från proben förstärks i en hög-impedans förstärkare (PAS 0.1-40) innan den samlas in i SNAP-systemet. En schematisk bild av uppställningen visas i Figur 4. Ultraljudssignalen togs upp och samplades med ett digitalt oscilloskop, PicoScope 6000, vilket har en samplingsfrekvens på 2.5 GS/s. Datafilerna sparades i PicoScope´s egna mjukvara med antingen MATLAB- eller LabVIEW-format (i senare delen av projektet endast MATLAB-format). Olika typer av ultraljudsprober användes initialt i projektet men tillslut stort det klart att den bästa för ändamålet var en prob från Olympus, modell D7054, som har en diameter på 13 mm (0.5”), två D-formade element (en för longitudinella- och en för transversella vågor) samt en centerfrekvens på 5 MHz.

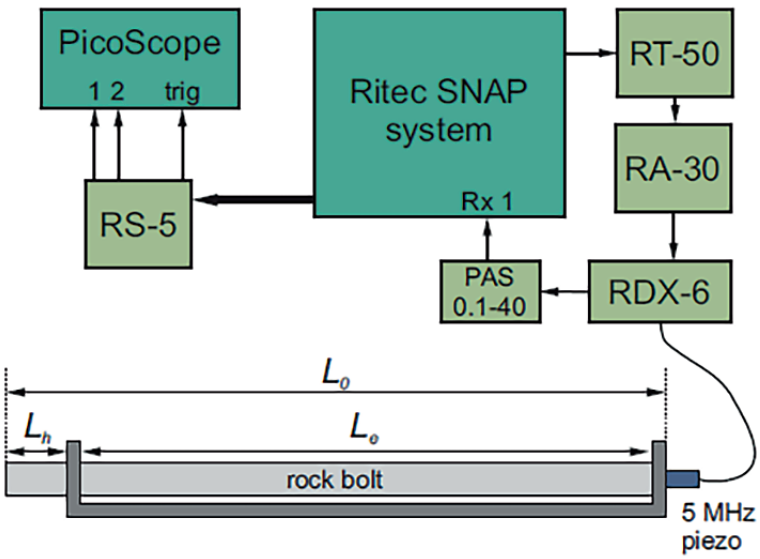

Figur 4 Uppställning för hårdvara under experiment/mätningar i labb.

De första mätningarna som gjordes i projektet med SNAP-systemet utfördes på olastade bultar av olika längd. Detta var för att få en uppfattning om vad SNAP-systemet, proberna och insamlingsdelen var kapabla till och då få en känsla för om effekten var tillräcklig för att mäta på långa bergbultar. Även försök med olika frekvenser gjordes (0.5, 1 och 5 MHz) och det visade sig snabbt att 5 MHz var den mest lämpliga frekvensen (av de tre

nämnda) för bergbultar. Figur 5 visar ultraljudsresponsen från den första mätningen med SNAP-systemet. Bulten är olastad och i sammanhanget bara 154mm lång men att så många ekon är synliga visar ändå på att det är möjligt att nå långt med ultraljud i en bergbult. Alla mätningar i detta projekt är gjorda med en så kallad ”puls-eko” uppställning vilket innebär att samma prob är både sändare- och givare av ultraljud. I fallet nedan i Figur 5 innebär det att första ekot runt 50µs är responsen av ultraljudet då det färdats 2 x 154 mm = 308 mm. I Figur 5 kan man urskilja nio ekon vilket representerar en bultände på 2772 mm (9 x 308 mm). Denna första mätning gav hopp om att det skulle vara möjligt att mäta de längder som behövs för att kunna kontrollera monterade bergbultar.

Metoden, som beskrivits i kapitlet Teori, för att bestämma spänning/klämkraft i en bult kräver två typer av ultraljudsvågor och därav var det av stor vikt att optimera utrustningen så att tillräckligt med energi fortplantar sig in i bulten för att mätningar på långa bergbultar skulle vara möjlig. Skjuv-vågen (S-våg) är svårare att inducera i ett objekt då det kräver att proben sitter fast/klibbar mot objektet. Således måste en speciell typ av kopplingsmedium användas om piezoelektriska prober används. I detta projekt användes ett kommersiellt kopplingsmedium (kan liknas vid melass) från Olympus som är optimerat för att användas till inducering av S-vågor. Att bara lyckas mäta på långa bultar med P-våg hade inte hjälpt detta projekt och på grund av den svagare S-vågen så fanns en oro om att det inte skulle gå att mäta på allt för långa bergbultar. Figur 7 och Figur 8 visar ultraljudsresponsen från P- respektive S-vågor på en bult med länden 1.97 meter. Där kan man se att det är fyra ekon synliga för P-vågen (Figur 7) och tre ekon för S-vågen (Figur 8) vilket representerar 16 meter respektive 12 meter väg för ultraljudet. En 8 meter respektive 6 meter lång bult skulle således ge ett eko var. Dock är mätningarna i Figur 5-Figur 8 uppmätta i labb på bultar som är frilagda, det vill säga inte ingjutna. En ingjuten bult kommer tappa (”läcka”) energi till omgivningen på grund av att den akustiska impedansen mellan bult och betong/berg är mycket närmare varandra än bult kontra luft. Luft som omgivning är nästa optimalt för bevarande av energi och ger nästan ingen förlust till omgivningen. Merparten av förlusten i en sådan mätning kommer från ultraljudets studsar i ändarna samt stålets mikrostruktur. Resultaten från dessa mätningar säger således något om hur långa bultar det ens är möjligt att mäta på med den utrustning som används här i projektet.

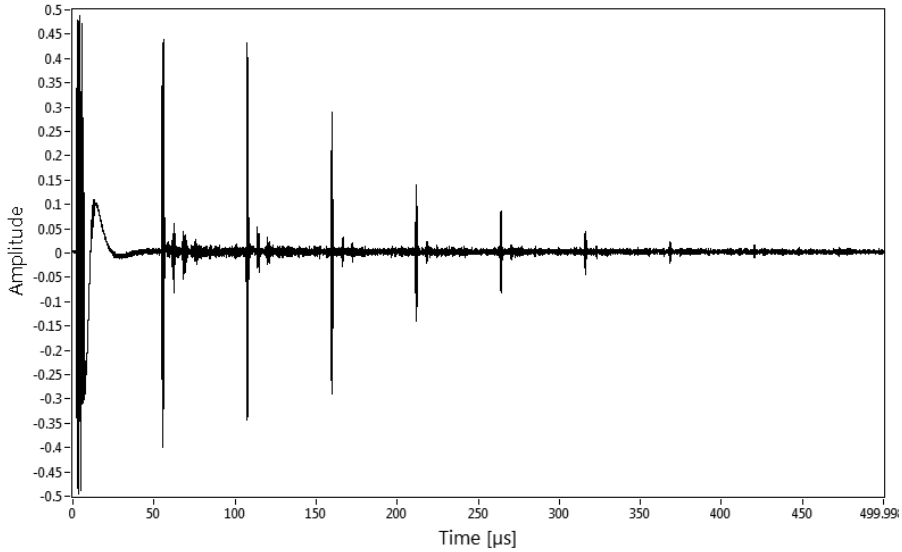

*Figur 5 Första mätningen på bult med SNAP-systemet. Längd på bulten var 154mm och varje eko representerar responsen då ultraljudet rört sig fram-och-tillbaka i bulten. I första ekot har således ultraljudet rört sig 2*154mm, andra ekot 4*154mm etc.*

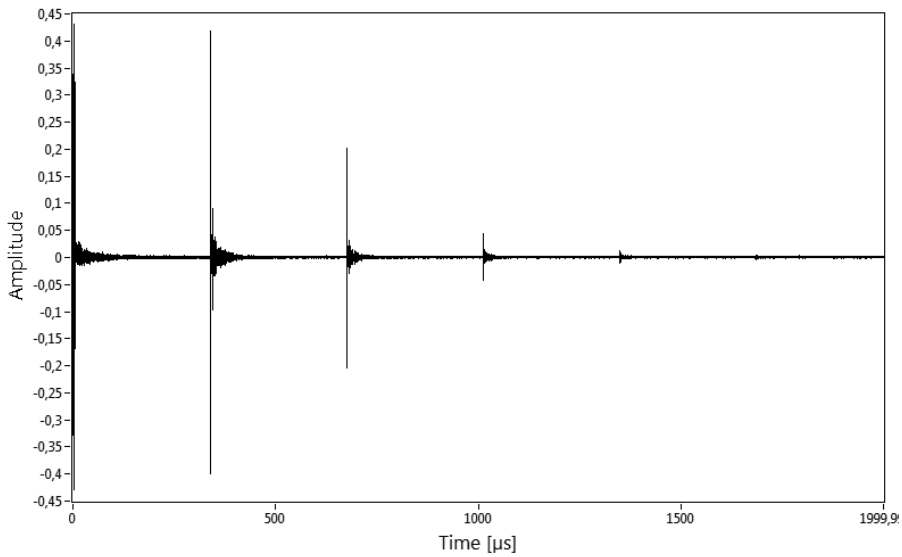

Figur 6 Ultraljudsrespons (P-våg) från mätning på 1 meter lång bergbult i labb.

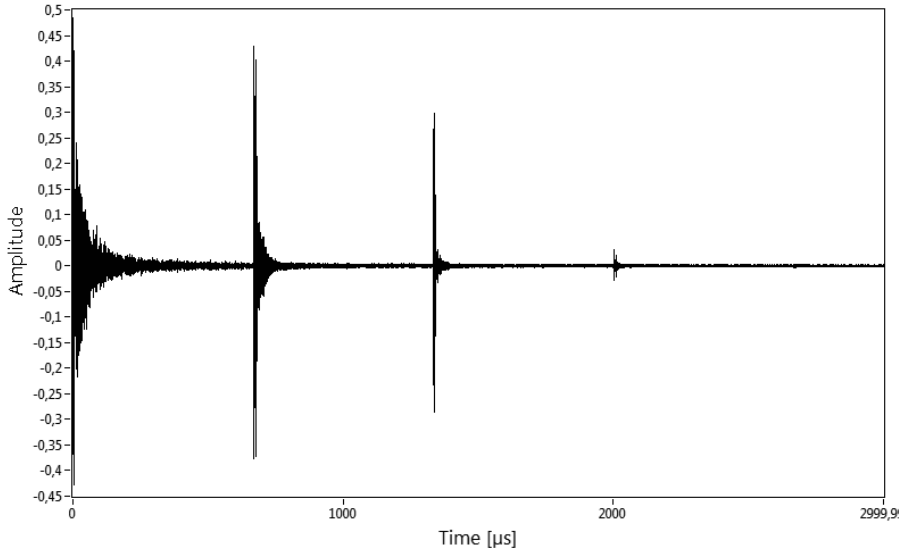

Figur 7. Ultraljudsrespons (P-våg) från mätning på 1.97 meter lång bergbult. Fyra ekon kan urskiljas vilket ger 16 meter gångväg för ultraljudsvågen.

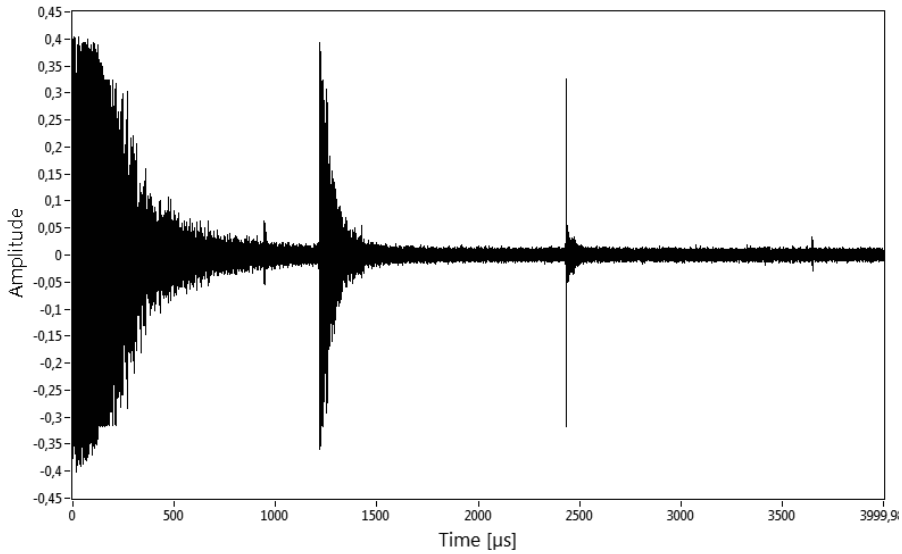

Figur 8 Ultraljudsrespons (S-våg) från mätning på 1.97 meter lång bergbult. Tre ekon kan urskiljas vilket motsvarar 12 meter gångväg för ultraljudsvågen.

Efter ett flertal mätningar på längre och längre bultar och optimering av ultraljudssignalen konstruerades en rigg för att kontrollerat kunna belasta bergbultar och samtidigt mäta på dem med ultraljud. Det konstruerades olika riggar för detta ändamål där de första varianterna hade sina begränsningar och var i behov av förbättring.

4.1.1 Rigg nr.1

Den första versionen av riggen för belastning av bergbultar visas schematiskt i Figur 9. Man belastade bergbulten genom att skruva in en mindre bult in mot den uppmonterade och fixa bergbulten. Man tryckte således ihop bergbulten vilket inte är riktigt representativt för ”verkligheten” för en monterad bergbult där den snarare skulle uppleva en dragkraft vid till exempel skjuvningar i berget. Fysiken bakom vad som händer med ultraljudet i objektet då det är under last är dock detsamma oavsett tryck- eller drag och därför användes initialt denna något enklare uppställning då metoden skulle verifieras med kontrollerade dragningar av bergbulten.

Något som tidigt hände vid belastning av bergbulten i denna version av rigg var att själva riggen inte klarade kraften som lastades på bulten. Riggens sidor ”säckade ihop” och botten böjde sig under belastning (~200Nm), se Figur 10.

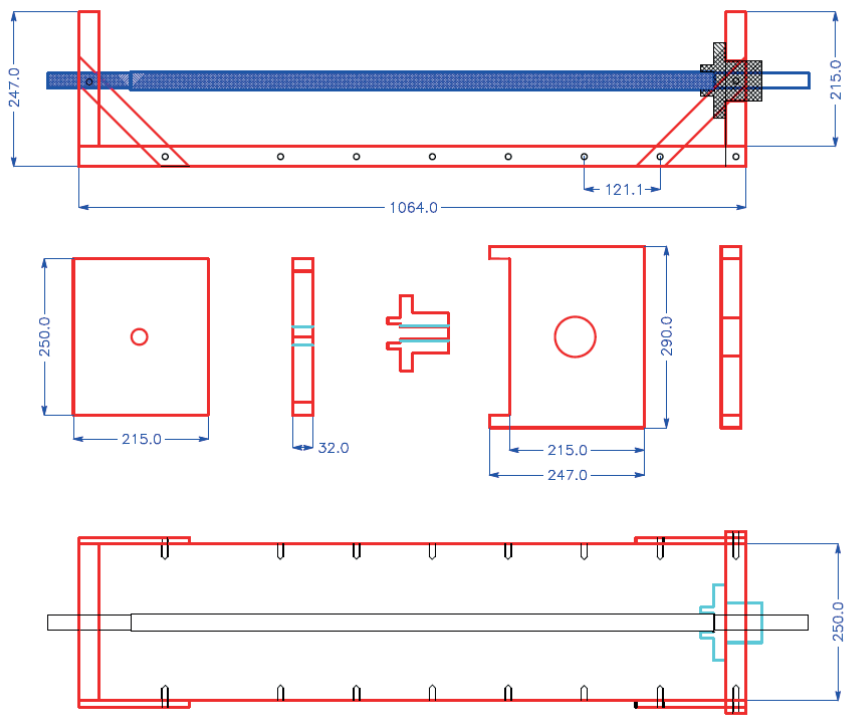

Figur 9 Schematisk bild av bergbultsrigg - version 1.

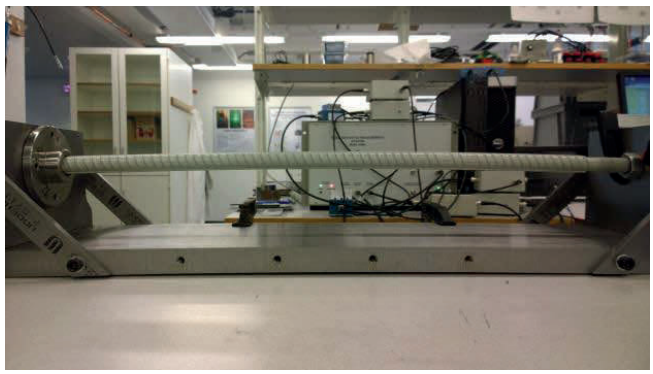

Figur 10 Version 1 av bergbultsrigg. Man ser tydligt hur botten bågnar under belastning, här redan vid ~200Nm.

4.1.2 Rigg nr.2

Version 2 av riggen var en modifiering av version 1. Två stycken rejäla överliggande stag monterades för att allt skulle stabilisera sig och förhoppningsvis hålla ihop bättre under belastning. Här belastade man på likadant sätt som i version 1, det vill säga genom att skruva in en mindre (kortare, samma diameter dock) bult på bergbulten och således komprimera bergbulten.

Denna version visade sig vara stabilare och hållbarare än version 1, vilket såklart var väntat, men den höll ändå inte måtten vid högre belastningar. I Figur 11 ser man riggen under belastning och det syns tydligt hur de övre stabiliserande stagen tryckts ihop och bågnar. Ett annat problem som uppstod vid höga belastningar med denna rigg syns i Figur 12. Gängorna i bulten som drogs med momentnyckeln klarade inte påfrestningarna utan havererade. Detta är lite lurigt då man inte ser vad som händer under själva åtdragningen men blev väldigt tydligt så snart man började lätta på kraften. I Figur 13, som visar moment (enligt inställning på momentnyckel) som funktion av kvoten mellan skjuv- och longitudinell våghastighet, ser man också tydligt att något händer som inte är kopplat till den verkliga kraften i den monterade bulten. Det ska vara ett linjärt samband men redan vid tredje mätpunkten avviker punkterna från ett linjärt samband. I detta fall är det en kombination av att riggen inte håller måttet och att gängorna i bulten går sönder.

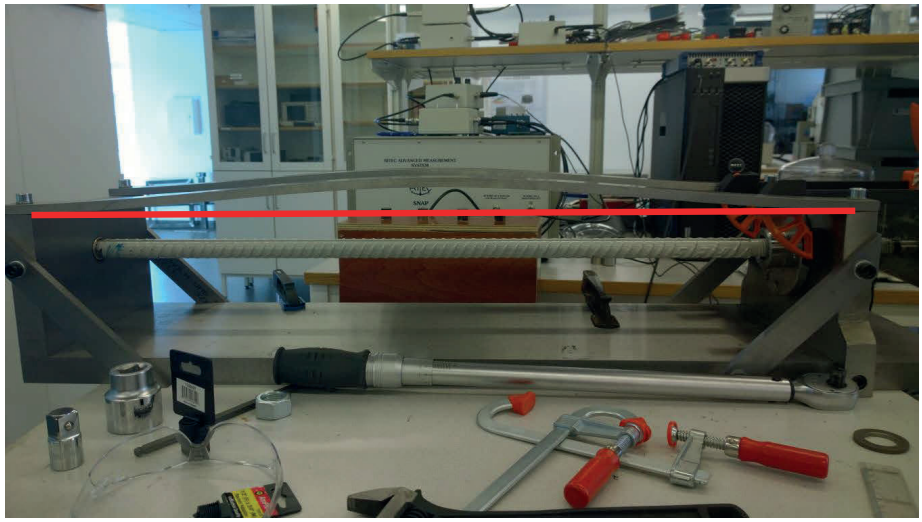

Figur 11 Utseende rigg version 2 under belastning. Man ser tydligt på de överliggande stagen att riggen säckar ihop (jmf. stag med inritad/rak röd linje).

Figur 12 Bult som havererat under belastning. Den höga belastningen gör att gängorna inte orkar hålla emot längre. Resultatet blev att momentnyckeln upplevde en mycket högre kraft än vad som var verkligt, den upplevda kraften var i stället friktion på grund av trasig gänga.

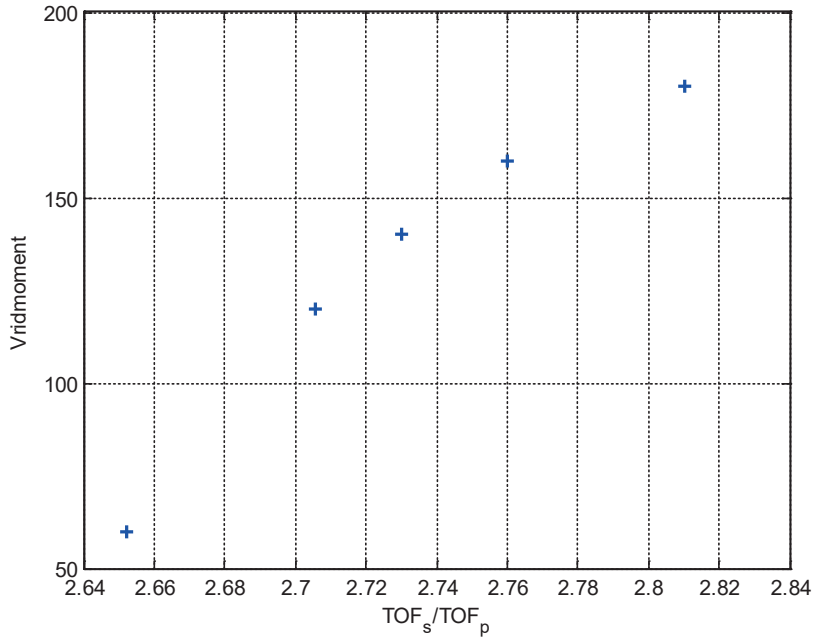

Figur 13 Resultat från ultraljudsmätningar på belastad bult där bulten är monterad i rigg version 2. Vridmoment (enligt inställning på momentnyckel) är plottad som funktion av kvot mellan skjuv- och longitudinell våghastighet. Man ser tydligt att resultatet inte är linjärt och att mätresultaten avviker från en rät linje redan vid den tredje mätpunkten.

4.1.3 Rigg nr.3

I den tredje versionen på riggen, se Figur 14, så var lösningen så att bergbulten gängades på båda sidorna och fastmonterades med bult (M24) på riggen. På så sätt kunde man dra i bergbulten istället för att trycka ihop den och på så sätt minimera belastningarna på själva riggen samt gängorna. Detta förfarande är dessutom mer likt verkligheten då monterade bergbultar i de allra flesta fall upplever dragkrafter och inte tryckkrafter. För ultraljudsmetoden som används här spelar det dock ingen roll om det är tryck- eller dragkraft. Även här smörjdes alla gängor och bultar väl för att minimera alla typer av friktion.

Figur 14 Version 3 av rigg. Till skillnad mot tidigare riggar drar man här i bergbulten genom att skruva in muttern på änden.

4.1.4 Olika typer av bergbultar

Mätningar utfördes på olika typer av bergbultar: rostfria, epoxybelagda kolstålsbultar samt kolstålsbultar utan beläggning. Signalkvalitéten var lika bra för de två bulttyperna av kolstål och epoxybeläggningen påverkade inte ultraljudet överhuvudtaget (inte mätbart här i alla fall). Resultatet från försöken på rostfria bergbultar var däremot av sämre kvalité. Det gjordes ett flertal försök med olika prober (frekvenser) och inställningar på SNAP-systemet men det var i de rostfria bergbultarna inte möjligt att få igenom något ultraljudseko ens i en 10 cm lång bergbult. Detta kan jämföras med fyra ekon i en 110cm lång kolstålsbult. Den faktiska orsaken till detta var inte helt klar då mätningarna utfördes men det fanns en vetskap om riskerna med ultraljudsmätningar på rostfritt material.

Vi valde att polera upp en av ytorna på den rostfria bergbulten för att genom mikroskopiska studier kunna få en uppfattning om hur mikrostrukturen i bergbulten såg ut och om det kunde vara en förklaring till svårigheten att få ultraljudssignalen att transportera sig genom materialet. Mikroskopet skannades i steg om 0.5µm över en yta som var cirka 0.3mm x 0.3mm. Mikroskopbilderna kan ses i Figur 15 där den vänstra bilden visar fördelningen austenit (blå del) och ferrit (röd del). Sidorna är 300µm x 300µm och från det kan man dra slutsatsen att dämpningen av ultraljudssignalen i alla fall inte beror på kornstorlek/struktur i materialet då respektive område (se Figur 15) är i storleksordningen tiotalet mikrometer vilket inte är ett problem för de ultraljudsfrekvenser som testades här. Så frågan kvarstod: varför kunde inte ultraljudssignalen färdas genom bergbulten?

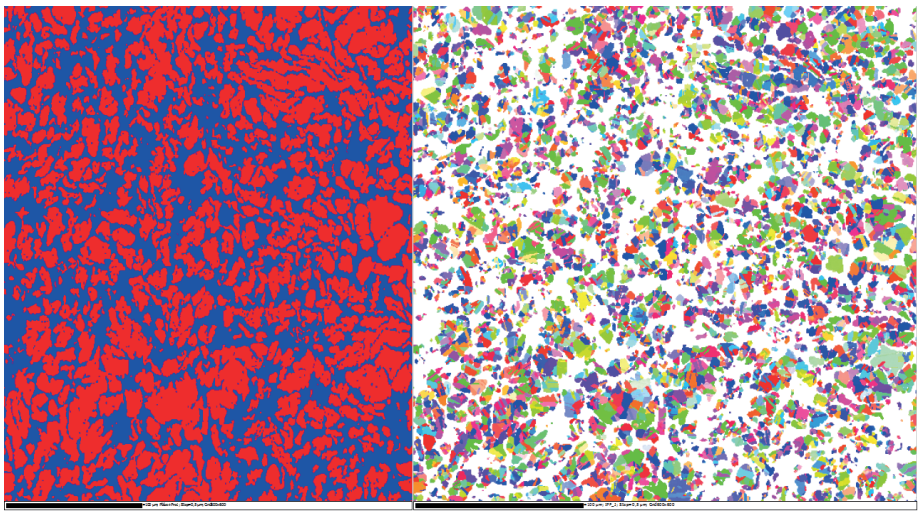

Figur 15 Mikroskopbilder av toppen på bergbulten gjord av rostfritt material. Bilderna är tagna ”sett från änden”. Kornstorlek och struktur i materialet är i storleksordningen några tiotal mikrometer och borde inte påverka ultraljudssignalen så kraftigt som mätningarna visade.

Efter diskussioner med personer som har stor kunskap om rostfritt stål, tillverkningsprocesser etc. så fattades beslutet att också snitta den rostfria bergbulten längs längdriktning för att se om förklaringen var så enkel att mikrostrukturen (sett från ett håll) skiljer sig märkbart beroende på från vilket håll man tittar (anisotrop). Resultatet, som kan ses i Figur 16, visade på en synnerligen stor skillnad i mikrostrukturen och ger en tydlig förklaring till varför ultraljudssignalen inte kan färdas någon längre sträcka i bulten. Dessa bilder är cirka 500µm x 750µm stora och man kan se att de långa delarna är flera hundra mikrometer långa vilket är direkt förödande för ultraljud på megahertz-skalan. Det ska tilläggas att det inte är kornen som är utdragna åt ett håll utan att det är faserna (ferrit/austenit) som är separerade i stråk som är flera millimeter långa.

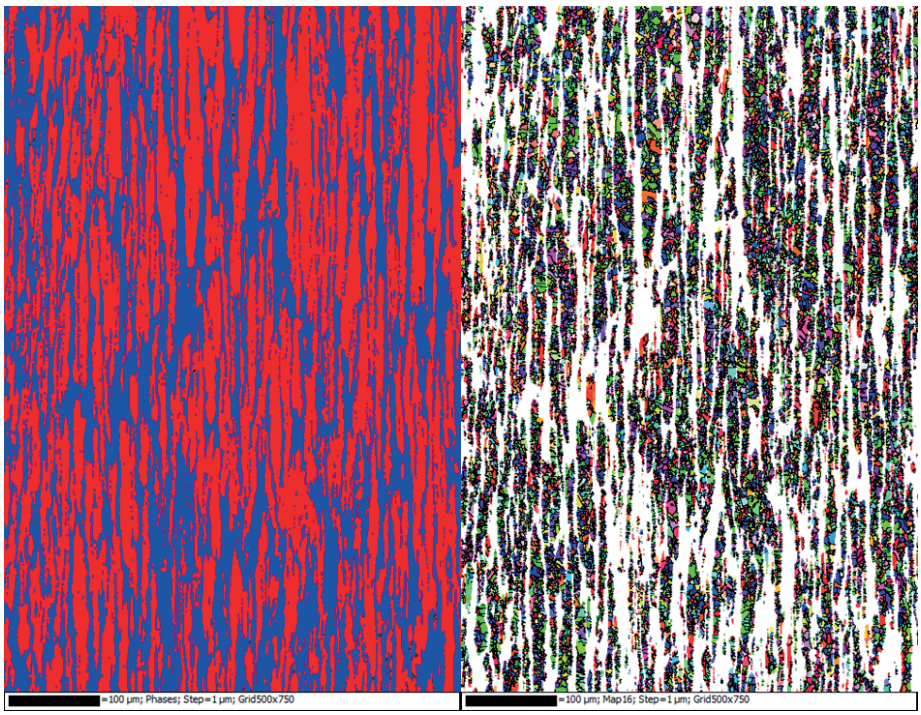

Figur 16 Mikroskopbilder från snitt längs med bergbulten gjord av rostfritt material. Bilderna är med andra ord tagna "sett frånsidan". Kornstorleken är även här liten och faserna (austenit/ferrit) är separerade i stråk som sträcker sig flera millimeter. Detta visar tydligt på orsaken till varför ultraljudssignalen inte orkar igenom ens korta sträckor av bergbulten. då millimeterlånga strukturer är direkt förödande för ultraljud i megahertz-regionen.

5 Resultat

5.1 Mätningar i labb

Under mätningarna i labb då bergbultar under last skulle undersökas så användes två förfaranden för att, mer eller mindre, kontrollerat ha kontroll på lasten i bulten: en momentnyckel av märke AmPro som kan ställas in på moment 150-800Nm (intervall 50Nm) samt en automatisk skruvdragare från Atlas Copco (modell PowerMACS) som monterades på bultriggen. Den automatiska skruvdragaren användes i de senare försöken och har en mycket större kontroll på kraft, grader etc. än momentnyckeln där den mekaniska enheten som ställer önskat moment är mycket grov samt att man egentligen inte har någon koll på om applicerad kraft är i bergbulten eller om det bara är friktion i gängorna. Hur skruvdragaren från Atlas Copco monterades i riggen visas i Figur 17. PowerMACS styrs med en mjukvara utvecklad av Atlas Copco. Den version av mjukvaran som användes i detta projekt innefattade mängder med inställningar och möjligheter som inte användes här. Installationen var lite knepig samt krävde ett operativsystem av äldre snitt (Windows XP) men projektet fick låna en dator från Atlas Copco för detta ändamål.

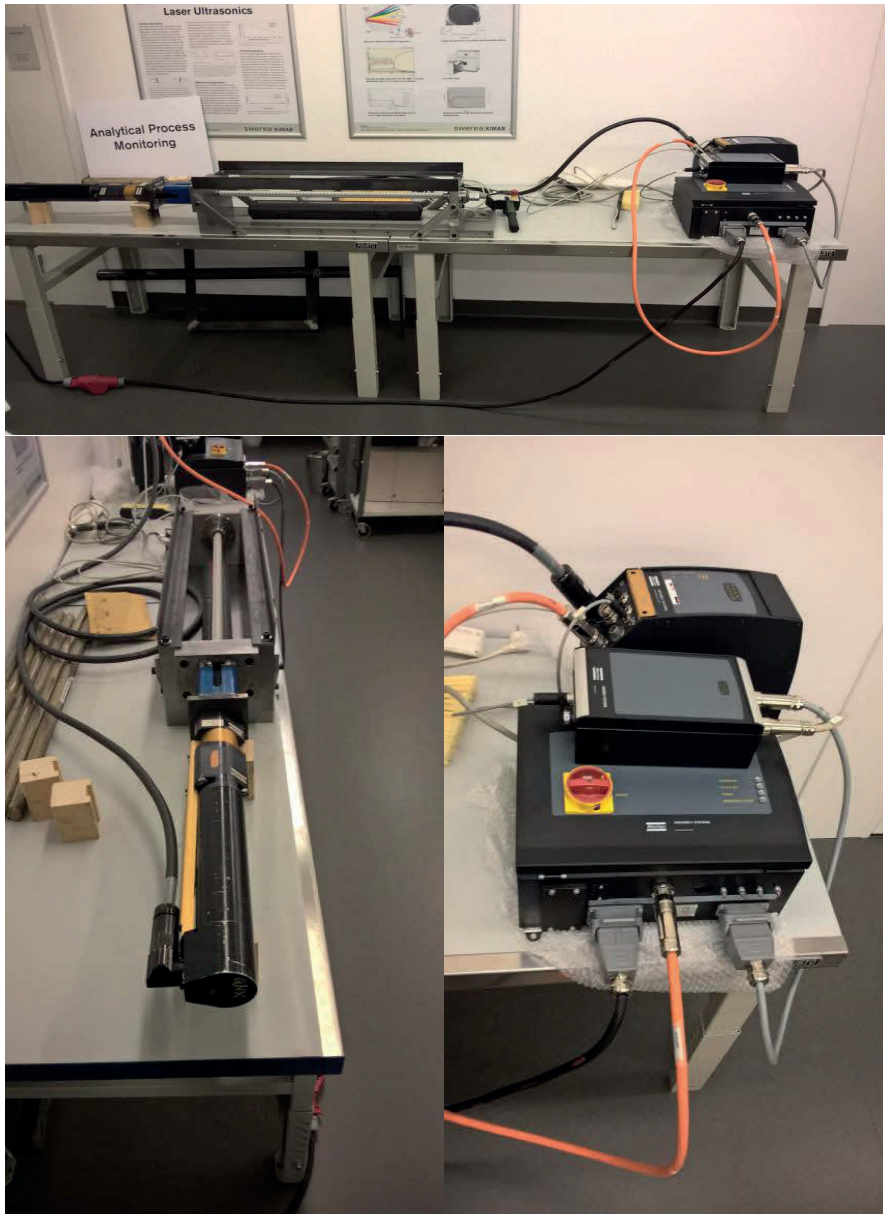

Figur 17 Bilder på automatiska skruvdragaren från Atlas Copco monterades i riggen. Bilden längst upp visar uppställningen från sidan, nere till vänster är själva skruvanordningen som är monterad så att den skruvar in en bult och således drar i själva bergbulten. Bilden nere till höger visar styrenheterna samt kraftaggregatet.

Det utfördes ett flertal mätningar på monterade bergbultar med PowerMACS och det framstod ganska omgående att dessa mätningar hade en klart större tillförlitlighetsgrad jämfört med de tidigare mätningarna utförda med momentnyckel. PowerMACS möjliggör mätningar där man styr på vinkel i stället för kraft (uppmätt med tryckgivare) vilket generellt också är bättre och tillförlitligare vid denna typ av mätningar. I Figur 18 visar en mätning med PowerMACS där momentet plottas som funktion av grader. Här har muttern skruvats in med steg om 15 grader upp till maxtaket vilket är då motor inte orkar skruva längre (cirka 600Nm). Systemet visar sig väldigt linjärt från olastat till 600Nm vilket också R^2-värdet visar.

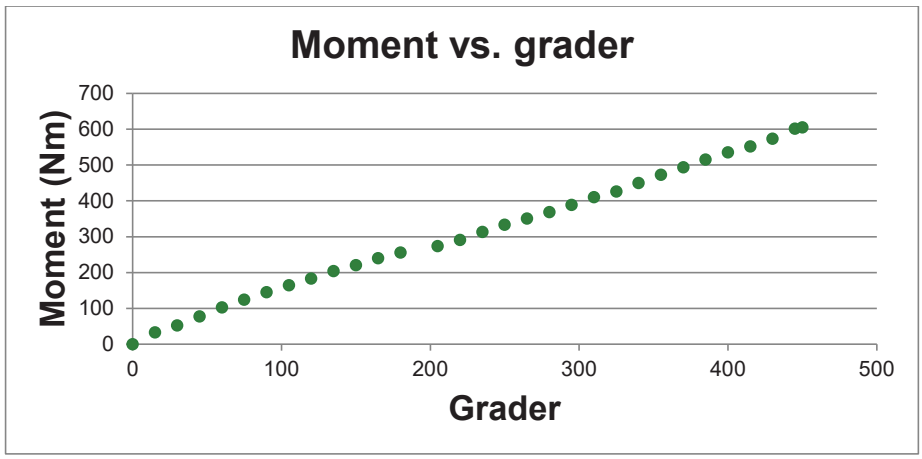

Figur 18 Mätning med PowerMACS där moment plottas som funktion av grader (inskruvad mutter).

Vid varje lastpunkt med PowerMACS-systemet utfördes 32 stycken mätningar (”skott”). Det går väldigt snabbt att göra dessa mätningar men tyvärr sattes denna begränsning av mjukvaran som skötte uppsamlingen. Mjukvaran var PicoScopes egenutvecklade men om man vill sampla data med, i detta fall, tillräckligt hög samplingsfrekvens så sattes begränsningen till 32 mätningar. Alla mätpunkter som redovisas från mätningar i labb och från fältförsöket är ett medelvärde av 32 skott.

I Figur 19 visas ultraljudsresponsen från en mätning i labbet på bergbult fastmonterad och fastspänd med PowerMACS-systemet. Den övre- och undre bilden är responsen från P-vågen respektive S-vågen. I den övre bilden kan man urskilja det fjärde ekot (efter den röda markeringen) medan i plotten för S-vågen är det endast tre ekon som är synliga. För beräkningen av TOF används två ekon från varje vågtyp (P- och S-våg) och dessa är i Figur 19 markerade med en blå respektive en röd ruta. I Figur 20, som är de valda ekona, finna samma markering av ekona. Man kan se där att de senare ekona (röda) är något bredare vilket tyder på viss dispersion men som det diskuterats tidigare i rapporten var det inte kritiskt för beräkning av TOF.

Analysen av all data utfördes initialt i projektet på två sätt, båda tidigare beskrivna i kapitel 3.2.1och i kapitel 3.2.2. I senare del av projektet användes dock bara den kurvanpassade korskorrelationen då den är mycket stabilare och inte lika känslig för till exempel dispersion. I Figur 21 är analysresultatet från båda analysmetoderna plottade tillsammans. Resultaten är från mätningar i labbet där bergbulten belastats med PowerMACS-systemet (styrt på vinkel) och där TOF-ration för P- och S-vågen är plottat som funktion av vinkel. De två analysmetoderna är utförda på samma data och det framgår tydligt att den demodulerade korskorrelationen fungerar mycket bättre än standardvarianten av korskorrelation. Den blåa respektive röda linjen i Figur 21 är respektive datas linjäranpassning och den kurvanpassningen till data analyserat med den kurvanpassade korskorrelationen är nära helt linjär vilket är förväntat. Avvikelsen från den linjära anpassningen kan eventuellt bero på att riggen/bulten ”sätter sig” då man drar åt och/eller att bulten man skruvar in halkar lite i hylsan.

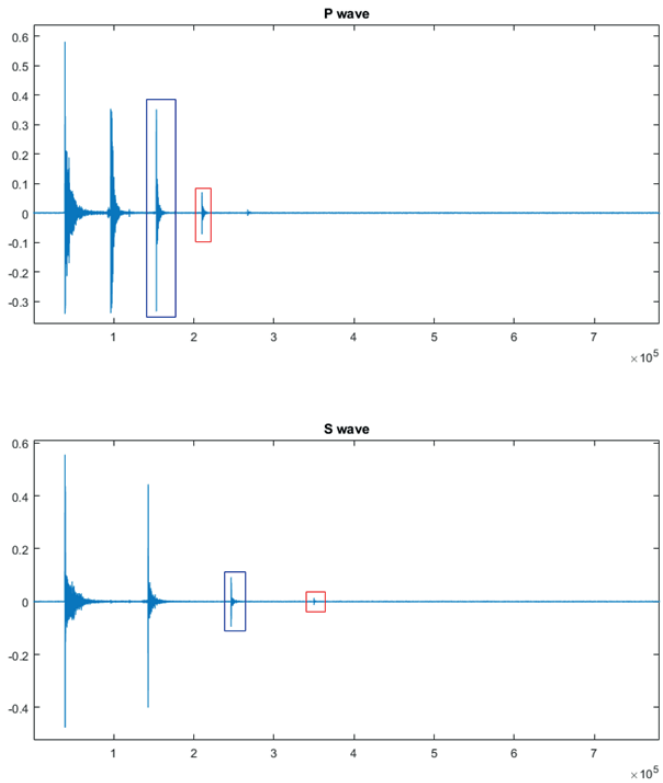

Figur 19 Ultraljudsresponsen från en mätning i labbet på bergbult fastmonterad och fastspänd med PowerMACS-systemet. Den övre- och undre bilden är responsen från P-vågen respektive S-vågen. I den övre bilden kan man urskilja det fjärde ekot (efter den röda markeringen) medan det endast syns tre ekon från S-vågen.

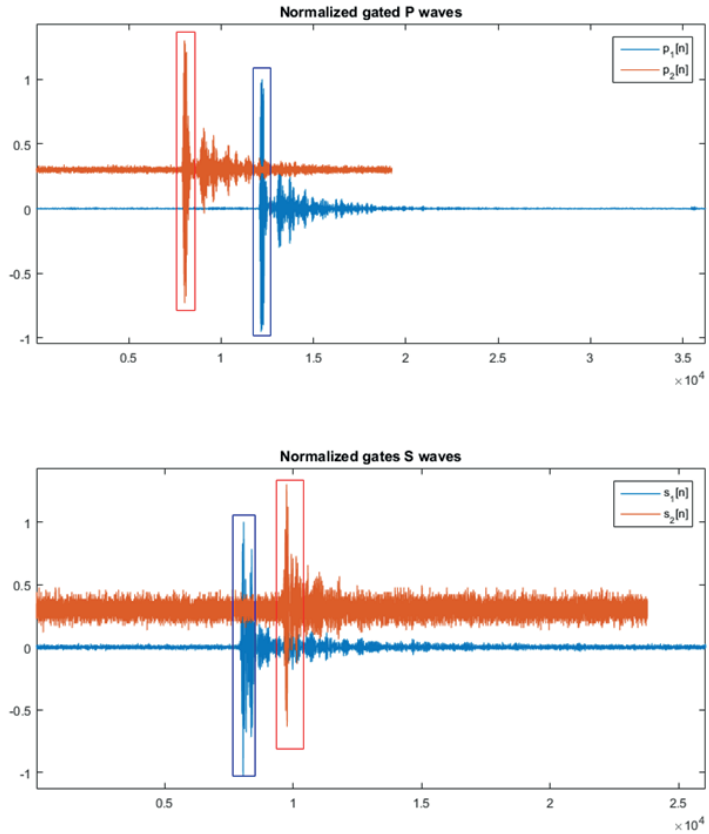

Figur 20 S-vågorna i Figur 19 men något inzoomade. Man kan se att det senare ekot (rött) är något bredare vilket tyder på viss dispersion men som det diskuterats tidigare i rapporten är det inte kritiskt för beräkning av TOF här.

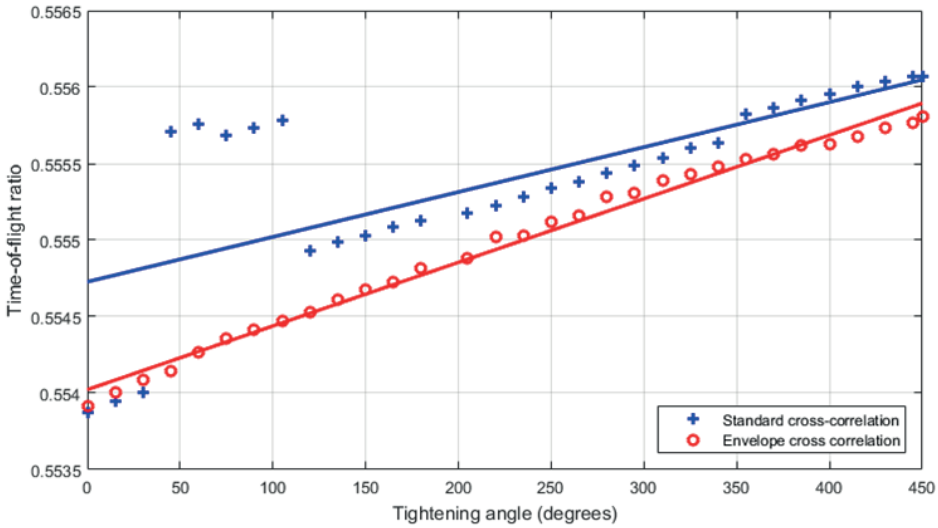

Figur 21 Analysresultatet från båda analysmetoderna plottade tillsammans. Resultaten är från mätningar i labbet där bergbulten belastats med PowerMACS-systemet (styrt på vinkel) och där TOF-ration för P- och S-vågen är plottat som funktion av vinkel. De två analysmetoderna är utförda på samma data och det framgår tydligt att den demodulerade korskorrelationen fungerar mycket bättre än standardvarianten av korskorrelation.

5.2 Mätningar i fält

Ett av målen, vid lyckade labbmätningar, med projektet var att utföra mätningar i fält på i berg monterade bergbultar. Detta var bland annat för att undersöka robustheten i själva mätsystemet (hårdvaran) men också för att se om till exempel handhavande i mätproceduren och/eller miljö hade avgörande inflytande över signalkvalitéten. Fältförsöket utfördes i slutet av projektet i en servicetunnel till Citybanan som vid mättillfället inte hade öppnat än. I denna servicetunnel finns det sedan tidigare ett antal (22 stycken) bergbultar monterade i just forskningssyfte. Bultarna var monterade för att användas som teststation för Boltometern, se diskussion i kapitel 1. Då Boltometerns syfte är att undersöka ingjutningskvalitéten för en bult har dessa testbultar blivit monterade med olika ingjutningar, skador och längder snarare än med olika klämkraft. Det passade dock detta projekt väldigt bra då inte bara robusthet och dylikt kunde undersökas utan potentialen att upptäcka andra eventuella defekter också kunde undersökas.

Projektdeltagare Kjell Windelhed på ÅF var behjälplig med att ordna tillstånd till tunnlarna för projektets mätningar och dessa utfördes under två dagar. En pickup lånades på plats i vilken utrustningen transporterades till mätplats. Utrustningen hade inte specifikt anpassats för tuffa fältförsök utan den såg ut som under labbmätningarna. Miljön vid mätplatsen var mycket tuffare än i labbet då t.ex. temperaturen var mycket lägre (cirka

5 grader Celsius) och luftfuktigheten högre. Detta gjorde bland annat att kopplingsmediet som användes blev väldigt svårarbetat och behövde lite förarbetning innan man kunde applicera det på bultänden och/eller ultraljudsproben. All utrustning som behövdes för mätningen placerades på två vikbord och ström (en fas, 10A, 220V) togs från ett närliggande strömskåp (efter anvisning). Bergbultarna hade god åtkomst och var monterade i lämplig höjd för mätningarna och ingen stege eller ställning behövde användas. I Figur 22 kan man se några av de 22 monterade bultarna och ungefär i vilket tillstånd/tillgänglighet de hade. Alla bultar var planslipade i ytterändan vilket är ett krav för att metoden som används i detta projekt ska kunna fungera. Information om hur ändan monterad inne i berget såg ut var vid mättillfälle inte tillgängligt och inte heller vid analysen. Detta diskuteras vidare senare under Sammanfattning men kort är orsaken att detta är information som undanhålls medvetet då projektet önskar gå vidare och vill utföra nya mätningar på dessa bultar utan att då heller veta facit.

I mätningarna på de monterade bergbultarna blev signalkvalitén godkänd till bra på 19 av 22 stycken bultar. Orsaken till att signalen inte var bra på just dessa tre är inte riktigt klarlagt men en möjlig förklaring är att två av dem har väldigt stora defekter i sig alternativt (än mer troligt) ej planparallella ändar vilket är av yttersta vikt för att mätmetoden ska fungera. Fallerandet med den tredje bulten är antagligen kopplat till den mänskliga faktorn så, i det fallet, samplingstiden var för kort inställd. I

Tabell 1 finns en tabell som sammanfattar alla fältmätningar. I tre ytterligare bultar gick det bara att få igenom P-vågen och inte S-vågen. Detta räcker för att uppskatta längden men möjliggör inte uppskattning av klämkraften. Så sammantaget: 22 bultar undersökta, 16 bultar med lyckade kompletta mätningar, tre bultar med bara P-våg och tre bultar utan några synliga ekon alls.

Tabell 1 finns uppmätt TOF för respektive bult, uppskattat läng på respektive bult, en kommentar samt beräknad kvot TOF_S / TOF_P. Denna kvot är, som tidigare diskuterats, linjär mot klämkraften. Även om det utan kalibrering inte går at säga hur hårt respektive bult sitter så ser man på spridningen i resultaten, som är liten, att de sitter med ungefär samma klämkraft. Detta var väntat av två orsaker: först var bultarna initialt monterade med samma klämkraft. Den andra orsaken är att bultarna sitter ganska nära varandra, området är ungefär 15 x 2 meter, och inga variationer i berget där är väntade.

Figur 22 Bergbultar monterade vid teststationen Citybanan. Sammanlagt 22 bergbultar med olika längd, defekter och ingjutningskvalitét är monterade och samtliga undersöktes vid fältförsöken.

Tabell 1 Sammanställning av resultaten från mätningarna under fältförsöken i Citybanan. Kolumnen till vänster, "ID" är samma markering som bultarna har markerat på sig i tunneln. I tre av fallen har bara P-vågen gått att mäta vilket resulterat i en uppskattning av längd men utan möjlighet till beräkning av kvot.

ID	TOF_P [ms]	TOF_S [ms]	Uppskattad längd [m]	Kommentar	Kvot (S/P)
20	700	1238	2,03		0,565428
21	701	1240	2,03	2st P-eko	0,565323
22	703	1244	2,04	2st P-eko	0,565113
23	703	1244	2	2st paket med P-ekon. Märkliga reflektioner/ekon i första och andra paketet.	0,565113
24	699	1238	2,03	2st paket med P-ekon. Märkliga reflektioner/ekon i första och andra paketet.	0,56462
25	702	1244	2,04	2st paket med P-ekon. Märkliga reflektioner/ekon i första och andra paketet.	0,564309
26	702	1243	2,04	2st paket med P-ekon. Märkliga reflektioner/ekon i första och andra paketet.	0,564763
27	701	1241	2,03	2st paket med P-ekon. Märkliga reflektioner/ekon i första och andra paketet.	0,564867
30	-	-	-	Inga synliga ekon	--------
31	1041	1852	3,02	Dubbelstuds i båda P- och S-ekon.	0,562095
32	1040	1862	3,02	Dubbelstuds i båda P- och S-ekon.	0,558539
33	1041	1862	3,02	Dubbelstuds i båda P- och S-ekon.	0,559076
35	1040	1861	3,02	Multipla reflektioner av P-ekon.	0,558839
36	x	x	x	Inga synliga ekon	--------
37	1042	1863	3,02	Multipla reflektioner av P-ekon.	0,559313
350	x	x	x	Inga synliga ekon	--------
351	1211	x	3,51	P synligt, S kapad för tidigt?	--------
352	1211	2174	3,51	Multipla reflektioner av P-ekon.	0,557038
353	1211	x	3,51	Bara P-våg sunlig	--------
354	1212	2175	3,51	Multipla reflektioner av P-ekon.	0,557241
355	1210	2172	3,51	Multipla reflektioner av P-ekon.	0,55709
356	1212	x	3,51	Svag P-våg. S kapad för tidigt?	--------

6 Diskussion och slutsatser

Grunden till projektet var tanken på en ultraljudsmetod med vars hjälp man skulle kunna bestämma klämkraften hos till exempel en bergbult. Under projektets gång har inte bara metoden utvecklats och förfinats utan infrastrukturen runt en testbädd för att kunna undersöka belastade bultar har byggts upp. Metoden är testad på olika typer av bergbultar (rent kolstål, epoxybelagd kolstål och rostfritt) i labbmiljö och ger tillförlitliga resultat. Ett av de tidiga frågetecknen var om ultraljudssignalen skulle kunna färdas så långt som det skulle behövas för att undersöka monterade bergbultar som kan vara uppåt 6 meter. Efter en del optimering av mätsystemet och tester av olika frekvenser på proberna stod det klart att systemet klarade av att få signal igenom och mäta i en minst 12 meter lång bergbult. Denna bult var dock inte monterad i berget utan hade bara luft omkring sig men detta gav oavsett ett tydligt svar på att det går att skicka bulkvågor genom en väldigt lång bult. Metoden för att bestämma Time-of-Flight (TOF) mellan olika ekon i signalen vilket ligger till grund för att kunna bestämma klämkraften visade sig vara väldigt pålitlig. En av orsakerna till det var att den förväntat kraftiga dispersionen uteblev och att signaltopparna förändrades förvånansvärt lite. Labbmätningarna visade på tydligt linjärt beteende mellan TOF, kvot av TOF (P- och S-våg) samt klämkraft vilket var vad som efterfrågades. Avvikelsen från helt linjärt beteende beror bland annat på svårigheten med att mäta klämkraft då till exempel friktion och gängkvalitét spelar in.

I slutfasen av projektet testades systemet under ett fältförsök i Citybanan. Där fanns sedan tidigare, monterade under ett annat projekt, ett antal bergbultar ingjutna som var av varierande längd, ingjutningskvalitét och med olika defekter. Bultarna hade inte gjutits in med avseende på att ha olika klämkraft men gav ändock en bra indikation på om systemet och metoden skulle fungera i andra, tuffare, miljöer än i labbet. Kalibrering av metoden på de monterade bultarna saknades vilket medförde att belastning i sig inte kunde mätas. Däremot visar fälttesten att man kan få de signaler man behöver, det vill säga tillräckligt många ekon av respektive vågtyp samt med sådan kvalitét att metoden med sannolikhet går att använda på redan ingjutna bultar under fältmässiga förhållanden.

Systemet och metoden som har utvecklats i detta projekt är avsett för mätning av gångtider (TOF) genom bult vilket gör att själva amplituden och frekvensinnehållet på signalen inte nyttjas. Detta ger en viss robusthet mot komplikationer som variationer i kopplingen mellan prob- och bult som andra metoder kan uppleva där handhavandet är väldigt kritiskt. Variationer i amplitud och/eller frekvensinnehåll skulle dock kunna användas för att eventuellt få ut mer information ur signalen än vad som gjorts här där klämkraften var frågan. Sprickor, ytnära defekter, korrosionsskador etc. är några saker som det finns potential att gå vidare med då projektet visat att det är möjligt att undersöka långa bultar.

7 Tillkännagivanden

Ett stort tack riktas till Formas (projekt 252-2012-1906) samt BeFo (projekt 325) för det finansiella stödet till detta projekt. Stor tacksamhet riktas också till den hjälpsamma och kreativa referensgruppen som projektet träffat två gånger per år.

8 Referenser

[1] J. D. a. N. Cheeke, ”Fundamentals and Applications of Ultrasonic Waves,” *CRC Press,* 2002.

[2] C. B. S. a. L. E. Drain, ”Laser Ultrasonics,” *CRC Press,* 2015.

[3] M. H. a. H. Ogi, EMATs for Science and Industry, Springer, 2003.

9 Appendix

9.1 Litteraturstudie

Tidigt i projektet gjorde en litteraturstudie för att få en fördjupad koll på omvärlden och vad som gjorts tidigare angående ultraljud och belastade strukturelement. Studien, ”*The evaluation of pre-loaded structural components - A literature survey with focus on rock bolt axial load evaluation employing the ultrasonic bi-wave technique in a non-contact mode*”, bifogas här som ett appendix.

The evaluation of pre-loaded structural components

- A literature survey with focus on rock bolt axial load evaluation employing the ultrasonic bi-wave technique in a non-contact mode

Content literature survey

Summary

As rock bolts are grouted into e.g. cement or epoxy, only one end is accessible for the analytical technique in question, ultrasonic methods are being considered valuable non-destructive techniques for estimating the bolt integrity. The conventional acoustoelastic ultrasonic technique for deducing the axial loading of pre-stressed bolts is based on variations in the time-of-flight of a single longitudinal bulk wave with loading. A main drawback of this mono-wave technique is the required pre-knowledge of the initial bolt length and the initial loading condition. The bi-wave method on the other hand allows the axial load in the stressed state to be calculated from the time-of-flight ratio of two different wave types, without pre-knowledge of measurement in the unstressed state.

Commercial piezoelectric probes exist that simultaneously generate and detect both longitudinal and transverse bulk waves, and the bi-wave technique has successfully been used for deducing the axial load of 50-215 mm long bolts. Piezoelectric transducers, however, require an intimate contact with the bolt end why errors rise from various surface conditions and couplant properties. The primary advantage of EMAT transducers over piezoelectric transducers is the ultrasonic wave generation and detection through electromagnetic forces, without requirements for intimate contact with the bolt end. The main drawback of the EMAT systems is, however, the generally low signal-to-noise ratio compared to piezoelectric transducers. Currently no commercial EMAT probe exists for bi-wave applications, however, an EMAT bi-wave prototype equipment has proven capable to measure the axial load condition of bolts with lengths up to 500 mm.

Keywords: ultrasound, bi-wave technique, bolt axial load, non-destructive testing, EMAT, piezoelectric

9.2 Sammanfattning

Konventionella ultraljudstekniker används allt oftare för oförstörande kvalitetsbedömning av skruvförband och inspända bultar, men den gängse monovågstekniken för att mäta axiell belastning av förspända bultar bygger på variationer i time-of-flight hos den longitudinella bulk-vågen, vilket kräver förkunskap om både initial bultlängd och initialt belastningstillstånd. Tvåvågstekniken baseras istället på det simultant uppmätta hastighetsförhållandet mellan två olika vågtyper, longitudinella och transversella bulkvågor, och kringgår därför behovet av initiala mätningar genomförda på den obelastade bulten. Experiment med simultan generering och detektion av längsgående och tvärgående bulkvågor har tidigare genomförts med kommersiella piezoelektriska prober, och man har i dessa arbeten uppmätt den axiella belastningen hos långa inspända bultar. Piezoelektriska prober kräver dock en direkt kontakt med mätytan och stora fel kan introduceras genom både bultens egna yttillstånd och kopplingsmedlets egenskaper. Fördelen med EMAT-proben är istället att ultraljudvågorna genereras och detekteras genom elektromagnetiska krafter, varför ingen tät kontakt krävs. Den huvudsakliga nackdelen med EMAT-prober är emellertid den generellt lägre signalstyrkan jämfört med piezoelektriska prober. Idag saknas kommersiella EMAT-prober för

tvåvågsteknik, men en prototyputrustning har kunnat uppvisa kapacitet för mätning av den axiella belastningen hos långa inspända strukturer.

Nyckelord: ultraljud, tvåvågsteknik, axiell bultspänning, oförstörande provning, EMAT

9.3 Introduction

9.3.1 Background and aim of the study

Rock bolts are extensively used to secure the stability of underground constructions. In the tunnel and mining industries, rock bolts are used in order to keep tunnel shapes intact. Because of their role as primary rock support, it is crucial to ensure that the rock bolt is not carrying excessive load and/or that it is not near failure. Due to stress redistribution in the surrounding rocks and other aging effect, the force on the rock bolt will change with time. Even though they are closely located, the tensile stresses in different rock bolts also differ because of the different anchorage conditions. In order to ensure the safety and reliability, the axial load (also called preload or clamping load) of the bolt has to be carefully controlled during installation and maintained during service. In addition to increasing the safety, accurate methods for characterizing and monitoring the conditions of rock bolts would also aid to optimize the use of the bolts and enable development of new materials. The evaluation of rock bolt integrity has been addressed by various groups around the world. Destructive methods including pull-out tests and over-coring methods are time consuming and expansive, but also a number of nondestructive evaluation techniques have been developed for evaluating the integrity of long bolts in the field, both for evaluating the grouting (or bonding) quality as well as for determining the loading conditions.

The main focus of the survey is techniques for deducing the axial loading condition of ~5 m long rock bolts. For deducing the axial loading condition, the majority of the scientific works published have however been performed on shorter bolt structures, i.e. for infrastructures and automotive applications. For the long specimens of relevance, the material attenuation is a limiting factor also for ultrasonic techniques. In addition to this, the bolts are not free standing, but grouted into e.g. cement and epoxy. This also means that also only one end of the bolts is accessible to apply the monitoring equipment for the analytical technique in question. Recent years, ultrasonic methods have been considered valuable non-destructive techniques for estimating bolt axial load - and a more specific aim of the current study is to employ the so called bi-wave technique using EMAT transducers, i.e. probes which do not require intimate contact with the bolt end.

9.3.2 Techniques for determining bolt integrity

A number of non-destructive testing methods have been developed for evaluating bolt integrity with focus on the grouting (or bonding) quality, ranging from bolts for thinner lap-joint structures to rock bolts of several meters. Some techniques require access to both ends of the bolt, while for some application one end is unreachable, as for rock bolts. Existing methods presented below are impulse-based techniques, impedance-based methods, and various techniques based on ultrasonic waves.

9.3.3 Impulse-based techniques

Impulse based method employ by e.g. a pneumatic or solenoid device. A commercial technique that has been available since 1997 is GRANIT^{TM} (Ground Anchorage Integrity Testing), developed at the University of Aberdeen[1]. The GRANIT system operates by application of a controlled tensile axial impulse of small amplitude at the bar using a pneumatically-driven piston in order to measure load stress. The system is readily deployable and does not need the end of the bolt to be prepared specially. The vibrational response in the bolt is measured with an accelerometer positioned on the impact device. A disadvantage of the GRANIT system is that the dynamic response has to be compared to results obtained at installation, i.e. pre-known data is required. Any changes in response then indicate a potential change in integrity of the anchorage. It is, however, complicated to determine the relationship between the dynamic response of the anchorage and its post-tension level. The vibration signals that arise from this impulse are complex and nonlinear in nature, and the response requires interpretation by neural networks to determine the condition of the bolt. The technique also does not provide any indication of the load distribution along the bonded length[1 2 3].

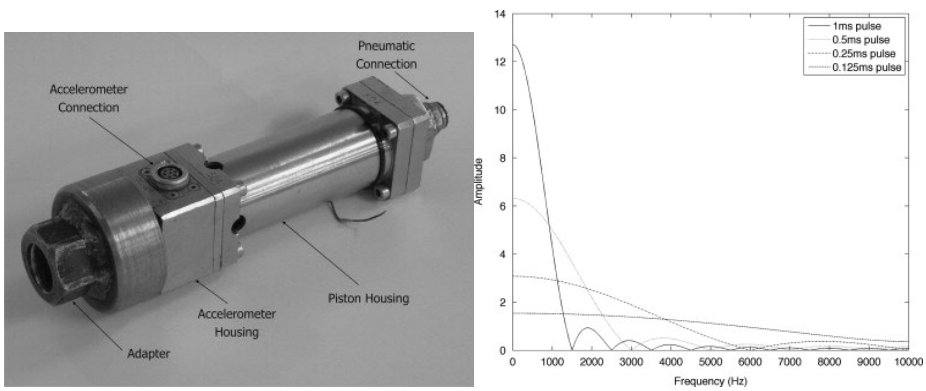

Figure 1. The GRANIT device and a typical impulse input spectrum.

9.3.4 Electromechanical impedance techniques

For shorter bolts, the electromechanical impedance method employs a piezoelectric transducer, where the electrical impedance across the transducer is coupled with the mechanical impedance of the tested structure onto which it is attached. Changes in the mechanical impedance are

attributed to the mass or stiffness changes. For instance An and Sohn[4] illustrated an integrated impedance and guided wave based damage detection technique by utilizing impedance and guided wave signals simultaneously obtained from surface-mounted piezoelectric transducers for the detection of bolt loosening. The piezoelectric impedance method has a high sensitivity to the local structure damage and a large frequency bandwidth. It is specially fitted for monitoring bolted joints which are dominated by local dynamics of high frequency characteristics. While it has a better applicability to more complex structures than the ultrasonic wave techniques, it has a shorter sensing range.

9.3.5 1.2.3. Ultrasonic techniques

The use of ultrasonic signals in general is well known method for monitoring the stress levels in the pre-stressed waveguides as strands, bars, rock bolts. Ultrasonic waves can travel long distances in solid materials and can provide information regarding a materials microstructure through variations in phase velocity, attenuation and nonlinearity. The attenuation, or internal friction, occurs as the propagating waves are scattered, reflected and absorbed by different material/structural boundaries. The acoustic nonlinearity originates from lattice non-harmonities, damping mechanisms and microcracks[5]. The velocity of the propagating waves is one of the most important parameters in ultrasonic testing. For bulk waves, the velocity is constant, while guided waves (which are a wave that follows a certain geometry either in bulk or at the surface), for example a bolt) are dispersive with velocities changing with frequency.

In 1978, Thurner proposed that loss of ultrasonic wave energy could be used to test the quality of a bolt in a bore. This lead to the development of the first instrument for non-destructive in-situ testing of grouted rock bolts, the Boltometer (Geodynamik, Sweden)[6]. It is designed for full bar anchors preferably with diameters between 20 and 30 mm, and can be used on both cemented grouted bolts and some resin grouts[7]. The Boltometer uses piezoelectric crystals to transmit and detect elastic waves into the bolt, and evaluates the bonding quality of the rock bolts from the amplitude of reflected wave. The longitudinal and transverse waves propagate through the bolt, reflect at the inner end and the echo is received by the sensor. When the waves travel along the bolt, some energy is transferred through the grouting into the rock and thus the wave amplitude decreases. The reflected waves are recorded at the outer end of the bolt by means of the piezo-electric crystals. While good grouting absorb most or all of the wave energy into the rock, leaving only small echoes returning to the sensor, an insufficient grouting result in a distinct echo. The Boltometer can, however, only indicate the overall grout quality and cannot give quantitative information or find the location of bad grouting in non-uniform grout. Due to the rather fast attenuation of these waves, the main limitation is the penetration depth, which restricted by the presence of a length of good grout[8]. Additionally, if the impedance between the grout and surrounding rock are to similar, the wave energy will dissipate into the rock before it could reach a major defect and the result will look as if the grouting is “good”[1].

The amplitude of the reflected waves is seriously dependent on the coupling conditions between the transducer and the rock bolt. The free end of the bolt has to be cut and/or ground plane and a special contact paste is required at the bolt end in order to obtain a good wave transfer.

More recently, guided ultrasonic waves has been proposed for determining the integrity of long rock bolts [1,7–9]. Guided wave propagation refers to the ultrasonic waves that propagate in solid media with boundaries[7]. The quality of the grouting and the location of the defect can be

determined. Also specific modes can be selected that are less sensitive to differences in impedance compared to the Boltometer. As guided wave testing only requires baseline reference measurements, no previous data of the specific rock bolt is needed[1]. One of the most important features of guided wave is that waves with different frequencies have different velocity and attenuation characteristics when propagating in a waveguide. Moreover, the propagation properties are related to the geometrical structure and bonding quality of the rock bolts and anchored objects[10]. A guided wave is generated in the bolt on the free end of the bolt, which is then reflected from the bolt end and from any major defects. From the reflection arrival time and knowledge of the wave velocity dispersion curves, the positions of the defects or the bolt length can be calculated. The maximum test range is limited by the extent of the attenuation that the wave experiences as it propagates. For testing of long grouted rock bolts also the wave attenuation and energy dispersion thus pose difficulties. For a free bolt, where wave attenuation due to energy leakage does not occur, it is easy to pick up many clear echoes reflecting back and forth during tests. For a grouted bolt, however, wave attenuation and energy dispersion complicate the problem. It is therefore very important to identify suitable frequencies and wave modes, which would incur low attenuation and less energy dispersion in grouted rock bolts so as to increase the penetration range of the ultrasonic wave test[8 10].

In 2003, Beard and Lowe[9] used transducers with low and high frequencies to investigate the defect of cylindrical steel bars. Standard rock bolts of 21.7 mm diameter and up to 3m long were grouted in epoxy resin. They investigated the effect of guided wave modes, frequencies and excitation periods in order to find the best guided wave mode for defect detection. It was found that grouted bolts should be tested by exciting the first axially symmetric longitudinal mode known as the L(0,1) mode, in its low frequency, and the first non-axially symmetric longitudinal mode known as the L(1,1) mode, in its high frequency range.

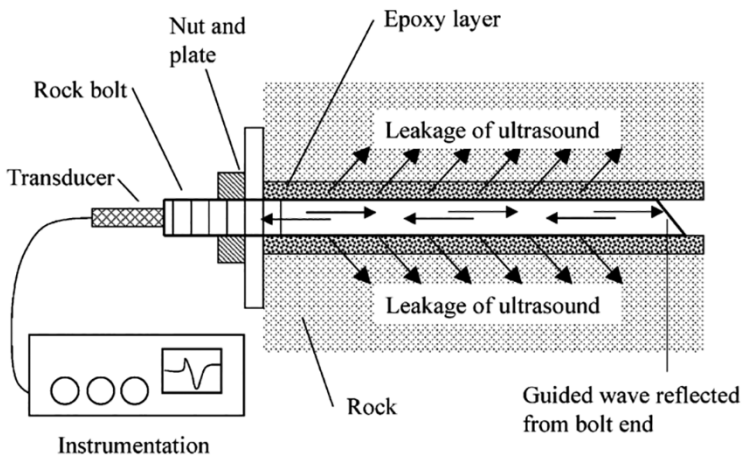

Figure 2. The laboratory set up of a rock bolt grouted in epoxy resin[9].

The bolts were successfully tested with both the fundamental L(0,1) mode and higher frequency low-leakage modes. The behavior of the high and low frequency modes were, however, very different, and neither approach offered a complete testing The low frequency test could identify defects such as partial bolt encapsulation and possibly corrosion patches near the bolt surface.

On the other hand, the high frequency test is not sensitive to surface defects, but could provide a reliable indication of the bolt length. As high frequency waves are attenuated by curvature, they also allowed the possibility of determining whether or not bolts are deformed.

In 2008, Buys[7] further developed the method of Beard and Lowe and employed guided ultrasonic waves for determining the condition of 1.5 m resin-anchored rock bolts, using the L(0,1) mode in its lower frequency range. A free standing bolt and a perfectly embedded bolt were used as the base reference. Also finite element models were built for a partially encapsulated bolt and for a bolt with a simulated local corrosion crack, respectively. Experimental bolts were then installed in a testing block and typical responses were compared to finite element models of different defect scenarios. It is apparent that it is critical to choose the correct frequency for optimized reflection. It was concluded that at higher frequencies, the energy propagates more along the center of the bolt; consequently the higher frequency modes will be less sensitive to partial grouting. It is recommended that lower frequencies should be used for detection of defects.

In 2006, also Edwards, Dixon et al.[11] employed electro-magnetic acoustic transducers (EMATs) to generate and detect a low-frequency (50 kHz to 1 MHz) wide-band guided surface waves for defect detection on railhead samples. As guided waves provide modes that can travel great distances in rails, as well as take into account the entire volume of the rail, it provides large benefits for surface defect detection compared to the fast attenuating bulk waves of small volume coverage. Although less efficient at generating or detecting ultrasound than piezoelectric transducers, the use of non-contact EMATs allows standoffs of several millimeters above the sample as well as working without couplants. This allows surface roughness on the millimeter scale to be measured without preparation. Any changes in detected amplitude due to changes in standoff can be compensated for by e.g. using an array of EMATs, such as a generator EMAT with a receive EMAT in front and behind. For the rail applications was found a meander coil configuration generated a large amplitude signal for working in single-shot mode. In all, the depth of the maximum crack present in the railheads provided by the EMATs agreed well with the depths measured using other methods.

9.3.6 Techniques for determining bolt tension (introduction)

Various techniques measure the load/tension condition of bolts. Some are however limited to measure shorter items. For longer bolts and rods, such as those of relevance for this study, several existing studies are however limited to free standing structures. For the application of interest, the rock bolt is analyzed while grouted in cement, epoxy or other high density grouting material. Existing methods presented below are the conventional torque wrench technique, various pre-mounted sensors, and techniques based on ultrasonic waves.

9.3.7 Torque wrench

Current practice relies on the torque wrench technique. However, with this technique, load dissipated in the friction of the bolt threads, and between the nut and the part prevents accurate measurements of the axial load. This situation leads to over- designing for safety and in turn

increases both weight and cost. The torque wrench method has been used for decades to estimate the axial load from a torque applied to clamp the bolt[12] . This technique, however involves large errors, which is mainly assigned to friction loss in the conversion of torque energy to clamping force. Friction has been estimated to consume as much as ~90% of the torque energy, with 50% dissipated in the bolt head and 35% in the bolt threads. This means that only a minor amount of the torsional work is converted to tension in the bolts. The friction can vary substantially, even between similar bolts, and errors as high as 50% are common even with perfect torque control[13]. Other sources of error that are difficult to control are the state of lubrication, surface quality of the plans in contact, alignment of the assembly, and manufacturing tolerances. The load can also not be evaluated without twisting the fastener and disturbing the joint [14 15].

9.3.8 Techniques employing pre-mounted sensors

Several types strain gauge techniques exist for determining axial loads on pre-stressed bolts, apart from traditional mechanical- and vibrating wire strain gauges[16]. The electrical resistance strain-gauged load cells has a load-sensing spool element made from high strength heat-treated steel that withstands severe environments (Figure 3). The physical size of the structure controls the deflection experiences under load, thus the capacity rating of the cell.

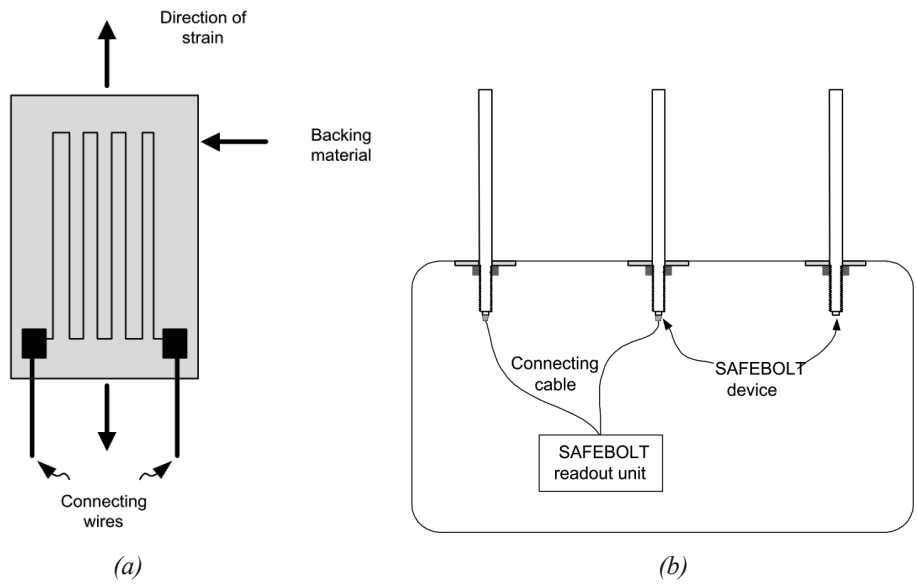

Figure 3. (a) A typical electrical resistance strain gauge and (b) the Safebolt system components [16].

A rock bolt load device based on anelectrical resistance strain gauge inserted in the bolt head is the SAFEBOLT (Stress And Force Evaluator in Bolts). The system consists of the SAFEBOLT device installed in the bolt head, a readout unit and a connecting cable (Figure). A zero strain

reference, A, is determined before any load is applied to the bolt, i.e. prior to installation. As the load is applied, the readout unit register a signal of magnitude R, why the axial strain due to applied load will be represented by the quantity R-A. The device can be installed on any type of rock bolt or rebar and the sensor and can monitor the bolt load to and past the yield point. The precision of load calculation is said to be subject to an error of ± 0.05 tons, and the sensor is also sensitive to temperature variation and to bolt inclination with the rock surface. As the gauge might break before the failure load is attained, monitor of the load to the ultimate strength of the bolt cannot be guaranteed.

In 2001 Mitri et al.[17] proposed a metal-based strain gauge based on placing a strain gauge directly in the bolt head prior to installation by drilling a central blind hole that extends beyond the threaded portion (Figure 4a). Once installed, the coupler load cell enables the monitoring of the bolt axial force exerted on the face plate. The metal-based strain gauge has a stretch capacity that is much greater compared to the traditional vibrating wire strain gauge used with hollow load cells. As the strain limit of the metal gauge is larger than the yield strain of the bolt steel material, the design allows measurements of the bolt yield load. Drawbacks are the need to transport the bolt back and forth to the mine, and that the hole drilled in the bolt head reduces its capacity by about 3%. As the gauge is installed in the bolt itself, it is thus unable to measure the ultimate or breaking strength of the rock bolt. More recently, Mitri et al.[17] suggested a new concept made of a coupler instrumented with a metal strain gauge placed in the blind borehole along the axis of the coupler (Figure 4b). The coupler load cell is fitted onto the rock anchor, and once installed which it allows the monitoring of the anchor head axial load. As the yield load of the coupler is greater than the ultimate breaking strength of the rock anchor, it ensures a complete load path monitoring of rock support performance until failure.

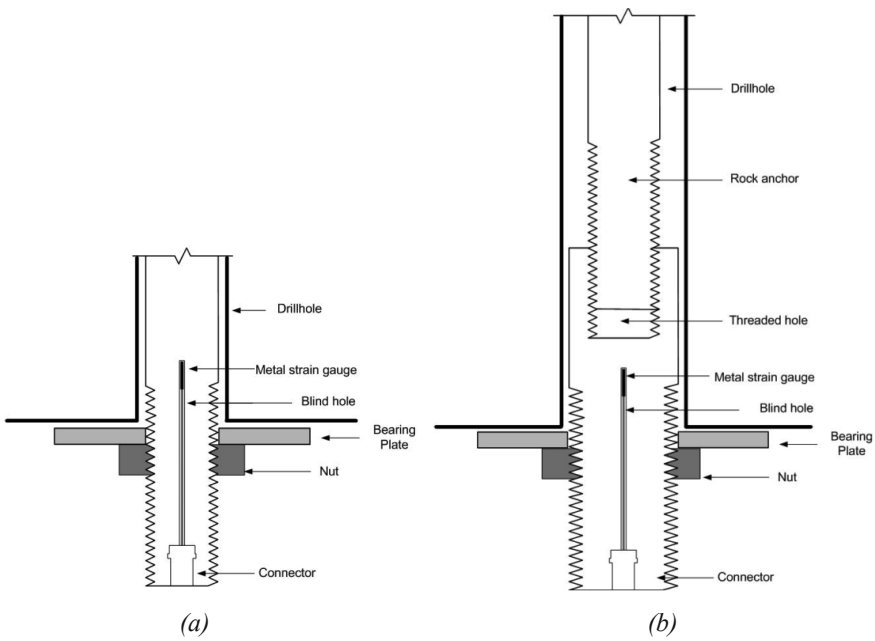

Figure 4. (a) The original metal-based strain gauge design and (b) the developed coupler load cell design[17].

Lately also elasto-magnetic (EM) sensors have been suggested as a promising technique for stress monitoring of in-service steel structures. Pre-fabricated EM sensor takes the form of a hollow cylinder through which steel elements such as a wire, strand, cable or bar passes through it during construction. The sensor consists of primary, secondary and compensating windings, mounted in a protective steel shield and sealed with an insulating material. The EM sensor has no mechanical contact with the measured element and its characteristics is estimated not to alter for more than 50 years[18].

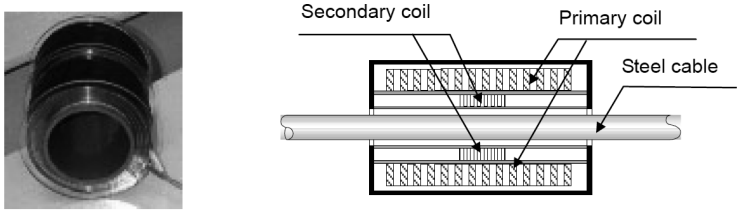

Figure 5. A schematic description of an EM-sensor.

The DYNAForce sensor from DYWIDAG-Systems International[19] employs the elastomagnetic technology (EM) to measure stress level in pre-stressed strands or bars installed on ground anchors or post tensioning tendons[20]. The sensor can be used to rapidly read the change in load during proof and performance tests and compare with the pressure gauge and during the life on the anchor to monitor existing lock-off load. It can be used also to determine the load along the bonded length of the anchor allowing the contractor to increase or decrease this length[20]. By passing current through primary coil, ferromagnetic material is magnetized. Sensing coil picks up induced electromotive force that is proportional to change rate of the applied magnetic flux and relative permeability. As permeability of core changes, output voltage changes. The output voltage is calibrated to measure force. In most cases, the monitoring accuracy is within 2% for strand tendons and within 5% for bar tendons[19].

9.3.9 Ultrasonic techniques

In general, the conventional ultrasonic methods for the detection of bolt load can be divided into two groups, based on either wave-propagation or vibration/resonance. With the wave-propagation-based techniques, it is possible produce various types of elastic waves. This dissipation process is recorded in the form of attenuated signals. For the vibration-based approach, the entire structure is excited and search for features that reflect damage- induced changes to the dynamic response. Recent years, the ultrasonic methods based on bulk waves have been considered a valuable method to estimate the bolt axial load, and the method is based on the fact that the velocity of an ultrasonic wave that propagates along a bolt depends on the axial stress. Being the focus of the survey, the determination of the axial load employing longitudinal and transverse bulk waves and the acoustoelastic theory is described more in detail in Chapters 2 and 3.

Experimental work for monitoring stress levels in long stressed structures have, however, also been performed employing surface- and guided ultrasonic waves, and some examples are presented below.

Chaki and Bourse[21] proposed a methodology for monitoring the stress levels of pre-stressed steel strands subjected to a uniaxial loading. For this was used guided ultrasonic and the acoustoelastic theory presented in Chapter 2. This experiment, however, requires the acoustoelastic coefficient of the material from calibration experiments conducted on non-loaded specimens of known length. Measurements were performed on the core wire of an assembled strand with the propagating mode L(0,1) at frequency 230 kHz. The resulting acoustoelastic coefficient was further used for in situ stress evaluation in similar strands to those used in the calibration test.

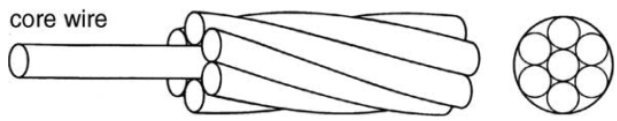

Figure 6. A pre-stressed steel strand structure.

A model was built with four pre-stressed strands (Figure 7) inside a plastic duct not yet injected by cement grout. The strands were loaded at various stress levels using a hydraulic jack device. As both ends of the strands were free, the stressed and total lengths (l_s and l_t) were measured using a tape-measure (±1 mm). The phase velocity at zero loading was measured on a 2087 mm long strand.

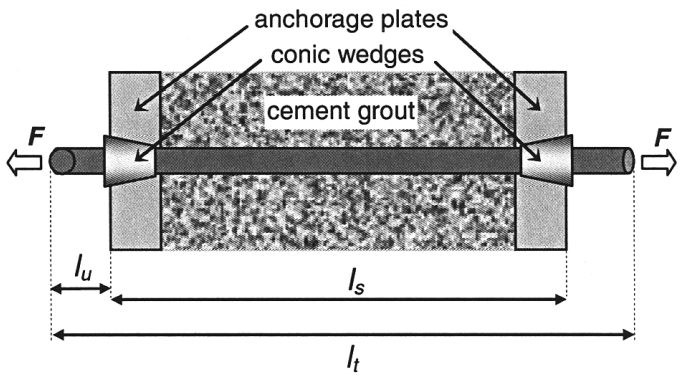

Figure 7. A pre-stressed strand in an industrial anchorage. Here l_s is the stressed length and l_u is the unstressed length.

The use of L(0,1) mode was justified by the fact that longitudinal waves are more sensitive to tensile stresses than other wave types, and secondly it can be generated purely and simply using commercial piezoelectric transducers working in piston mode. Two simplified acoustoelastic formulations were derived from the acoustoelasticity theory according to the loading type, i.e. a tensile testing machine for the calibration test and a hydraulic jack for the industrial loading of strands. These formulations based on the relative phase velocity change, of L(0,1) mode at frequency 230 kHz, enabled the characterization of the acoustoelastic effect in the tested strands by performing measurements only on the straight core wire. For case of tensile loading, the stress distribution homogeneity in the seven-wire steel strand was demonstrated, thus a uniform normal stress in each individual wire was assumed. Except for the low load, which was located in the nonlinear part of calibration curve, the evaluated stresses for the pre-stressed strands were

in reasonable agreement with the applied stress. Before implementing the methodology on longer pre-stressed stands for industrial applications, it was concluded that the short-range of the ultra- sonic energy provided by piezoelectric transduction would be insufficient. Ongoing studies seek to exploit the potential of other transduction technologies, such as magnetoelasticity in order to devise miniature magnetostrictive transducers being able to be introduced into each strand during its installation.

More work has employing guided waves have been performed on shorter bolts. For instance Yang and Chang[22] provided an ultrasonic attenuation-based method to identify loosened short bolts joining composite panels. Ultrasonic waves propagating through contact interfaces between solid bodies are sensitive to contact conditions such as the contact pressure and the true area of contact. This sensitivity can be related to the fact that the load at the contact is supported by surface asperities and by increasing the nominal load the contact area may increase. It has been shown that the transmission and reflection coefficients of the ultrasonic wave are sensitive to the contact pressure or other contact parameters. Theoretically, the normal and tangential stiffness of the contact interface govern the transmission/reflection coefficients and can be used as parameters to characterize the contact condition. However, weak and incomplete interfaces, formed by rough surfaces in partial contact, show a highly nonlinear behavior also when they are excited under free vibrations. In particular, the amplitude of the second harmonic is a relevant index of the contact stiffness, and the nonlinear response is strongly influenced by the nominal contact pressure applied to the boundaries[23]. The ratio between the amplitudes of the second harmonic and the fundamental can be related to the nominal force applied at the boundary. The interface of the two contact surfaces is restricted to discrete areas at the tips of the surface asperities (Figure 8). The true contact area is known to be smaller than the nominal contact area and varies with the contact pressure. By increasing the fastening torque, the true contact area will increase and the wave will propagate across the interface with less energy loss.

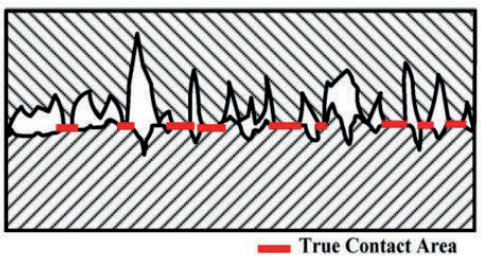

Figure 8. Schematic view of an imperfect interface[24].

Ultrasonic waves were generated and transmitted through the imperfect interfaces between the fastening components. Depending on the amount of pre-load at the bolted joints, the contact condition at the imperfect interfaces varies, and as a result the guided waves along the interfaces reveal different dissipation patterns. The energy dissipation at an imperfect contact interface can be examined as the transmitted wave propagation mainly occurs in the true contact area. The amount of transmitted wave energy is proportional to the true contact area, which in turn is proportional to the square root of the pressure applied to the contact surface. By analyzing the transient responses of the sensor signal measured by the embedded sensors, information about the fastener integrity can thus be deduced in terms of the torque levels of the monitoring bolts.

Amerini et al.[23] developed the power spectral density (PSD) of the recorded signal to assess the loosening state of joint structures. By assuming a theoretical model of the nonlinear interface stiffness, the stiffness of the contact interface was described as a function of the nominal contact pressure. Next, this theoretical model was experimentally tested, and a different index based on the power spectral density (PSD) of the recorded signal was developed and validated to assess the loosening state of joints by studying the signal energy.

The ratio between the second harmonic amplitude and the fundamental frequency amplitude was found to be a reliable parameter from which the information about the amount of nonlinearity associated with the contact could be extracted - and it is a clear index of the loosening state of a joint. This index decays following an analytical power law with the clamp force. These experimental results were validated by an analytical model able to reproduce the nonlinearity generated by the non-perfect contact, by adopting a nonlinear spring applied at the contact location.

Recently, also Martinez et al.[25] implemented a synthetic phased array surface acoustic wave (SAW) sensor to estimate the tension/clamping force of a 6.4 mm grade 8 threaded bolt in a 12.7 mm thick steel plate. The interaction of various acoustic wave modes with the boundaries of rough surfaces takes place at the points where the propagation surface and the external body are directly in contact with each other (points of real contact). The real area of contact (RAC) is the sum of all these individual contact points (Figure 9).

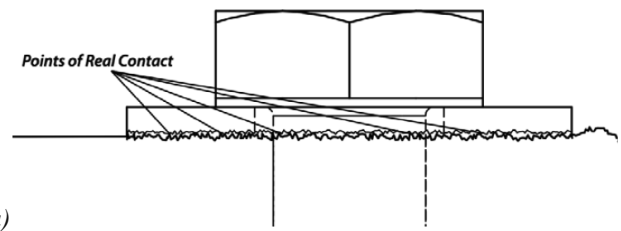

a)

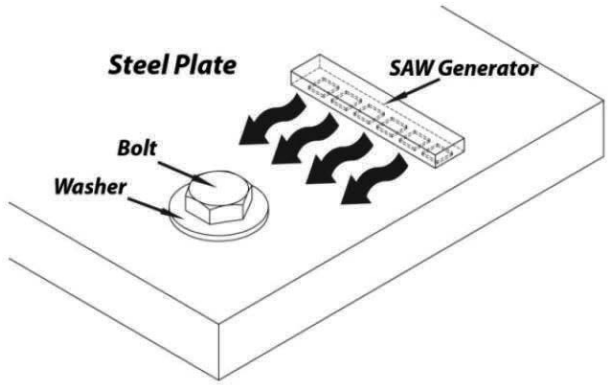

(b)

Figure 9. Schematics of (a) The real contact area (RAC) of a clamped plate and washer and (b) the methodology used.

Waves created by a SAW generator are directed towards a bolted joint. As the tension at the bolt is increased, the position of the reflective boundary is expected to move from the edge of the joint towards the outer washer perimeter. It is hypothesized that the increase in the bolt tension results in a proportional increase in the RAC. The synthetic phased array was formed by a single angle beam transducer actuated from several positions within a linear array. The array pitch was selected as 250 μm corresponding to less than half the wavelength. An array with 50 elements was used corresponding to the total array length of 12.5 mm that results in 1.25 mm beam diameter at 29 mm away from the center of the array. The study employed used a 5 MHz bulk piezoelectric transducer, attached to an ultrasonic wedge that is specifically designed for converting the longitudinal bulk wave into SAWs in steel. In all, the study presented the first step towards the development of a bolt tension sensor based on surface acoustic waves, where bolt tension was estimated using the reflection of SAWs created by the bolted joint interference.

9.4 The acoustoelasticity theory

The bulk wave types used for load measurements on bolts are the longitudinal and transverse waves (Figure 10).

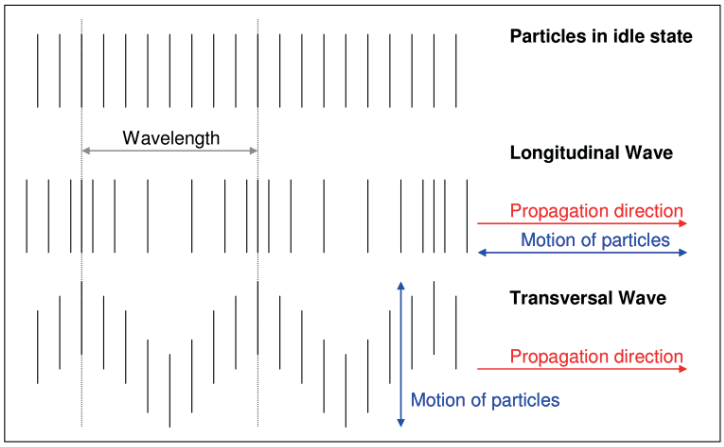

Figure 10. Ultrasonic wave types for load measurements

For longitudinal waves, the particles in the bolt swing in the same direction as the bolt's axis, while for transversal waves the particles swing perpendicular to this axis. Also the velocities of the both waves are significantly different. For standard steels the typical longitudinal wave velocity is ~5.900 m/s while the corresponding transversal wave velocity is ~3.200 m/s. The propagation of the ultrasonic waves is sensitive to both residual and applied stresses in materials, where stresses in a material cause a modification of its elastic behavior. The elastic wave propagation depends on the direction of the applied stress as well as on the direction and polarization of the waves.

The ultrasonic methods to estimate the bolt axial load from bulk waves propagating along the bolt are thus based on the fact that the wave velocity depends on the axial stress. The tightening of the bolt is followed by elongation, which in turn increase the time it takes for the wave to return. The alteration in wave velocity induced by the stress in the bolt, called the acoustoelastic effect, however causes a larger time delay than what is expected from the elongation factor alone[26]. A sensor or transducer is put on one of the bolts ends and convert an electronic signal into a mechanical vibration. As the wave travels through the bolt, it is reflected at the end and travels back to be converted back into an electronic signal.

The acoustoelasticity theory relates nonlinear elasticity and ultrasonic acoustics. In the case of plane waves and for a homogeneous and isotropic material subjected to a uniaxial state of stress, the velocities of longitudinal (V_L^σ) and transverse (V_T^σ) waves, which propagate in the same direction as the applied stress, can be written at the first order as[8:]

$$V_L^\sigma = V_L^0(1 + A_L\sigma) \quad , \quad V_T^\sigma = V_T^0(1 + A_T\sigma)$$

Where V_L^0 and V_T^0 are the respective velocities in the unstressed states, σ is the stress, and A_L and A_T are the longitudinal and transverse acoustoelastic coefficients. The velocities and acoustoelastic coefficients are in turn functions of the second-order Lame's constants, λ and μ, and of the third-order Murnagan's constants, l, m and n, respectively.

$$V_L^0 = \sqrt{\frac{\lambda + 2\mu}{\rho}} \qquad V_T^0 = \sqrt{\frac{\mu}{\rho}}$$

,

$$A_L = \frac{1}{2(\lambda + 2\mu)(3\lambda + 2\mu)}\left(\frac{\lambda + \mu}{\mu}(4\lambda + 10\mu + 4m) + \lambda + 2l\right)$$

$$A_T = \frac{1}{2\mu(3\lambda + 2\mu)}\left(4\lambda + 4\mu + m + \frac{\lambda n}{4\mu}\right)$$

As the acoustoelastic coefficients are negative, the wave velocities will decrease with an increased stress.

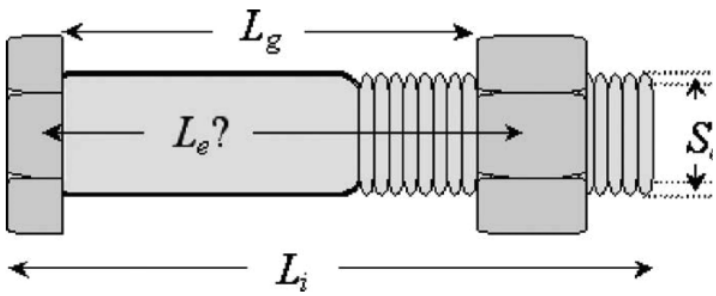

Figure 11. An axially loaded bolt [27]

For a bolt that is subjected to an axial load, the initial length, L_i, will consist of parts that is both stressed and unstressed. This means that $L_i = L_0 + L_e$, where L_0 constitutes the unstressed part and L_e is the effective length assumed to subjected to a uniform stress, $\sigma=F/S$ where F is the axial load and S is the cross section area.

The time-of-flight for the longitudinal and transverse waves respectively then becomes

$$t_L^\sigma = \frac{2L_e(1 + E^{-1}\sigma)}{V_L^0(1 + A_L\sigma)} + \frac{2L_0}{V_L^0} \qquad t_T^\sigma = \frac{2L_e(1 + E^{-1}\sigma)}{V_T^0(1 + A_T\sigma)} + \frac{2L_0}{V_T^0}$$

,

Where $L^\sigma = L_e(1 + \sigma/E)$ is the stressed length and E is the Young's modulus of the bolt material.

Introducing the time-of-flights for the respective waves that travel the way through the bolt and back in the initial unstressed length, as:

$$t_L^0 = \frac{2L_i}{V_L^0} \quad t_T^0 = \frac{2L_i}{V_T^0},$$

9.5 The mono-wave technique

The use of transversal waves generally requires special so called shear-wave sensors, as well as measuring equipment that is able to handle the two independent echoes. Most ultrasonic devices in the market use solely longitudinal waves for the determination of clamp loads.

This conventional time-of-flight method is based on variations in the time-of-flight of the single longitudinal bulk wave with load. Here the first order development of the time-of-flight can be approximated as:

$$t \cong t_0 \left[\frac{L_e}{L_i} (E^{-1} + A)\sigma + 1 \right]$$

Once the relationship between F and Δt (the change of time-of-flight due to axial load) is calibrated, and the time-of-flight data for both the stressed and unstressed states are measured, the bolt axial stress can be determined from the calibration curve.

The main drawback of the method is the requirement for pre-knowledge of the initial loading conditions as well as the initial bolt length. For fastened bolts in a structure, it is impossible to loosen the bolt to measure the length and the time-of-flight of the ultrasonic wave.

This linear ultrasonic technique for estimating the axial load is also especially unsuitable for short and highly stressed bolts. First, the change in the time-of-flight of the ultrasonic wave caused by the change in the axial load is so small that a very high resolution and reliability of the time-of-flight measurement is required. The linear method also neglects nonlinear deformation, such as deformation of the bolt head and non-ideal elastic properties of the threaded parts[28].

Several works have been performed on short bolts[29] [30]. Since the variation of ultrasonic velocity in the range of actual stress acting in the bolt, especially for short bolts, is very small, Jhang et al. [30] employed the phase detection method for a more precise measurement compared to the conventional pulse-echo technique which is more sensitive to noise. The experiment used the bolt M16/10.9T, and 5MHz ultrasonic transducers were located on the top and bottom of the sample to measure the TOF and the experiment results show that the ultrasonic velocity decreases linearly corresponding to increases in stress. Figure 12 shows the resulting calculated change-rate of the ultrasonic velocity versus stress.

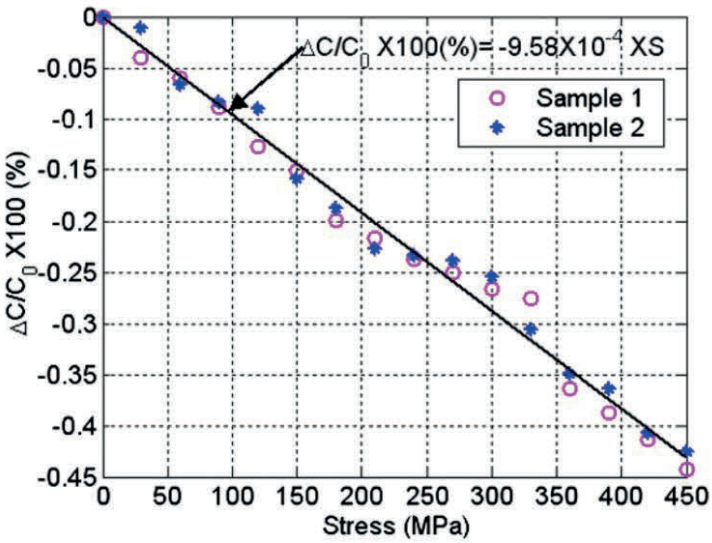

Figure 12. The resulting tensile testing results for change-rate of ultrasonic velocity vs. stress

Among work performed on longer bolts and rods, i.e. Liew et al.[31] used an ultrasonic pulse-echo for determining the change in wave velocity due to axial load for mild stress bars of the diameters 19 mm and 25 mm respectively. Since the accuracy of the applied stress is proportional to the effective length of the bar, the length was chosen to 1.5 m. The load was introduced with a torque wrench, ranging from 70 to 335 Nm. The study was conducted on three physically identical specimens for each nominal diameter. Both 19 and 25 mm nominal diameter bars showed a trend of decreasing ultrasonic wave velocity with applied load. The 25mm samples, however, showed a significantly larger variation between samples. This was assigned to the larger dimension and a presumed lower microstructural homogeneity. Also a higher and more consistent strain deduced at the smaller diameter indicate that the effect of acoustoelastic is more obvious and in a smaller diameter bar. The resulting decrease in wave velocity was assigned to degradation or loss of strength of the material.

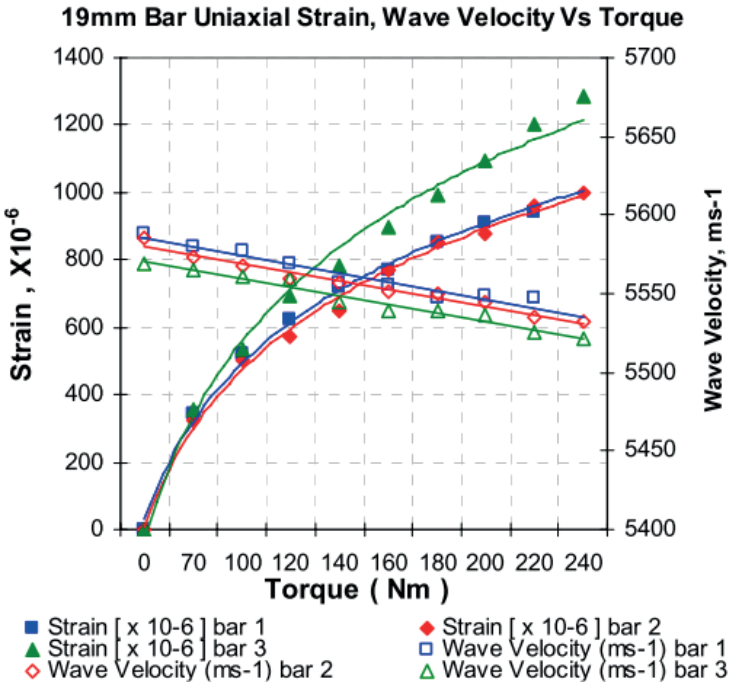

Figure 13. The 19mm bar axial strain and wave velocity versus torque.

Washer et al.[32] measured changes in ultrasonic velocities as a function of stress in pre-stressing tendons of both rod and seven-wire helical strand geometries over a constant gauge length using a set up with EMATs. The primary advantage of EMATs over piezoelectric transducers is that no mechanical coupling is required, which allows non-contacting operation and reduces effects of coupling variations on measurements. The sensors can also be moved independently along the specimen being tested. For acoustoelastic measurements this allows ultrasonic velocities can be measured at different stress levels without changing the distance between transducers. The system for velocity measurements consisted of three EMATs. A transmitter EMAT driven with a tone burst of three cycles at 320 kHz was used to generate the wave in the specimen. The wave was detected by a pair of receivers that were placed at a known and fixed distance apart. The distance between the receivers was nominally 0.5 m (Figure 14).

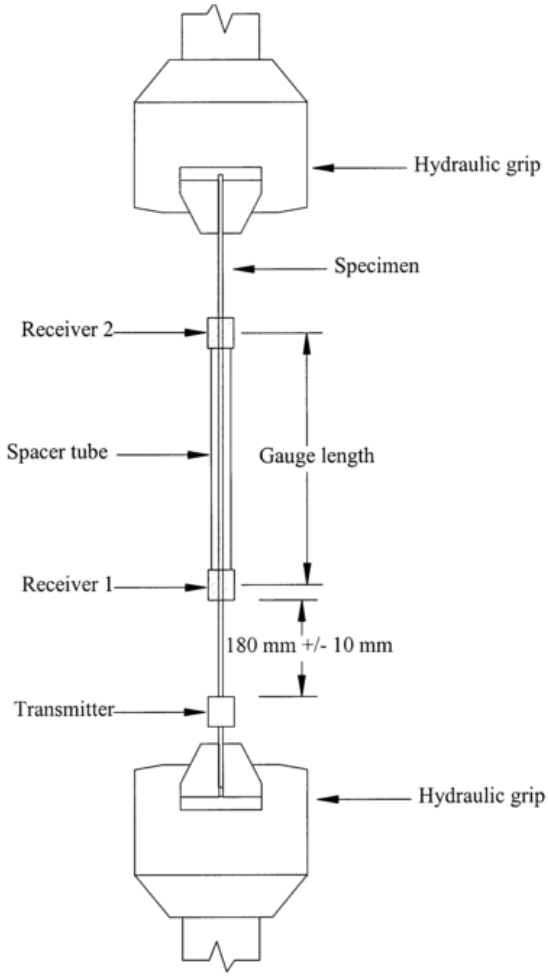

Figure 14. The setup with one EMAT transmitter and two EMAT receivers.

As the changes in velocity due to variations in stress are very small, also the effects of dispersion need to be considered. Due to Poisson's effect, the diameter of the waveguide will be reduced when a tensile stress is applied. The phase velocity of a longitudinal wave propagating in a circular waveguide will increase as the ratio of to the waveguide radius to wavelength decreases. This means that an increase in wave velocity will counteract the acoustoelastic effects. Nonlinear effects were observed and explained. In all, it was found possible to relate wave velocity changes to applied stress in a seven-wire strand, introducing a new approach for developing health-monitoring instrumentation for pre-stressing tendons. The experiments, however, also found the wave velocity and velocity constants to vary significantly for materials with the same specifications, but manufactured at different times or by different manufacturers. This would have significant impact on the practical application intended.

9.6 The bi- wave technique

For a bolt in uniform tension, the travel times of the longitudinal and transverse waves propagating along the axis of a bolt can be used to calculate the stress acting on the bolt. This is true because the material's elastic and acoustoelastic characteristics can be measured independently and the only remaining unknowns affecting the travel times are the bolt's length and the magnitude of the stress. Because the variation of shear velocity with stress is different than that of the longitudinal velocity, the two measurements are sufficient to eliminate the bolt's length and evaluate the stress.

The requirement for initial data from state before actually tightening the bolt can therefore be avoided if longitudinal and transverse waves can be generated simultaneously.

The velocities of the both waves are significantly different. As the two waves travels the same distance, they carry with them different acoustoelastic effects As the dependence on propagation length is eliminated by the phase ratio of the two waves, the acoustoelastic response can be extracted.

The first order development of the time-of-flight ratios can then be approximated as:

$$\frac{t_T^\sigma}{t_L^\sigma} \cong \frac{V_L^0}{V_T^0}\left[1 - \frac{L_e}{L_i}(A_T - A_L)\frac{F}{S_e}\right]$$

However, the length L_e and the difference between the acoustoelastic coefficients, $A_T - A_L$, are needed. By performing calibration tests on bolts made of the same material, but with different dimensions and tightening configurations, these unknown can be deduced[8].

Taking the derivative with respect to F, the following slope is obtained:

$$\beta = -\frac{V_L^0}{V_T^0}\frac{L_e}{L_i}\frac{(A_T - A_L)}{S_e}$$

Provided both the longitudinal and transverse wave velocities are known, no time-of-flight measurement for the unstressed state is required, and that it is possible to measure the effort in already tightened bolts without previous measurements or knowledge of the exact length of the unstressed bolt[8]

Since the velocity variations resulting from the load conditions of relevance are very small, the analytical equipment requires a high resolution for measuring the time-of-flight values. Piezoelectric transducers exists that can generate both longitudinal and transverse bulk waves simultaneously, thus removing the errors connected with repeatedly changing the position of

analysis. However, for piezoelectric transducers, the required contact with the bolt surface will still depend on the surface conditions and cause errors associated with the mechanical coupling.

In general, bolts are not uniformly loaded. Instead, they have regions at the ends which are either free of stress (that part of the bolt which extends past the nut) or are subject to a lower level of axial stress than is the shank of the bolt. In the case of short bolts, these regions can be a significant portion of the total length and must be accounted for. Unstressed portions can be accounted for by introducing a correction term[14]. For accurate results for short bolts a precise time measurement is required. As the longitudinal and transverse waves were excited simultaneously, the time resolution could be enhanced compared to traditional measurements.

While the bolt material is assumed to be isotropic, it is also more correctly characterized as transversely isotropic - with the axis of the bolt being the axis of symmetry. However, since the waves will travel along the axis of symmetry and the stress will act along this same axis, this anisotropy will not affect the measurements or the analysis, regardless of the extent to which the isotropy assumption may not hold[14].

The models for calculating the tightening stress based on acoustoelasticity theory all involve parameters that requires calibration tests, i.e. the material parameters of the bolts (elastic constants, acoustoelastic coefficients) and their tightening configurations (effective length under stress). As the bolt material may have been heat treated for high strength, and the material might also be degraded due to long-term service and corrosion, the pure steel material may not be a relevant reference material to conduct calibration measurements on. This means that calibration tests for determining the acoustoelastic material constants can be complicated. It may therefore be useful to determine the elastic constants from separate measurement on the bolt head of the bolt to be analyzed. The bolt head is free of load and accessible for inspection even after fastening. The transducer is then connected to the side of the bolt head, and its size deduced by e.g. a micrometer.

The method is also not only influenced by the stress in the bolt but also by temperature and plastic elongation leading to some limitations which have to be observed[26].

Being the focus of the survey, various experimental work employing the bi-wave method are presented in greater detail in Chapter 3.

9.7 Techniques based on resonance frequency

The resonance method uses the variation of resonance frequencies of bolts for stress measurement.

In the 70ies, Heyman[33] used nonlinear ultrasonics to correlate the frequency shifts with load caused by bolt elongation in the longitudinal direction. With the assumption that complete reflection occurs at the flat and parallel ends of a bolt, a simple one-dimensional isolated resonator model was applied to ultrasonic waves propagating in a bolt. The work combined the pulse-echo and the continuous-wave (cw) ultrasonic techniques, where in the latter the sample acts as an acoustic resonator – with changes in the mechanical resonant frequency is linearly

related to the applied stress. Since the frequency can be deduced with a higher accuracy than the time-of-flight data of the pulsed ultrasonic techniques, the resulting resolution is superior. Continuous wave techniques may however be difficult to perform practically without transducers on both ends of the item inspected. In the combined technique employed by Heyman, known as the pseudo-continuous-wave technique, however a transducer was connected to one end of the sample and excited by a source of variable frequencies. This excitation signal was periodically interrupted, when the transducer instead acted as receiver for the ultrasonic waves. The signal obtained was used as a control signal to maintain the frequency of the source to the mechanical resonance peak of the sample.

In the 80-ies, Joshi and Pathare[34] employed a pseudo-continuous-wave technique based on carrier phase detection to monitor changes in mechanical resonant frequency of 100 mm bolts made from a high-strength steel. The diameter was 12.5 mm and the ends were machined flat and parallel to each other. Transducers with fundamental resonant frequencies of ~5 MHz were used to generate longitudinal waves in the bolt. To determine the resonant frequencies, the bolt was treated as a simple one dimensional acoustic resonator and it was assumed that complete reflection occurred at the flat and parallel ends of the bolt. The bolts were loaded in tension with stresses up to 270 MPa, and the frequency shift was measured for different values of applied stress. Figure 15 shows the resulting change in mechanical resonant frequency as a function of the applied stress.

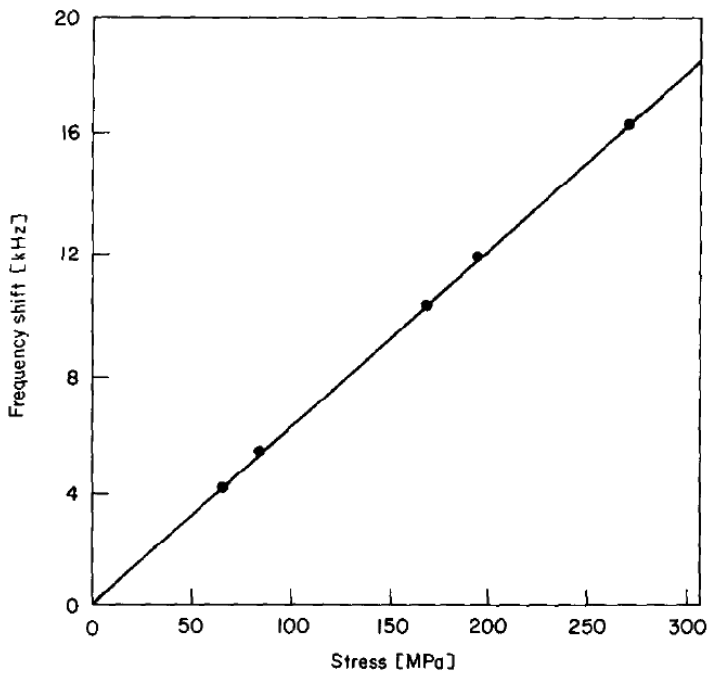

Figure 15. The change in mechanical resonant frequency as a function of the applied stress.

The frequency was found to change linearly with the applied stress, the change being ~60 Hz/MPa of applied stress. This means that the sensitivity of the technique is high, even to small

variations in bolt stress. To confirm that friction did not affect the measurements, as when using a torque wrench, experiments were conducted with varying friction conditions. The change in was found to be less then +/-2%. Additionally, the instrumentation used in this work allowed compensation for temperature variations. A change in the ambient temperature produces a change in the length of the bolt as well as in its acoustic velocity. This creates a problem when strain in a bolt is monitored over a long period of time, as results from temperature changes could be mistaken for changes in bolt stress. In the present experiment, the phase shift was able to compensate for temperature variations of approximately +/- 10 °C. This, however, requires operating away from the mechanical resonant frequency, thus may result in reduced sensitivity to changes in bolt stress.

Also the axial shear-wave EMAT, which generates and detects the shear (transverse) wave propagating in the axial direction of the bolts, can also be useful for resonance measurements focused on the outer surface region[5]. The wave energy of the fundamental mode is concentrated to the outer surface region on a cylinder, and as the mode becomes a higher overtone the peak amplitude moves to the inside. Then it is possible to evaluate the radial gradient using different resonance modes. Figure 16 shows an EMAT for generating axial shear (transverse) waves in a bolt head.

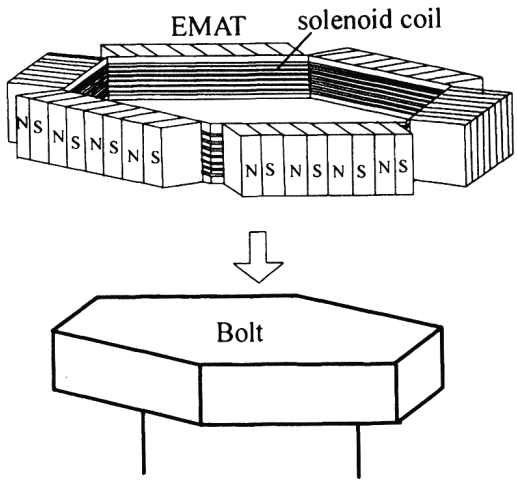

Figure 16. An EMAT for generating axial shear (transverse) waves in a bolt head[5].

The thin permanent magnets are arrayed to serve the alternating bias fields normal to the side faces, and the solenoid coil wound in a hexagonal shape. When the driving current is applied, the shearing forces in the axial direction arise periodically and generate the shear waves propagating in the circumferential direction – with the polarization along the bolt axis. For a cylindrical rod, the axial shear resonance modes can be easily determined. At a lower resonance mode, the shear/transverse wave propagates near the outer surface region, and as the mode becomes higher the vibration penetrates inside. This is especially the case for hexagonal rods. The bolt head plays a role of transmitting axial force, and its small volume is subjected to complicated elastic deformations of tension, bending and shearing. This stress field is axis-

symmetric and develops as the tightening advances. The method, however, requires the pre-knowledge of material constants and bolt lengths.

In 2001, Hirao, Ogi and Yasui[35] presented an ultrasonic method to monitor the acoustoelastic response and deduce the bolt axial stress using a shear-wave EMAT. The axial stress was estimated using both the resonance frequency shift and from the phase method (i.e. based on the time-of-flight of the echoes), using the same instruments. By eliminating error sources associated with the use of contacting piezoelectric transducers, the contactless aspect of the EMAT allows a higher reproducibility. The EMAT for generation and detection of the polarized shear waves along the bolt length consisted of a pair of Nd–Fe–B permanent magnet blocks and a spiral elongated coil under the magnets with an effective area of 8.5 × 12 mm^2. The polarized shear wave was generated with the magnetostrictive mechanism at the bolt top face.

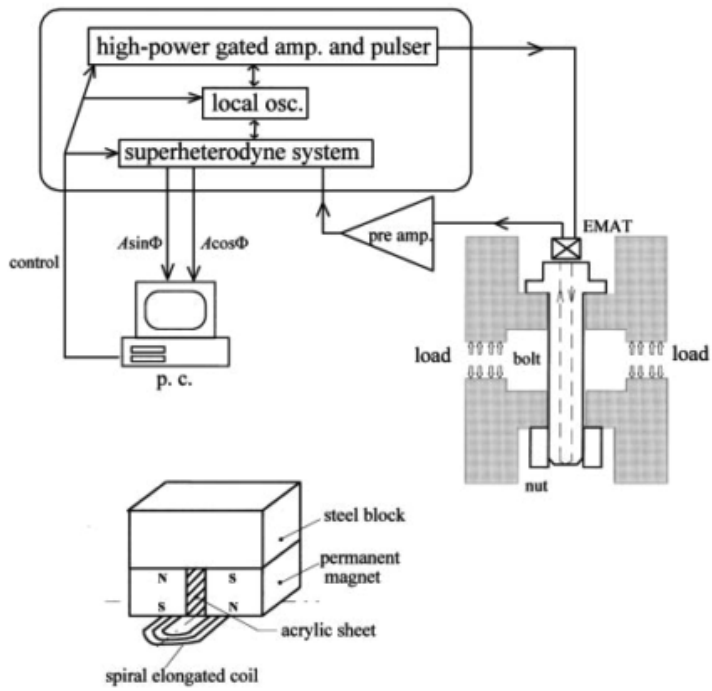

Figure 17. The set-up and the shear-wave EMAT used.

For short bolts also the stress distribution at the nut-joint portion influences the apparent acoustoelastic response. As the stress resolution decreases for short bolts, the choice of the phase or resonance method should also be based on the bolt length. While the phase detection is more suitable for long bolts, the resonance measurement is more applicable for short bolts. The two types of bolts investigated, aimed for automotive applications, both had flanges at the heads. The shorter Bolt A was measured with both techniques, and had an initial length of 27.5 mm and a diameter of 10.5 mm. The longer Bolt B had an initial length of 53.7 mm and a diameter of 8.6 mm. The phase change was also measured for a standard M24 bolt with length 155 mm.

For the resonance method, the EMAT was run with long tone bursts of 200 ms duration to excite the overlapping multiple reflections in the bolts. The resulting shift in resonance frequency versus loading for bolt A is displayed in Figure 18. The non-linearity observed, particularly at low loads for bolt A, indicates that the stress distribution under the nut change with load.

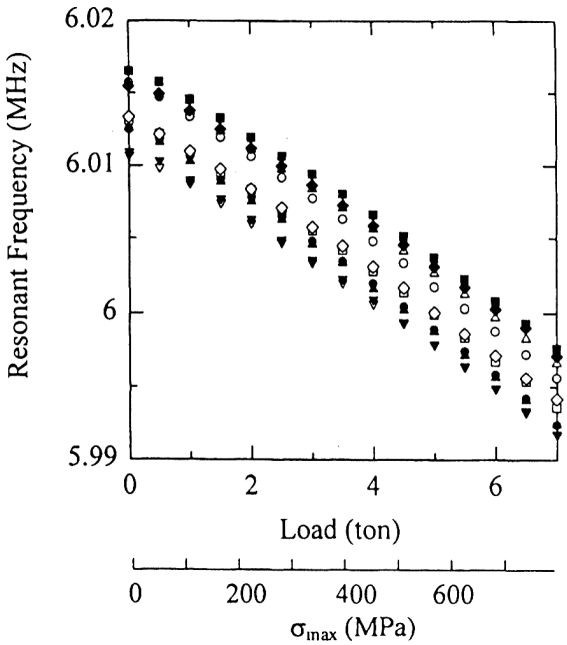

Figure 18. The shift in resonance frequency versus loading for several bolts of type A.

For the phase measurement the EMAT was used with 5 MHz tone bursts at ~300 V, and two echoes where selected from the received train of reflections. As seen in Figure 19, the phase difference for Bolts A and B was proportional to the load.

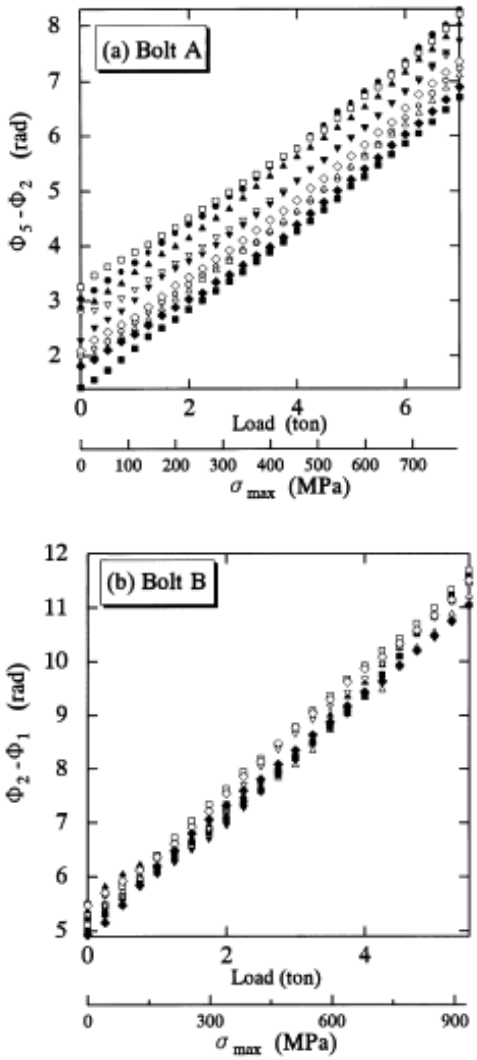

Figure 19. The phase shift versus loading for several bolts of type A and B, respectively.

The scattering between different bolts of each type A and B was mainly attributable to small variations in bolt length (< 0.04 mm for both types). For an ultrasonic velocity of 3240 m/s this variation would correspond to ~ 0.7 tons. Also, the temperature has an influence on the phase measurements. In all, the phase methods and the resonance methods using shear-wave EMAT showed a high accuracy (~5% for 5 ton) for measurements of axial stress, also for short bolts. The phase measurement on the longer M24 bolt showed a linear dependence on stress, as well as the expected higher accuracy compared to the shorter bolts. The methods, however, requires measurements of the initial state, i.e. before tightening of the bolt.

9.8 Experimental work employing the bi-wave technique for deducing bolt stress

9.8.1 Free bolts of lengths 80-160 mm, employing an elder sing-around technique

In an early work from 1986, Johnson et al.[14] used an ultrasonic sing-around technique which allowed both longitudinal and transverse waves to propagate along the axis of a bolt.

In total 23 bolts of Grades 5 and 8 with diameters of 19.1 and 22.2 mm were analyzed, and the lengths varied between 80 and 160 mm. The known load was applied to the bolt with a tensioning device (Figure 20), and the effects of bending forces were minimized by supporting the head of the bolt.

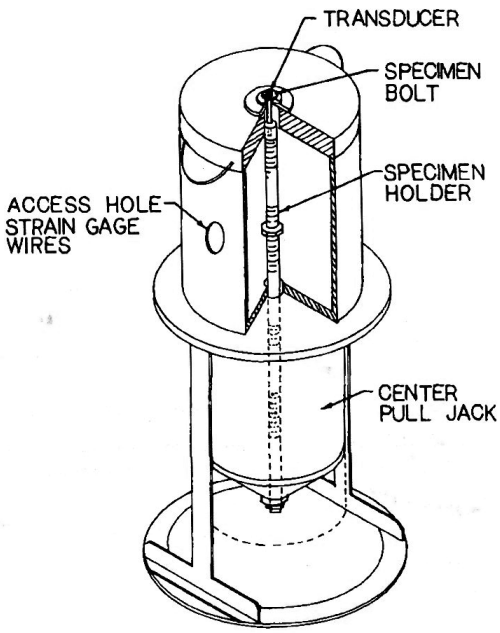

Figure 20. The bolt-tensioning device used.

The RF tone burst from the gated amplifier drives a transducer with either a 10 MHz longitudinal wave element or with a 5 M Hz shear wave element. The equation used to resolve the stress, T, was:

$$T = \frac{t_1 V_{10} - t_2 V_{20}}{t_1 V_{10} d_1 - t_2 V_{20} d_2 - 2\kappa(d_1 - d_2)}$$

where t_1 and t_2 are the travel times for the longitudinal and transverse waves, respectively, V_{10} and V_{20} are the respective velocities in the unstressed bolt, and the correction factor κ accounts for the portion of bolt length that is actually unstressed. The acoustoelastic material coefficients, d_1 and d_2, were in turn defined as:

$$d_1 = \frac{D_1}{2(\lambda + 2\mu)} \quad d_2 = \frac{D_2}{2\mu}$$

$$D_1 = -[\lambda + 2\ell + (\ell + \lambda)(4\lambda + 10\mu + 4m)/\mu]/(3\lambda + 2\mu)$$

$$D_2 = -[4\lambda + 4\mu + m + \lambda n/4\mu]/(3\lambda + 2\mu)$$

where λ and μ are the second-order Lame's constants and l, m and n are the third-order Murnagan's constants.

In order to calculate the stress, the values of d_1, d_2, V_{10}, V_{20}, and κ were deduced by a series of calibration experiments. The values of V_{10} and V_{20} were acquired from time-of-flight measurements on ten short samples. As a high accuracy is required, a phase-detection method was used instead of the sing-around method. After measuring the initial lengths of a series of bolts of a particular diameter, the values of d_1, d_2 and κ were determined from the slopes of the curves for the time-of-flight versus load for the longitudinal and transverse waves, respectively. After this calibration, the bolt axial stress could be calculated without pre-knowledge of the initial load conditions.

Each bolt investigated was subjected to a sequence of loads up to ~70 % of its yield stress. At each load, time-of-flight measurements of the longitudinal and transverse waves, t_1 and t_2, were performed, and the resulting calculated stress was compared with the known applied stress. Figure 21 exemplifies the calculated stress versus ram pressure for one type of bolts, where each graph includes a reference plot of ram pressure versus bolt stress calculated from the known applied loads. The slopes were found to vary with the bolt diameter.

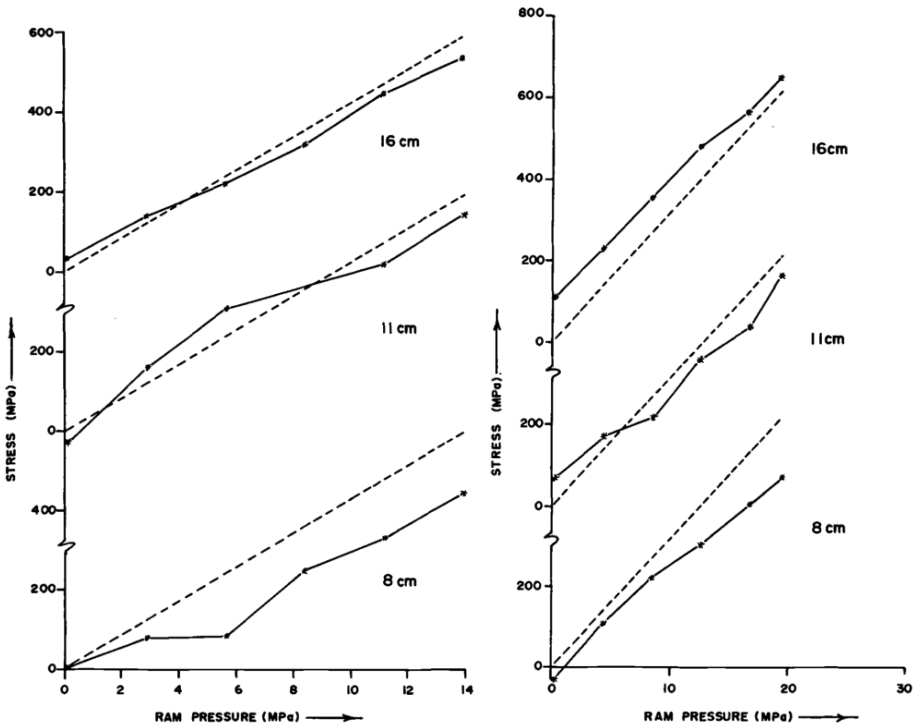

Figure 21. The calculated stress versus ram pressure for Grade 5 bolts with three different lengths and bolt diameters of (a) 19.1 mm and (b) 22.2 mm, respectively. The dashed reference line indicates the ram pressure versus bolt stress calculated from the known applied load and bolt cross-sectional area.

For applied stresses in the range of 0 to 600 MPa, the calculated stresses were generally found within 100 MPa of the known applied stress. In the higher stress range, the results showed 4-20 % reliability, while the largest percentage errors were found in the low stress region. The error is generally an increment of stress, rather than a percentage of applied stress.

In all, the resulting calculated stress acting on the bolt showed an improved accuracy compared to conventional mono-wave techniques at the time of the study. In this work, no measurements were conducted in order to deduce the possible effect from plastic flow.

9.8.2 Free bolts of lengths up to 50 mm for automotive applications

In work dated in 2000, Yasui et al.[28] used a combined L/S mode transducer for bi-wave measurements on short bolts for automotive applications during exposure to high axial loads. The results were also compared to analyses using the conventional linear method based on longitudinal waves only.

The experiments were conducted on 30 mm and 50 mm long bolts of the material SCM440. Both ends were finished to be flat and parallel, and the exact dimensions of bolts A and B are displayed in Figure 22.

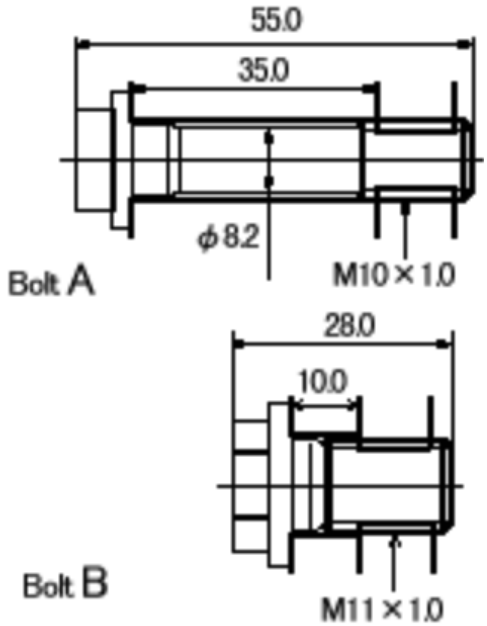

Figure 22. The bolt geometries used.

The bolts were fitted into a load cell where the axial load was applied by a torque wrench. The error in the axial load cell was found to be within ±1%. Different maximum loads were applied to the bolts A and B, respectively.

The combined ultrasonic transducer Panametrics-X1045 from Olympus simultaneously generated and received a 10 MHz longitudinal wave and a 5 MHz transverse wave. The transducer with 6.3 mm diameter was attached with a viscous coupling medium. The time-of-flight measurements were carried out with an ultrasonic pulser-receiver and an A/D converter with minimum sampling interval of 10 ns. Figure 23 displays the resulting waveform of the longitudinal (L) and transverse (T) waves of bolt B, along with their frequency spectra.

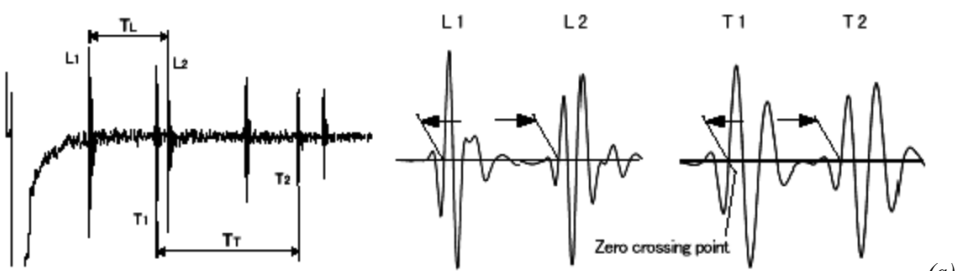

(a)

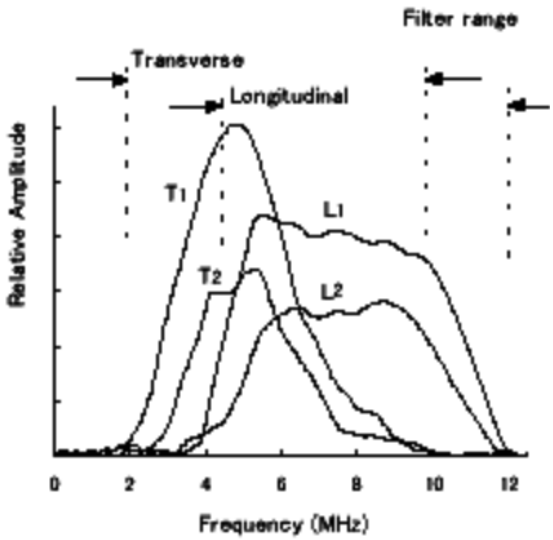

(b)

Figure 23. (a) The received waveform of the longitudinal (L) and transverse (T) waves of bolt B, with the zero-crossing method used for deducing the time-of-flight between echoes, and (b) the corresponding frequency spectra.

The result from the velocity ratio-method (bi-wave technique) was compared to the result when employing the change in time-of-flight for the longitudinal wave alone (conventional linear method). The both calibration curves are displayed in Figure 24.

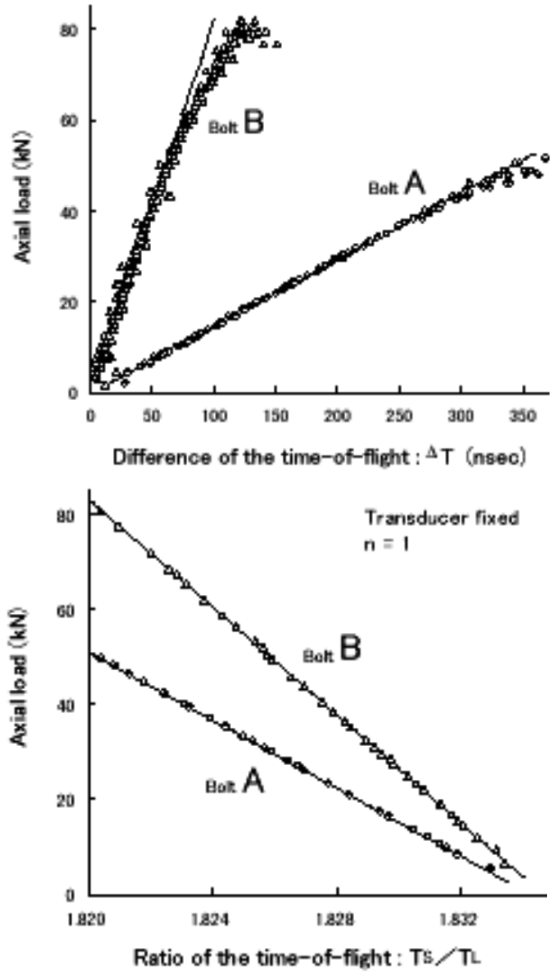

(a) *(b)*

Figure 24. The calibration curves obtained for 10 specimens of bolts A and B, respectively, employing (a) the linear ΔT-method and (b) the bi-wave velocity ratio-method, respectively.

In Figure 24a, the calibration curve of bolt A shows a linearity, while bolt B obtains a significant error subjected to nonlinear effects. This nonlinear extension of the stressed part of bolt B is caused by the geometry of bolts, where a high stress appears locally at the threaded portion and at the corner of the seating, respectively.

In Figure 24b, the calibration curves obtained by the velocity ratio was performed on only one specimen of the bolts A and B, respectively, and with the transducer being fixed. Both calibration curves show a better linearity compared to Figure 24a, and the deviation from linearity is quite small also at high loads for bolt B.

However, the calibration curves obtained by the velocity ratio for five different specimens of bolt B showed a lower correlation between different specimens (Figure 25). This indicates that even small variations in geometry and material properties of short and highly stressed bolts can provide non-negligible errors for the axial loads estimated.

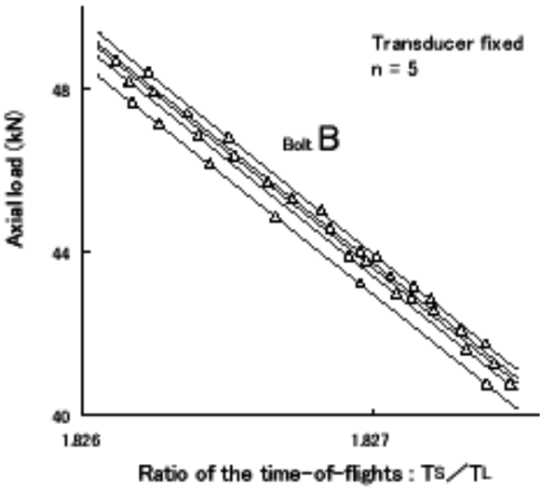

Figure 25. Calibration curves obtained for five different specimens of bolt B.

The repeatability obtained from the bi-wave method was also smaller for both bolts in trials where the transducer was repeatedly removed and attached (Figure 26). This error induced by frequent detaching the transducer was assigned to variations in thickness in the coupling medium.

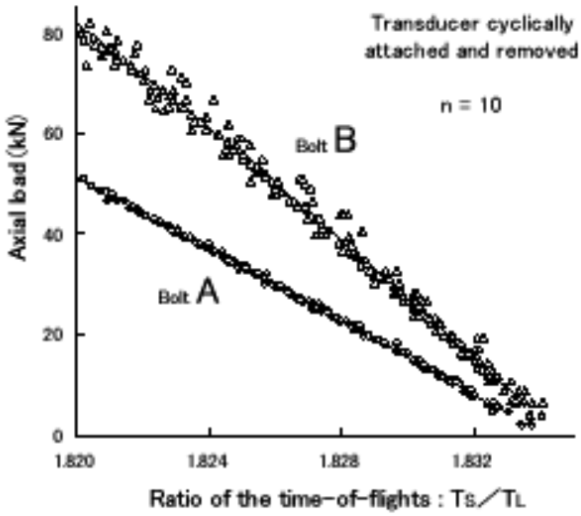

Figure 26. Errors induced by frequent detaching the transducer.

In all, the bi-wave method provided reasonable axial load for 50 mm long bolts, while noticeable errors were observed for shorter bolts of 30 mm. The technique also requires reduction in errors caused by the changes at the interface between the transducer and the bolt head.

9.8.3 Free 42CrMo4 steel bolts, up to 215 mm long

In work dated in 2007, Chaki et al.[27] used a combined ultrasonic transducer for simultaneous generation and detection of longitudinal and transverse waves for measurement of the tightening force in bolts. The study aimed at a simplified calibration procedure to obtain an absolute automation of tightening control.

The 42CrMo4 steel bolts were of diameters 12 mm (HM12) and 20 mm (HM20), respectively, and the longest bolts evaluated for each diameter were 207.38 mm (for d=12 mm) and 215.58 mm (for d =20 mm). The end faces of the bolts were finished to be flat and parallel.

For bolts tightened by a torque wrench, the state of stress generated is actually a combination of tension and torsion. The shear stress induced by torsion has, however, been found to have only small influence on the ultrasonic measurement of tightening tension[36]. The uniaxial stress loading was accordingly carried out in pure tension with an INSTRON testing machine, equipped with a force sensor and an extensometer. The ultrasonic measurements were carried out during loading and unloading, and the applied stresses were limited to 75 % of the yield strength in order to avoid plastic strains. To obtain a stable and reproducible system, each bolt experienced a loading cycle up to 20 % of its yield strength prior to the actual measurements.

The broadband normal-incidence transducers used emit and receive the longitudinal or transverse separately through an acoustic coupling layer. The probe diameters used were 12.7 mm and 6.35 mm, for the two bolt diameters, respectively. The path of the ultrasonic waves can include several round trips until complete dissipation of the ultrasonic energy, and the

signals were sampled and visualized at 500 MHz. Figure 27 shows an example of the longitudinal and transverse wave signals received after propagation in an unstressed 215.58 mm long HM20 bolt.

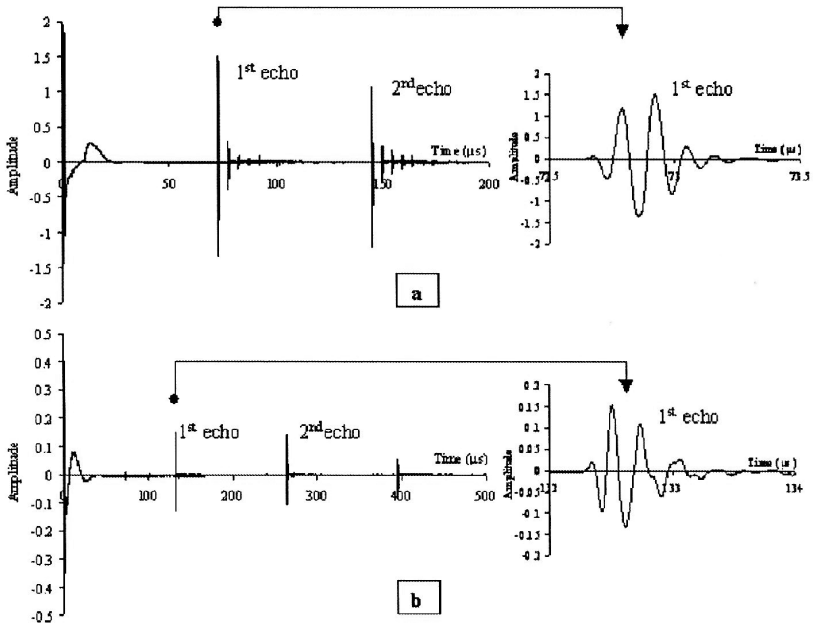

Figure 27. The waveforms of the (a) longitudinal and (b) transverse wave received for an unstressed HM20 bolt.

In order to calculate the load from the time-of-flight ratios of the longitudinal and transverse waves, the effective length, L_e, and the difference between the acoustoelastic coefficients, $A_T - A_L$, are required:

$$\frac{t_T^\sigma}{t_L^\sigma} \cong \frac{V_L^0}{V_T^0}\left[1 - \frac{L_e}{L_i}(A_T - A_L)\frac{F}{S_e}\right]$$

These unknown were deduced from calibration tests on totally threaded bolts made from the same material but with different dimensions and tightening configurations. For a bolt tightening configuration, j, with a given bolt diameter, the slope of the equation derivate with respect to the axial load, F:

$$\beta_j = -\frac{V_L^0}{V_T^0}\frac{L_e^j}{L_i^j}\frac{(A_T - A_L)}{S_e}$$

As the difference $A_T - A_L$ is dependent on the bolt material only, it will remain constant between two different tightening configurations. The value of $A_T - A_L$ can thus be eliminated by taking the ratios of the slopes for two different configurations.

$$\frac{\beta_j}{\beta_k} = \frac{L_e^j}{L_i^j}\frac{L_i^k}{L_e^k}$$

This allows calculation of the length L_e, after which also the value of $A_T - A_L$ is provided. In order to verify that the difference $A_T - A_L$ actually is entirely constant, additional calibration tests can be performed. For one total length, L_i, several grip lengths, L_g, may be used. Conversely, for one grip length several total lengths may be tested by cutting up the bolt. Here totally threaded bolts are preferably used since they enables an equivalent cross-sectional area, and thus provides an average stress. For a configuration, j, with a given bolt diameter, L_e is given by:

$$L_e^j = L_g^j + \delta L$$

The distance δL depends on the bolt geometry, such as head and nut thickness, diameter, and thread for a given tightening load. For two configurations, j and k:

$$L_e^j - L_e^k = L_g^j - L_g^k$$

As the lengths L_g^j and L_g^k are usually known from bolt geometry, the two lengths L_e^j and L_e^k can be calculated using pairs of all the configurations. Figure 28 shows the resulting calibration curve of t_T^σ / t_L^σ versus the axial load for a tightened HM20 bolt during loading and unloading.

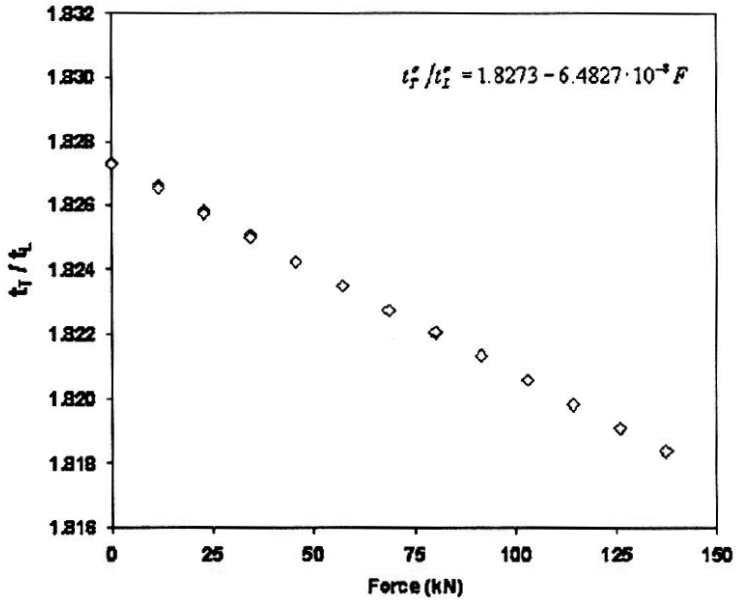

Figure 28. The calibration curve obtained for the HM20 bolt with L_i =215.58 mm and L_g=144.50 mm.

This linear relation allows the evaluation of the axial load, F, for similar bolts and tightening configurations without loosening the bolts. For a single tested bolt, the resulting measurement uncertainty was estimated with ±10 % at 95 % reliability.

The uncertainty of the velocity measurements alone was estimated to ±0.8 m/s for 95 % reliability. This estimation includes both the resolution of the instruments and the statistical measurements. For both longitudinal and transverse waves, the velocities slightly differed depending on the bolt diameter and length, L_i. These velocity differences were larger than the measurement uncertainty, and were assigned to diffraction phenomenon of elastic waves in a limited bolt geometry. For a given diameter, however, the ratio V_L^0/V_T^0 was almost identical for different tightening configurations. This means that for confined propagation, V_L /V_T^0 is insensitive to variation of the length but is sensitive to varying diameters.

In all, the axial load on a bolt of ~215 mm could be determined with an uncertainty of ±10 % at 95 % reliability. The determination of L_e and A_T–A_L requires only two calibration tests applied to one bolt under two grip lengths. Provided that parameters for V_L^0 /V_T^0, δL and A_T–A_L are characterized for different bolt materials and geometries, this allows for an absolute automation of tightening control.

9.8.4 Clamped bolts of length 115 mm tightened to yield

The determination of the residual load of bolts tightened into the yield is of interest for e.g. engine bolts such as cylinder head bolts and con rod bolts. Hartmann[26] used simultaneous generation and detection of both longitudinal and transversal waves in order to determine the residual clamp load of bolts tightened into yield. The bi-wave technique made it possible to

eliminate this unknown parameter, i.e. the plastic elongation for bolts tightened to yield, without need to disassemble the joint.

A bolt tightened into yield has a defined clamp load determined by the strength of the bolt. However, as soon as tightening tool stops, the torsional stress in the joint relieves and the residual stress drops slightly below yield. Further release of the stress in the bolt occurs as the joint settles, after which the joint is back in the elastic region.

The method for determining clamp load with the conventional linear method, employing a single longitudinal ultrasonic wave, is displayed in Figure 29. As the ultrasonic testing cannot differentiate between a purely elastic and a plastic deformation, the plastic elongation of the bolt becomes a problem. After being tightened into the yield (point A), the bolt can be further stressed to point B by external forces or different thermal expansion of the bolt and the jointed components. Although the plastic deformation at point A might have been determined previously, the plastic deformation at point B is unknown. As the joint is cooled down to room temperature to enable an ultrasonic clamp load testing, the load is further decreased along the elastic line. The actual load can only be determined by untightening the bolt and measure the difference in the ultrasonic time delay between point C and the completely unloaded bolt.

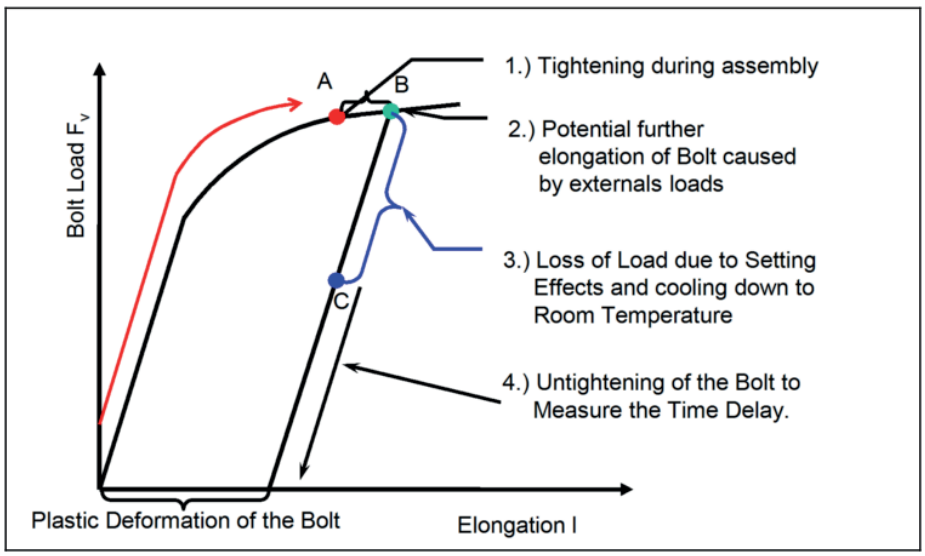

Figure. 29 Determination of the residual clamp load of a bolt tightened into yielding using the mono-wave ultrasonic method after untightening.

The solution when employing the bi-wave method is displayed in Figure 30. The experimental work employed a fatigue tester and the sampling rate of the ultrasonic transient recorder was set to 2000 Hz. In order to incorporate the influence of thermal elongation, the test rig was exposed to 150 °C for 5 hours and cooled down to room temperature to simulate a real engine application.

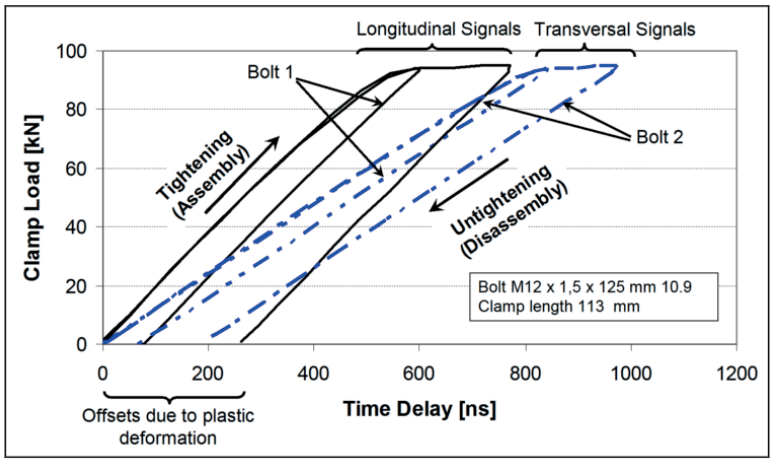

Figure 30. The behavior of longitudinal and transverse waves for an M12x1.5x125 mm bolt with a clamp length of 113 mm tightening into yield.

The influence of plastic deformation was found to be higher for the longitudinal waves compared to the transversal waves. This effect allowed for a compensation of the plastic deformation, after which the residual clamp load of bolts tightened into yield could be determined without disassembling the joint. After calibration at different levels of plastic deformation, a bi-linear equation was deduced to describe the bolt load as a function of the time delays of both waves. For 21 different bolt specimens of grade 10.9 and geometry M10x115 mm, the maximum deviation from the clamp load of the load cell was about ±4 %. The accuracy of the method may however be improved by employing a second order equation instead of a bilinear calibration function. The accuracy was found to decrease for shorter clamp length. Any changes in the bolt stress or elongation lead to higher changes in the ultrasonic time delay, which consequently leads to a better accuracy. The accuracy was also found to decrease for higher levels of plastic deformation. Additionally, the accuracy was found to be significantly better for bolts with their thread rolled after heat treatment compared to bolts that were rolled before heat treatment. Thread rolling not only induces residual stresses in the thread, but also locally work-hardens the material in the root of the thread. These changes in the microstructure are smaller for bolts that are heat treated after thread rolling, and it is assumed that the microstructure has an influence on the ultrasonic sound field.

9.8.5 **3.1.5. Free bolts of lengths up to160 mm using mode converted waves**

Simultaneous generation and measurement of both longitudinal and shear waves in bolts can also be made using mode conversion of longitudinal waves. Figure 31 describes the mode conversion of a primary longitudinal wave in a bounded solid immersed in fluid. A pair of transmitted longitudinal (L) and transversal (T) waves penetrates into the solid with specific refraction angles depending on the polarization of the waves. As the waves reach the surface of the solid, they produce a pair of mode-converted waves (LT, TL) back towards the front surface[13].

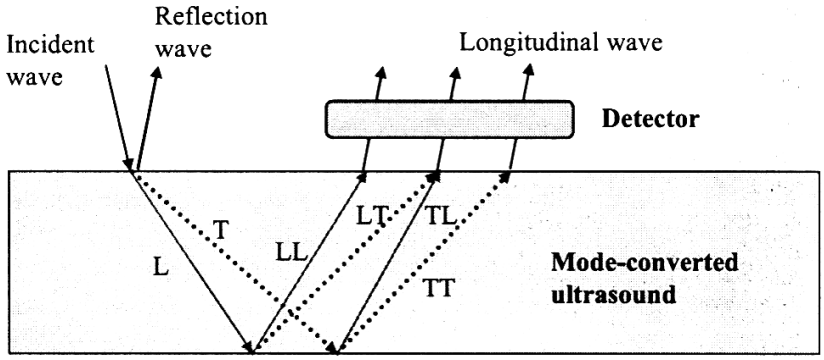

Figure 31. Mode-conversion of ultrasonic waves in a bounded solid[13]

Kim and Hong[13] proposed an ultrasonic technique employing mode-converted ultrasound for determining the axial stress in high-tension bolts. An acoustic transverse wave that propagates in a plane stress state undergoes a phase velocity change along its path. This is similar to the birefringence effect of polarized light in optics according to its wave vector. The method, however, applies only to plane stress normal to the propagation vector. In this work, however, a theoretical expression for axial stress in terms of the time-of-flight measurements was obtained by combining the velocity ratio method to calculate the tensile stress of bolts with the birefringence concept. The transverse TT-wave generally is weak due to strong attenuation. For this reason, the mode converted LT-wave, which contains both longitudinal and transverse wave velocities, was chosen for the analyses.

A single piezoelectric transducer was used, and the ultrasonic signals produced in the bolt were captured via an acoustic lens. As the time-of-flight calculation from the LT-wave requires knowledge of its wave path, a ray analysis was required. As the ray from a defocused spherical lens is incident on the cylindrical solid with a small angle, the path and time-of-flight of the mode-converted LT-wave can be deduced using Snell's Law and the geometric conditions. For a long enough cylinder, all refraction angles can be assumed to be very small. This simplification, and pre-knowledge of the acoustoelastic material coefficients involved, allows the calculation of the axial stress of the isotropic cylindrical material from the ratio of the longitudinal LL wave and the mode converted LT wave.

The determination of the acoustoelastic material constants is, however, not always straight forward. If the bolt material has been heat treated, or experienced degradation due to long-term service and corrosion, the pure steel material may not be a relevant reference material to conduct calibration measurements on. It may then be useful to determine the elastic constants from separate measurement on the bolt head of the actual bolt to be analyzed. The bolt head is free of load and accessible for inspection even after fastening. The transducer is connected to the side of the bolt head, and its size is deduced by e.g. a micrometer. In the work of Kim and Hong, the resulting accuracy after measuring on the side of the bolt head was ~5 %. The error was assigned to the different measurement points for measuring on the bolt head for calibration and for the actual analysis along the bolt axis. Also, long high-tension bolts are actually anisotropic, i.e. with different material properties along and transverse to the axis due to e.g. heat treatment and cold-drawing during manufacturing.

The bolts analyzed were of material and geometry M22 SCM435, but with the different lengths of 160 mm (Bolt A) and 134 mm (Bolt B). The bolts were subjected to tensions from 0 to 1.8 tons using a universal tensile machine. The increment steps were 200 kg and a 5 minutes holding time was employed at each load prior to ultrasonic analysis. The ultrasonic waves were generated and detected using a 10MHz transducer and an acoustic lens with a small aperture angle. The bolt head was cut from hexagonal to a round shape, and the transducer and acoustic lens were placed on the flat bolt head surface using a coupling medium.

The waveforms of the ultrasound for bolt B are exemplified in Figure 32.

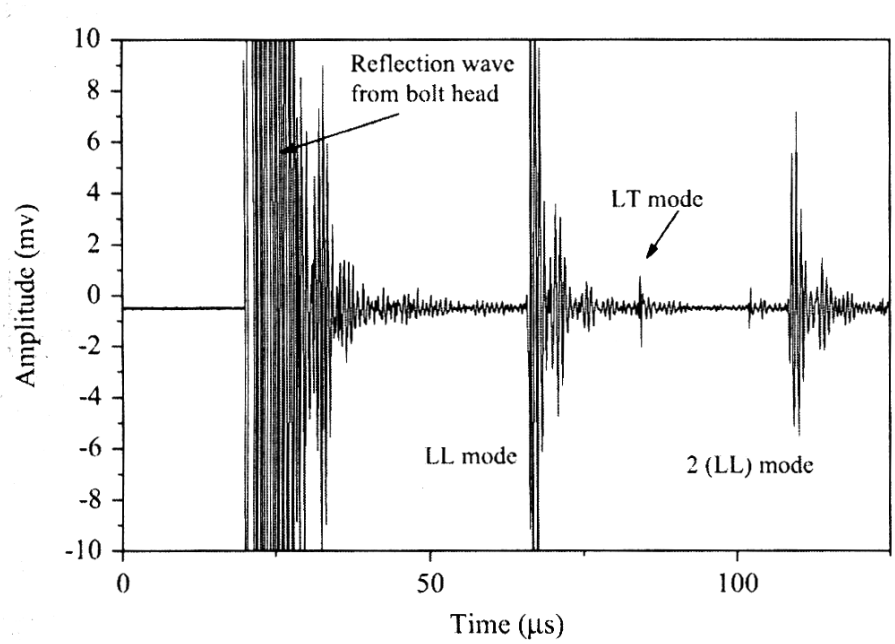

Figure 32. Waveforms for the longitudinal (LL) and mode converted (LT) waves.

Additionally Figure 32 shows the variation in time-of-flight for the LT wave with load. As the tensile strength expands the bolt, its acoustic velocity is reduced and the resulting time-of-flight is increased. This increase showed a nonlinear contribution assigned to the inverse proportional relation between the time-of-flight and the wave velocity, and to a nonlinear distribution of the axial stress in the bolt cross sections and along the axis.

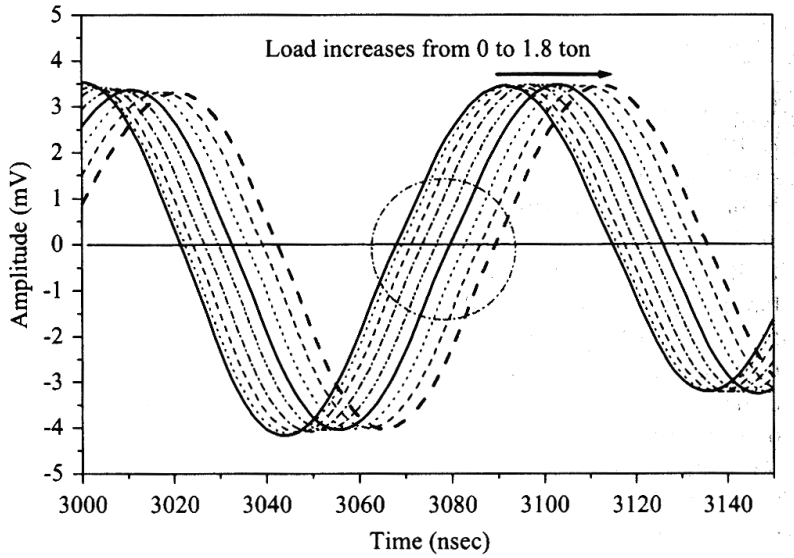

Figure 33. The variation in time-of-flight for the mode converted LT wave with load.

Figure 34 shows the resulting relationship for bolt B obtained between the tensile stress calculated from the measured TOF_{LL}/TOF_{TL}-ratios and the actually applied stress.

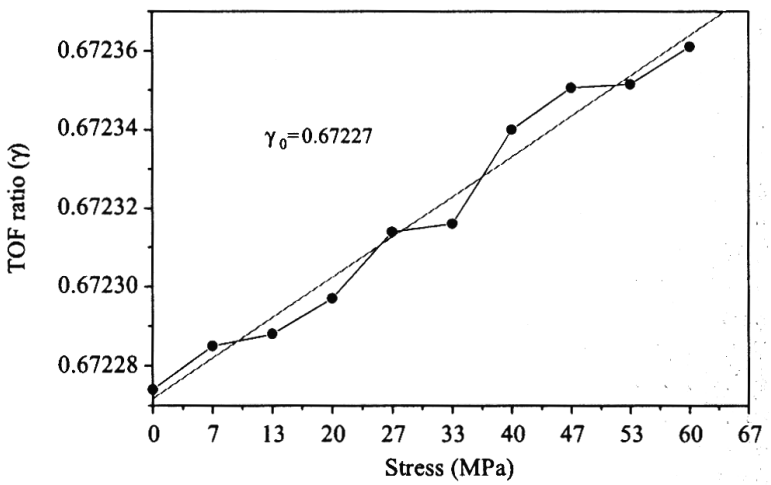

Figure 34. The relationship between the actually applied stress and the measured TOF_{LL}/TOF_{TL}-ratios.

In all, simultaneous velocity measurement of two differently polarized acoustic waves, LL and TL, were made with approximately 5 % error. The tensile stresses were possible to evaluate accurately down to less than 10 % of the yield stress of the bolt material.

9.9 Bi-wave analysis of bolts employing a single EMAT probe

9.9.1 A bi-wave single-probe EMAT applicable to non-magnetic metals

For non-magnetic metals, the Lorentz force mechanism allows the bi-wave technique to be employed with a shear-wave EMAT, which then allows a dual-mode EMAT with both longitudinal and transverse bulk waves. E.g. Hirao and Ogi[5] employed a shear-wave EMAT of 5 MH on a 320 mm long bolt of aluminium alloy 7075T771 and subjected to an axial stress. Figure 34 shows the resulting longitudinal, transverse and mode-converted echoes received.

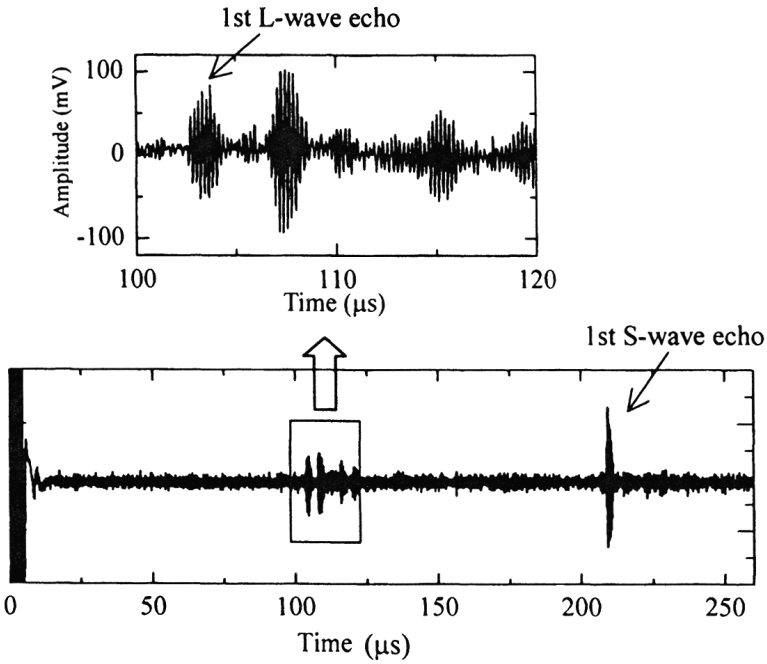

Figure 35. The received longitudinal, transverse and mode-converted echoes, with magnification of the first longitudinal echo, which is not subjected to mode conversion[5].

The first echo of the longitudinal wave and one echo from the shear wave were selected for deducing their phase response to stress. These echoes experienced no mode conversion at the lateral surface, and the measured phases showed a good linearity with the axial stress applied. Figure 35shows the normalized difference of the longitudinal and transverse wave phases, where the offset value was found to depend on the Poisson's ratio alone. While the pre-knowledge of the propagation length is eliminated employing this method, the acoustoelastic coefficients are still required from experiments.

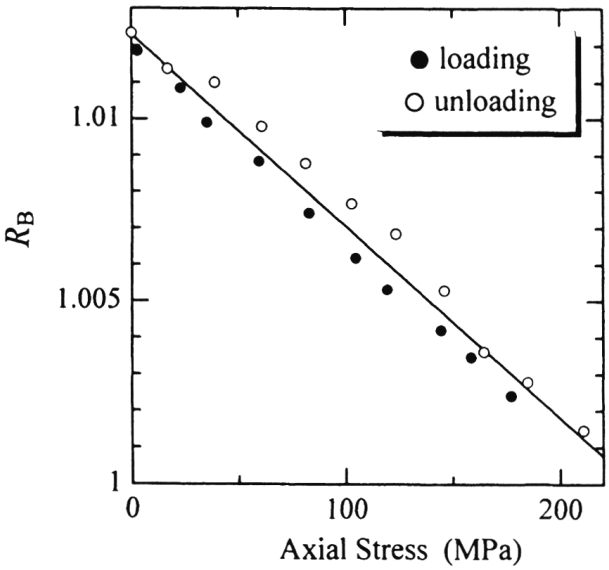

Figure 36. The axial stress in an aluminum bolt versus the normalized difference of the detected phase of longitudinal and transverse waves[5].

This method is, however, only applicable to nonmagnetic metals, while most bolts are made from ferromagnetic steels[5].

9.9.2 Free steel bolts up to 500 mm long using a single EMAT probe prototype

The French research institute CETIM[15 37] has developed a bi-wave technology to measure the axial stress on bolts using electromagnetic transducers (EMAT). This method is not industrialized yet, but CETIM employs a prototype. Being a non-contact transducer, the EMAT enables a repeatability which is difficult to obtain with traditional piezoelectric transducers.

Figure 36 displays the principle of electromagnetic generation of ultrasound, along with a resulting Fourier transform of echoes obtained on a 30 mm thick 35NCD16 specimen. The ultrasonic spectrum was found to be centered at ~6.5 MHz. The acquisition is performed with an oversampling with 100 MHz frequency, which leads to 500 MHz equivalent frequency. The time-of-flight is measured on the peak value of the longitudinal and transverse echoes, respectively. The best resolution for a stress level of 1kN has been observed at a sampling resolution of 2 ns.

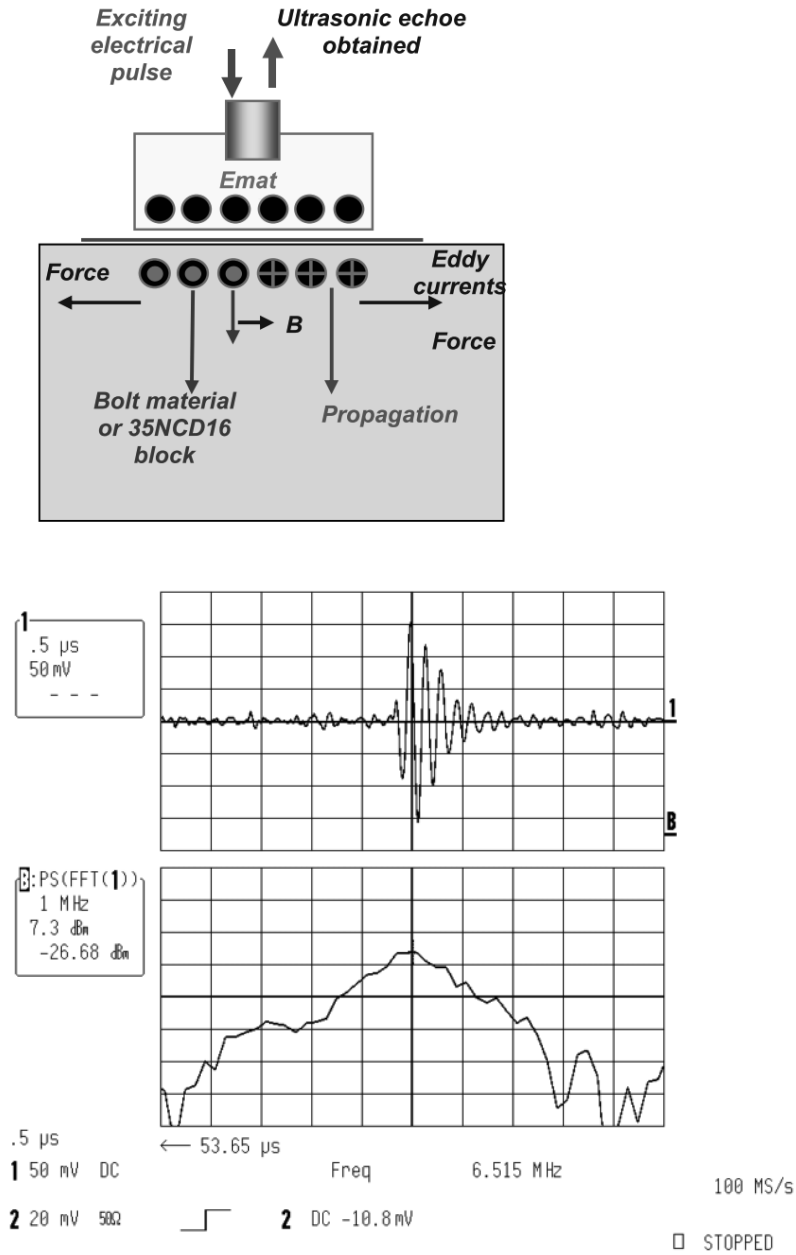

Figure 37. (a) The principles of EMAT generation of ultrasound, and (b) a typical spectrum for a 30 mm thick 35NCD16 specimen.

In order to deduce the axial load on bolts, the authors have performed[37] EMAT- measurements on bolts of various dimensions. Unpublished results exist for bolts of e.g. dimensions M14, M18 and M24, and with lengths from 64 to 152.5 mm.

From testing the same bolt after subsequently reducing its length, it could be confirmed that the ultrasonic measurement was independent on bolt length. Figure 38 shows an example were one of the bolts tested have obtained a subsequent reduction in length between measurements.

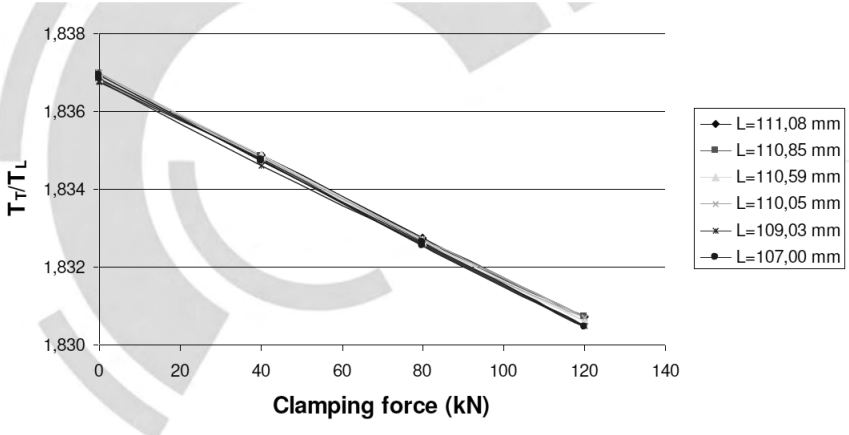

Figure 38. The resulting bi-wave calibration curve on a bolt after subsequently reducing its length from 111.08 mm to 107.00 mm.

Figure 39 displays the time-of-flight ratio for the longitudinal and transverse waves, TT/TL, versus load for a 520 mm long M30 bolt.

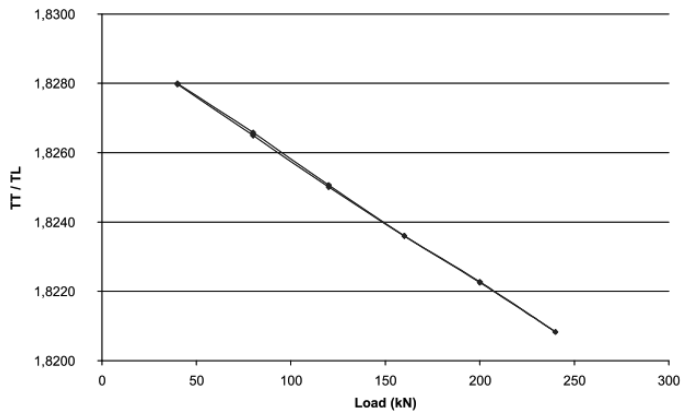

Figure 39. The resulting bi-wave calibration curve on a 520 mm long M30 bolt[15].

As the ultrasonic velocities are significantly affected by the temperature conditions, also the influence of temperature was measured in an oven on an unstressed bolt. Figure 40 exemplifies the linear relationship between the resulting velocity ratio and temperature.

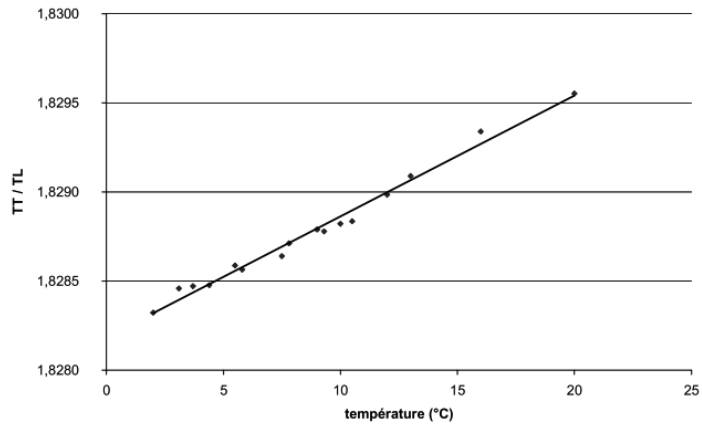

Figure 40. A temperature calibration curve, providing a load correction factor versus temperature.

The slope of the resulting calibration curves was also found to depend on the tightened length. Figure 41 shows an example were the actual tightened length of the bolt is varied.

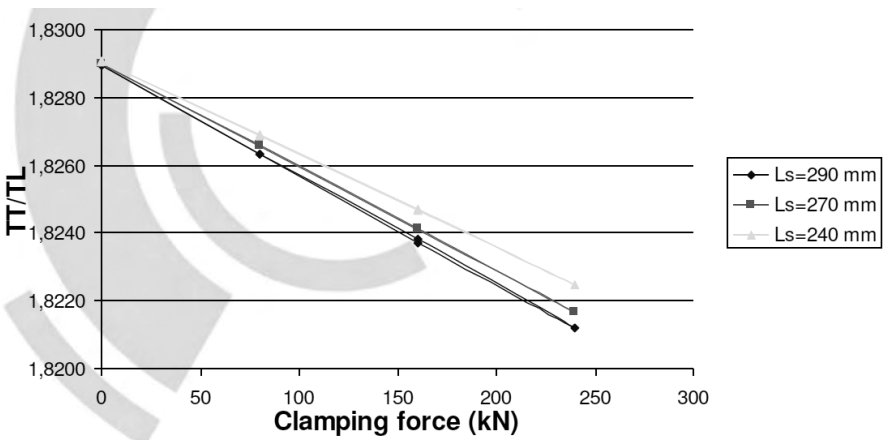

Figure 41. The slope of the calibration curve was also found to depend on the tightened length.

The ultrasonic measurements showed no effect for differences in torsional load (and also tightening torque) or by the presence of lubricants on the torque. However, flexion can disturb wave propagation and measurements. Additionally, the technique is dependent on the material, as well as on various heat-treatments. The method is currently also not valid on Titanium and Inconel bolts. As the ultrasonic velocity increases linearly with temperature, stability in temperature is of high importance for the analyses.

In all, the results showed a clear linear relationship between the load and the ratio of the transversal and longitudinal ultrasonic wave velocities, TT/TL. The bi-wave method thus

enables to perform the measurements in already tightened bolts with an uncertainty less than ±5 %. These results show that it is possibility to measure the load condition in already tightened bolts without pre-knowledge of the exact length of the unstressed bolt. While the one-wave method, employing only longitudinal waves, is not valid in the plastic region, the bi-wave method was found valid also in the plastic region. The tests were, however, only performed in a laboratory environment and not in the field.

9.10 Piezoelectric- vs EMAT ultrasonic transducers

A piezoelectric transducer induces ultrasonic waves by generation of a mechanical stress in response to an applied electrical potential. Portable instruments are commercially available for measurements of transit time/time of flight of bulk waves. The piezoelectric transducers, however, require an intimate contact with the bolt end. This can cause errors from the stamped mark, surface conditions and from unstable couplant properties[5]. The need for coupling fluids also means that the elastic waves not only propagate in the material but also in the coupling element and the transducer itself. This means disturbing echoes from interfaces within the transducer. Using piezoelectric transducer, the wave propagation angle in the test part is affected by Snell's law. As a result, a small variation in sensor deployment may cause a significant change in the refracted angle. Additionally, the method often is strongly dependent on the operator skills.

Contactless transducers include Electromagnetic Acoustic Transducer (EMAT), Laser-induced ultrasonics (LUS) and air-coupled transducers. In the case of rock bolts this would enable determination of the load of a mounted rock bolt without any prior knowledge regarding the object under investigation. While laser-based systems cannot be applied on such thick/long samples, EMATs allows investigations on longer samples.

The primary advantage of EMATs over piezoelectric transducers is that the ultrasonic waves are generated and detected through electromagnetic forces. This means that no mechanical coupling of acoustic energy is required, which eliminate measurement errors associated with the contacting transduction[38 5]. Since ultrasonic velocities can be measured at different stress levels without changing the distance between transducers, this is especially beneficial for acoustoelastic measurements. With contact-based piezoelectric transducers, the test surface has to be machined smoothly to ensure coupling. Using EMAT, the requirements to surface smoothness are less stringent. As the efficiency of the transduction decays exponentially with the distance between the sensor and the sample, the separation possible is limited to a few millimeters. However, this is enough to give a big advantage over piezoelectric transducers in some applications. It enables analyses at high temperatures as well as on moving samples[37].

Generally, three mechanisms are responsible for the electro-acoustic transduction of EMATs; the Lorentz force, the magnetostrictive force and the magnetization force. While the Lorentz force arises in any conducting material, the other two forces only occur in ferromagnetic materials[38 5]. Due to the forces arising due to magnetic interactions, the EMAT operation on steel is considerably more complicated than on non-magnetic metals as aluminium. Additionally, the lower electrical conductivity and higher density of steel will significantly reduce the EMAT efficiency in the Lorentz mode of operation for steel compared to e.g. aluminium. Figure 42 shows the mechanisms of bulk-wave-generation by Lorentz forces and

magnetostriction, respectively. For the effect of magnetostriction, the efficiency of the shear wave (or transverse wave) is considerably larger compared to the longitudinal wave[38].

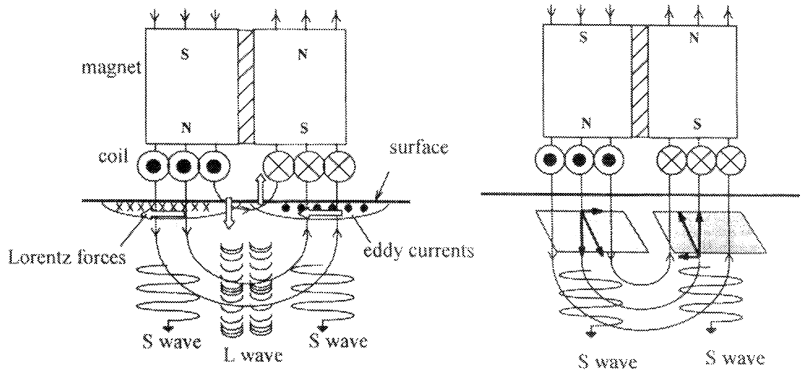

(a) *(b)*

Figure 42. Mechanisms of bulk-wave-generation by (a) Lorentz forces and (b) magnetostriction (a transverse wave, S-wave EMAT), respectively.

The main drawback of the EMAT systems is the generally lower signal-to-noise ratio compared to piezoelectric transducers. The low generation efficiency has limited the use of EMATs as ultrasonic generation sources. In order to compensate for their low efficiency, EMATs are typically narrowband in nature. The signal to noise ratio can also be greatly enhanced by filtering.

The EMAT is an ideal transducer to generate Shear Horizontal (SH) bulk wave mode, as well as Lamb waves and other guided-wave modes. Several types of EMATs exist, such as bulk wave EMATs, longitudinal-guided-wave EMAT, PPM EMAT, Meander-line coil SH-wave EMAT, various SH-wave EMATs, Rayleigh wave EMAT and EMATs for high temperature applications[5]. An EMAT can excite the orthogonally polarized horizontal shear (SH) plate or bulk modes. It is believed that this new transducer has many potential applications in the excitation of SH waves for both signal processing and nondestructive testing devices. These waves are important because of the absence of mode conversion when they strike surfaces parallel to their polarization and the resulting simplicity of the resulting signals. Previously they could only be excited by EMAT's using the periodic permanent magnet geometry[39].

A large market for EMAT probes today is quality inspections of welds or investigation of defects, employing both bulk waves and guided waves. Common to these analyses is that you only use one type of ultrasonic wave at the time. This simplifies the measurement and allows the probe to be small. Although small EMAT transducers do exist, commonly used transducers are large. For a probe for the generation of two types of waves simultaneously becomes a limitation to the probe head is small enough to fit on the measurement object without limiting the ability to measure long distances. While the bi-wave method, employing simultaneous generation and detection of longitudinal and transverse bulk waves, is applicable on already tightened bolts or screws, there is currently no EMAT equipment available on the market today. However, as previously described, the French research institute CETIM has employed a portable prototype equipment capable to measure on M14 bolts of lengths up to 160 mm[37] and

M30 bolts up to 500 mm[15]. Commercial piezoelectric probes exist that simultaneously generate and detect both longitudinal and transverse bulk waves. Olympus (www.olympus.com) provides a piezo electric probe/converter, which uses a combination of longitudinal and transversal wave. A combined EMAT- and piezoelectric probe with a sensor head of 25 mm diameter that allows the bi-wave application is however available at Inner Spec Technologies (www.innerspec.com).

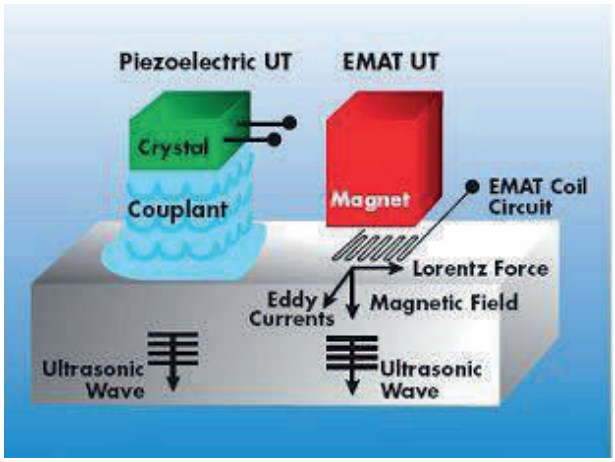

Figure 42. A schematic description of a piezoelectric- and an EMAT transducer, respectively.

9.11 Conclusive summary

In order to ensure the safety and reliability of rock bolts and other structural components, the integrity and load conditions have to be carefully controlled during both installation and service. A number of non-destructive testing methods have been developed for evaluating and monitoring bolt integrity, with focus on the grouting quality of long rock bolts. Some techniques require access to both ends of the bolt, while for the application one end is unreachable. The main focus of the survey is techniques for deducing the axial loading condition of bolts. The examples range from bolts joining thin lap-joint structures for automotive applications to long grouted bolts – often with both ends accessible.

Traditionally, the torque wrench technique has been used for evaluating the loading condition of rock bolts. However, as load to a large extent is dissipated in friction large errors are obtained for determinations of the axial load. Other commercial methods include strain gauge- and elasto-magnetic sensors, all which have to be pre-mounted onto each bolt for monitoring. Recent years, ultrasonic methods have been considered valuable non-destructive techniques for estimating bolt axial load. As rock bolts are not free standing, but grouted into e.g. cement and epoxy also only one end of the bolts is accessible for the analytical technique in question. In general, the conventional ultrasonic methods for the detection of bolt load can be divided into two groups, based on either wave-propagation or vibration/resonance. Several studies use nonlinear ultrasonics to correlate the frequency shifts with load caused by stress-velocity

relationships based on the acoustoelastic theory. The methods based on acoustoelastic effect use the fact that ultrasonic wave velocities vary proportionally with the axial stress. The methods, however, require the knowledge of the acoustoelastic coefficients of the bolt material investigated, which means that calibration tests have to be carried out on the bolt material. For certain application, calibration tests can be carried out on similar untightened bolts - but often the variation in material properties are too large due to e.g. heat treatments, ageing, or other variations between batches and material providers. For some applications calibrations can be performed on the bolt head of the tightened bolt in the field. For long specimens, a limiting factor for the ultrasonic bulk wave techniques is the strong attenuation while propagating in the material. Experimental work for monitoring the integrity and stress levels of free standing long grouted bolts have also been performed using guided ultrasonic waves, which can travel further along a structure. For studies employing guided waves, the focus has however generally been on crack- and flaw detection for long rods and even rails.

The conventional acoustoelastic ultrasonic technique for deducing axial loading is based on variations in the time-of-flight of a single longitudinal bulk wave with loading. A main drawback of this mono-wave technique is the required pre-knowledge of the initial bolt length as well as the initial loading condition. For many applications it can be difficult to deduce these data for already fastened bolts. These requirements can be avoided if two waves with different behavior are evaluated simultaneously. This so called bi-wave technique employs the time-of-flight ratio of both the longitudinal- and transverse bulk waves. As the two waves travel the same distance, they carry with them different acoustoelastic effects and travel with different velocities, and the dependence on propagation length is eliminated by the phase ratio of the two waves. Still, an extremely accurate time-of-flight measurement is required, especially for short bolts. Only small variations in the contact condition and measurement location of the piezo electric probe can cause a significant error in the time-of-flight measurement. Experimental errors induced from two different contact measurements of the two waves can however be avoided by employing a simultaneous generation and detection of both longitudinal and shear waves. Commercial piezoelectric probes exist that simultaneously generate and detect both longitudinal and transverse bulk waves, and the work has generally been carried out with a 10 MHz longitudinal wave and a 5 MHz transverse wave, respectively. The bi-wave technique has been employed for deducing the axial load for bolts between 50 and 215 mm long [29] [28] [27] [14].

Piezoelectric transducers, however, require an intimate contact with the bolt end which can cause errors due to various surface conditions or couplant properties. The primary advantage of EMAT transducers over piezoelectric transducers is that the ultrasonic waves are generated and detected through electromagnetic forces. This means that no intimate contact with the bolt end is required and that measurement errors associated with the mechanical coupling is avoided. The main drawback of the EMAT systems is, however, the generally lower signal-to-noise ratio compared to piezoelectric transducers. For the effect of magnetostriction, the efficiency of the transverse wave is considerably larger compared to the longitudinal wave. The lower electrical conductivity and higher density of steel will significantly reduce the EMAT efficiency in the Lorentz mode. For a bolt made of nonmagnetic material, an EMAT transducer generates simultaneously longitudinal and transverse waves in accordance with the Lorentz principle. For instance a 320 mm long bolt of aluminium alloy have been investigated while subjected to an axial stress[5]. However, on a magnetic material, the generation of longitudinal waves is very difficult and only transverse waves which are generated according to the magnetostrictive effect are exploited. There is currently no EMAT equipment available on the market for simultaneous generation and detection of longitudinal and transverse waves. The French research institute

CETIM has developed a bi-wave technology to measure the axial stress on bolts employing an EMAT prototype equipment which has been capable to measure the axial load condition of bolts with lengths up to 500 mm[37 16]. A combined EMAT- and piezoelectric probe with a sensor head of 25 mm diameter that allows the bi-wave application is commercially available.

9.12 References

1. Buys, B. J. *Rock Bolt Condition Monitoring using Ultrasonic Guided Waves*. (2008).

2. Ivanović, A. & Neilson, R. D. Non-destructive testing of rock bolts for estimating total bolt length. *International Journal of Rock Mechanics and Mining Sciences* **64**, 36–43 (2013).

3. Ivanović, A. & Neilson, R. D. Influence of geometry and material properties on the axial vibration of a rock bolt. *International Journal of Rock Mechanics and Mining Sciences* **45**, 941–951 (2008).

4. An, Y.-K. & Sohn, H. Integrated impedance and guided wave based damage detection. *Mechanical Systems and Signal Processing* **28**, 50–62 (2012).

5. Hirao, M. & Ogi, H. *EMATS FOR SCIENCE AND INDUSTRY - NONCONTACTING ULTRASONIC MEASUREMENTS*. (Kluwer Academic Publishers: 2010).

6. Thurner, H. F. Boltometer-instrument for non-destructive testing of grouted rock bolts. *The 2nd International Symposium on Field Measurements in Geomachanics* 135–143 (1988).

7. Buys, B. J., Heyns, P. S. & Loveday, P. W. Rock bolt condition monitoring using ultrasonic guided waves. 95–105 (2009).

8. Zhang, C. S., Zou, D. H. & Madenga, V. Numerical simulation of wave propagation in grouted rock bolts and the effects of mesh density and wave frequency. *International Journal of Rock Mechanics and Mining Sciences* **43**, 634–639 (2006).

9. Beard, M. D. & Lowe, M. J. S. Non-destructive testing of rock bolts using guided ultrasonic waves. *International Journal of Rock Mechanics and Mining Sciences* **40**, 527–536 (2003).

10. Wang, C., He, W., Ning, J. & Zhang, C. Propagation properties of guided wave in the anchorage structure of rock bolts. *Journal of Applied Geophysics* **69**, 131–139 (2009).

11. Edwards, R. S., Dixon, S. & Jian, X. Characterisation of defects in the railhead using ultrasonic surface waves. *NDT & E International* **39**, 468–475 (2006).

12. Frank, Y. Bolt torque equations predict stresses. *Product Engineering* **10**, 28 (1978).

13. Kim, N. & Hong, M. Measurement of axial stress using mode-converted ultrasound. *NDT & E International* **42**, 164–169 (2009).

14. Johnson, G. C., Holt, A. C., Cunningham, B. & Johnson, R. An Ultrasonic Method for Determining Axial Stress in Bolts. **14**, 253–259 (2013).

15. Walaszek, H. & Bouteille, P. Ultrasonic Stress Measurement: Application to Preload Assessment on Already Tightened Bolts. *Materials Science Forum* **524-525**, 459–464 (2006).

16. Mitri, H. S. Design and development of a new rockbolt load measuring device. (2002).

17. Mitri, H. Evaluation of Rock Support Performance through Instrumentation and Monitoring of Bolt Axial Load. 136–140 (2011).

18. Sumitro, S., Jarosevic, A. & Wang, M. L. Session 15. *Elasto-magnetic sensor utilization on steel cable stress measrement* 79–86 (2002).

19. DYWIDAGSystemsInternational http://www.dsiamerica.com/products/geotechnic/dynaforcesensor/system-description.html.

20. Bogdan, L. Dyna Force — An Elasto-Magnetic Sensor for Force Measuring of Ground Anchors (ASCE). *Problem Soils, and Geo-Support* 17–24 (2009).

21. Chaki, S. & Bourse, G. Guided ultrasonic waves for non-destructive monitoring of the stress levels in prestressed steel strands. *Ultrasonics* **49**, 162–71 (2009).

22. Yang, J. & Chang, F.-K. Detection of bolt loosening in C–C composite thermal protection panels: I. Diagnostic principle. *Smart Materials and Structures* **15**, 581–590 (2006).

23. Amerini, F., Barbieri, E., Meo, M. & Polimeno, U. Detecting loosening/tightening of clamped structures using nonlinear vibration techniques. *Smart Materials and Structures* **19**, 085013 (2010).

24. Wang, T., Song, G., Wang, Z. & Li, Y. Proof-of-concept study of monitoring bolt connection status using a piezoelectric based active sensing method. *Smart Materials and Structures* **22**, 087001 (2013).

25. Martinez, J., Sisman, A., Onen, O., Velasquez, D. & Guldiken, R. A synthetic phased array surface acoustic wave sensor for quantifying bolt tension. *Sensors (Basel, Switzerland)* **12**, 12265–78 (2012).

26. Hartmann, G. Potentials and Limitations of Ultrasonic Clamp Load Testing. (2007).doi:10.4271/2007-01-1668

27. Chaki, S., Corneloup, G., Lillamand, I. & Walaszek, H. Combination of Longitudinal and Transverse Ultrasonic Waves for In Situ Control of the Tightening of Bolts. *Journal of Pressure Vessel Technology* **129**, 383 (2007).

28. Yasui, H. & Kawashima, K. Acoustoelastic Measurement of Bolt Axial Load with Hypothetical Velocity Ratio Method. *Transactions of the Japan Society of Mechanical Engineers Series A* **66**, 390–396 (2000).

29. Tadolini, S. C. *Evaluation of Ultrasonic Measuremetn Systems for Bolt Load Determinations- RI 9332*. (1990).

30. Jhang, K.-Y., Quan, H.-H., Ha, J. & Kim, N.-Y. Estimation of clamping force in high-tension bolts through ultrasonic velocity measurement. *Ultrasonics* **44 Suppl 1**, e1339–42 (2006).

31. Liew, F. K., Hamdan, S., Osman, M. S. & Engineering, F. The Relationship between the Applied Torque and Stresses in Post-Tension Structures. 1–7 (2006).

32. Washer, G. A., Green, R. E. & Pond, R. B. Velocity Constants for Ultrasonic Stress Measurement in Prestressing Tendons. 81–94 (2002).doi:10.1007/s00164-002-0003-8

33. Heyman, J. S. A CW ultrasonic bolt-strain monitor. *Experimental Mechanics* **17**, 183–187 (1977).

34. Joshi, S. G. & Pathare, R. G. Ultrasonic instrument bolt stress. 270–274 (1984).

35. Hirao, M., Ogi, H. & Yasui, H. Contactless measurement of bolt axial stress using a shear-wave electromagnetic acoustic transducer. *NDT & E International* **34**, 179–183 (2001).

36. Rollins, F. R. Ultrasonic Analysis of Bolt Preloads. *Int. Adv. Nondestr. Test.* **5**, 229–253 (1977).

37. Bouteille, P. Combination of Longitudinal and Transverse Ultrasonic Waves for In Situ Control of Bolts Tightening. *Ultrasonc Control of Bolts TighteningBolts Tightening* (2009).

38. Ogi, H. Field dependence of coupling efficiency between electromagnetic field and ultrasonic bulk waves. *Journal of Applied Physics* **82**, 3940 (1997).

39. Thompson, R. B. Generation of horizontally polarized shear waves in ferromagnetic materials using magnetostrictively coupled meander-coil electromagnetic transducers. *Applied Physics Letters* **34**, 175 (1979).

BeFo

Box 5501
SE-114 85 Stockholm

info@befoonline.org • www.befoonline.org
Besöksadress: Storgatan 19, Stockholm

ISSN 1104-1773